Regulation of human Polo-like kinase 4 via phosphorylation and ubiquitin-dependent proteolytic degradation

Dissertation
zur Erlangung des Doktorgrades der Naturwissenschaften
der Fakultät für Biologie der Ludwig-Maximilians-Universität
München

Vorgelegt von
Jens Westendorf
aus Surwold

Dissertation eingereicht am: 03. August 2009

Tag der mündlichen Prüfung: 14. Dezember 2009

Erstgutachter: Prof. Dr. Erich A. Nigg
Zweitgutachter: Prof. Dr. Heinrich Leonhardt

Hiermit erkläre ich, dass ich die vorliegende Dissertation selbständig und ohne unerlaubte Hilfe angefertigt habe. Sämtliche Experimente wurden von mir selbst durchgeführt, soweit nicht explizit auf Dritte verwiesen wird. Ich habe an anderer Stelle weder versucht, eine Dissertation oder Teile einer solchen einzureichen bzw. einer Prüfungskommission vorzulegen, noch eine Doktorprüfung zu absolvieren.

München, den 03. Dezember 2009

1. Summary

Controlling centrosome numbers is crucial for proper bipolar spindle assembly and genomic stability. While defective centrosome duplication in S phase often leads to the formation of monopolar spindles, the assembly of excessive numbers of centrioles fosters multipolar mitoses. In either case, chromosome segregation is likely to be impaired and the probability of subsequent aneuploidy increases. Several kinases have been implicated in centrosome duplication, including members of the Cdk and Plk families. Recently, we and others could show that Polo-like kinase 4 (Plk4) is fundamental to this process (Habedanck *et al.*, 2005; Bettencourt-Dias *et al.*, 2005; Kleylein-Sohn *et al.*, 2007; Rodrigues-Martins *et al.*, 2007; Peel *et al.*, 2007). This present study aims at unraveling how Plk4 itself is controlled by upstream signals.

First, we set out to identify phosphorylated residues on Plk4 via mass spectrometry. We show that Plk4 is a highly phosphorylated protein throughout the cell cycle and identify several phosphorylated residues on this kinase. Next, we present a biochemical and functional characterization of the corresponding Plk4 phosphorylation site mutants in the context of centriole biogenesis.

Second, based on the finding that *Drosophila* Plk4 is degraded by the 26S proteasome dependent on the E3 ubiquitin ligase SCF^{Slimb} (Rogers *et al.*, 2009; Cunha-Ferreira *et al.*, 2009b), we show that Plk4 levels in human cells are tightly controlled by the homologues $SCF^{\beta TrCP}$ complex. Moreover, we prove that βTrCP binding is dependent on a phosphorylated consensus binding motif in Plk4 and provide evidence that autophosphorylation activity of Plk4 is required for its own controlled destruction.

Thus, we propose that active Plk4 constantly primes itself for degradation in order to restrain its own activity at the centrosome.

2. Introduction

Since the centrosome has been discovered by van Beneden and Boveri in the second half of the 19th century (Van Beneden, 1883; Boveri, 1887), this cellular organelle has fascinated cell biologists due to its complex and intriguing nature. In 1914, Theodor Boveri formulated his remarkable hypothesis that centrosomal abnormalities are linked to aneuploidy and tumorigenesis (Boveri, 1914), foreseeing experimental evidence that has been obtained many decades later (Lingle *et al.*, 1998; Pihan *et al.*, 1998; Carroll *et al.*, 1999).

With the advent of sophisticated microscopic and molecular biology techniques, the structure as well as the functions of this organelle have extensively been studied. The centrosome functions as the major Microtubule Organizing Center (MTOC) in interphase where it actively orchestrates numerous microtubule (MT)-dependent processes, such as cell shape, mobility, polarity and adhesion, as well as intracellular transport and the positioning of organelles (Bornens, 2008). When cells enter mitosis, the duplicated centrosome becomes a key player in proper bipolar spindle assembly by virtue of its MT nucleation capacity.

In addition to its role in organizing MTs, the centrosome is also pivotal to the process of ciliogenesis, in that the mature centriole of the centrosome templates the formation of the axoneme of cilia and flagella.

Despite this recent progress, many aspects in centrosome biology remain mysterious. In particular, the process of centriole duplication and its regulation are only incompletely understood. The interphase centrioles must duplicate exactly once per cell cycle in a strict one-per-one ratio of pre-existing to newly-formed centrioles (Nigg, 2007), as any numerical aberration fosters the formation of monopolar or multipolar spindles (reviewed in Godinho *et al.*, 2009). In fact, many tumors are characterized by excess numbers of centrosomes (Kramer *et al.*, 2005; Lingle *et al.*, 1998; Giehl *et al.*, 2005; Pihan *et al.*, 1998). This clearly demonstrates the requirement for a tight regulation of the centrosome duplication cycle – both in conjunction with the cell cycle and with regard to centriole copy number control.

In the following, we will present the current knowledge on centrosome structure and function, followed by an overview over the centrosome (duplication) cycle and its regulation. Finally, we will end the introductory part with a discussion on the role of the ubiquitin-proteasome system in cell cycle and centrosome cycle regulation.

2.1. Structure of the centrosome

As the cellular environment is highly unfavorable for any spontaneous MT nucleation, templated nucleation mechanisms evolved where γ-tubulin-containing multiprotein ring complexes (γTuRCs) accelerate the polymerization of tubulin dimers to dynamic MTs (Zheng *et al.*, 1995). The centrosome is the primary MTOC in animal cells that orchestrates this dynamic MT array, mainly through a concentration of γTuRCs within the cell.

The centrosome is a non-membranous organelle of about 1 µm in diameter that is usually found in close proximity to the nucleus (Fig. 1) (Doxsey, 2001). Despite its small size, the centrosome is of remarkable complexity. Its center is comprised of two loosely tethered centrioles, barrel-shaped structures with a nine-fold radial symmetry built of highly stable MT blades. These centrioles are embedded into an electron-dense, amorphous protein matrix referred to as pericentriolar material (PCM) (Doxsey, 2001; Azimzadeh & Bornens, 2007). There is an intimate relationship between centrioles and their surrounding PCM: While loss of centrioles leads to the dispersal of the PCM and thus to a loss of centrosome integrity (Bobinnec *et al.*, 1998), the PCM has *vice versa* been shown to be fundamental to the formation and stabilization of newly forming procentrioles (Fig. 2) (Dammermann *et al.*, 2004; Loncarek *et al.*, 2008).

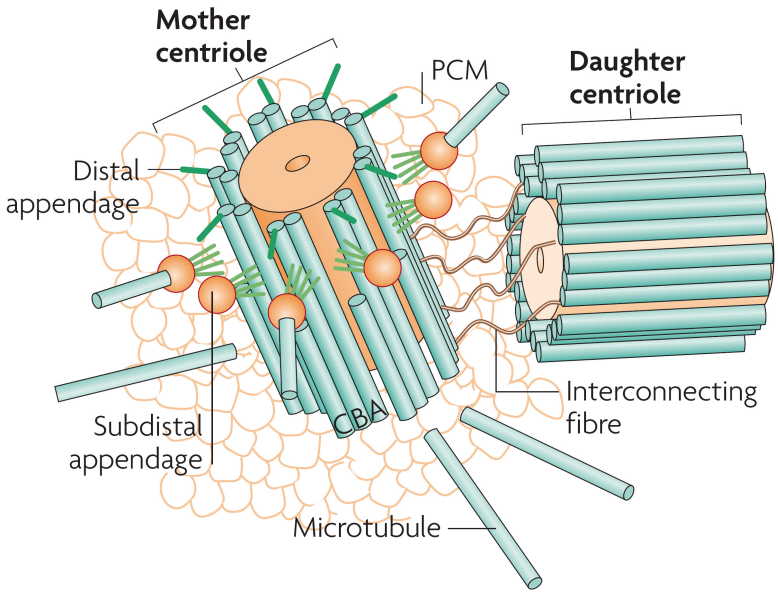

Fig. 1: Schematic diagram depicting the centrosome consisting of two centrioles in their surrounding PCM. In each triplet, the most internal tubule is called the A-tubule, the following one is the B-tubule and the most external one is the C-tubule. At its distal end, the centriole consists of doublets (adapted from Bettencourt-Dias & Glover, 2007).

The canonical centriole is a complex cylindrical structure with an outer wall formed by MT triplets (Bornens, 2002; Song *et al.*, 2008b). However, variations on this scheme have occurred over the course of evolution, exemplified by centrioles from flies and worms displaying MT doublets and singlets, respectively (Pelletier, 2004; Callaini *et al.*, 1997). Centriolar MTs dictate a polarization along the proximo-distal axis, with the MT minus ends forming its proximal end (Bornens, 2002). Post-translational modifications, such as polyglutamylation (Bobinnec *et al.*, 1998; Janke *et al.*, 2005), and additional structural proteins, such as tektins and ribbon proteins (Hinchcliffe & Linck, 1998; Steffen & Linck, 1988), are thought to account for the remarkable stability of centriolar MTs which withstand even harsh detergent and cold treatments. In addition, centrioles possess further structural features on their insides, including intraluminal spokes, filaments or tubes (Pelletier *et al.*, 2006; Nakazawa *et al.*, 2007; Hiraki *et al.*, 2007).

Although the two centrioles share an overall similar architecture, they are structurally and functionally distinct in that only the older one is fully mature (Azimzadeh & Bornens, 2007). Mature centrioles are characterized by two sets of nine appendages at their distal ends (distal and subdistal appendages) (Paintrand *et al.*, 1992), thought to be involved in anchoring MTs and in docking of centrioles at the plasma membrane during ciliogenesis (Azimzadeh & Bornens, 2007). Characteristic proteins present at appendages are ε-tubulin, ninein, Odf2, Cep170 or Cep164 (Chang *et al.*, 2003; Mogensen *et al.*, 2000; Ishikawa *et al.*, 2005; Guarguaglini *et al.*, 2005; Graser *et al.*, 2007).

The PCM has long been characterized only as amorphous, electron-dense material. With the development of highly sensitive protein identification techniques, in particular mass spectrometry, it has been shown that this matrix consists of more than one hundred different proteins, many of them carrying large coiled-coil regions known to mediate protein-protein interactions primarily in structural and motor proteins (Andersen *et al.*, 2003).

2.2. Functions of the centrosome

2.2.1. The centrosome as MTOC

The architecture of the interphase MT array depends not only on the dynamic instability of MTs themselves (Mitchison & Kirschner, 1984), but also on a balance between MT nucleation, MT release and MT anchoring at the centrosome (Bornens, 2002). Central to these processes is the PCM with its principal components belonging to the pericentrin and AKAP450 family of coiled-coil proteins (Moritz, 2004; Bornens, 2002). It constitutes a binding matrix for the γTuRC, that mediates the nucleation of MTs (Zheng *et al.*, 1995), and

for regulatory proteins, such as the MT severing protein katanin which drives the release of MTs into the cytoplasm (Bartolini & Gundersen, 2006). But also the mature centriole plays a role in MT organization, in that released MTs might be re-captured and subsequently anchored at the subdistal appendages, an activity known to depend on the protein ninein (Mogensen *et al.*, 2000). In addition, re-captured MTs may also be anchored within the PCM, however in close association with the mother centriole and dependent on the concerted action of the MT-associated protein EB1 with the dynactin subunit p150^{Glued} (Askham *et al.*, 2002).

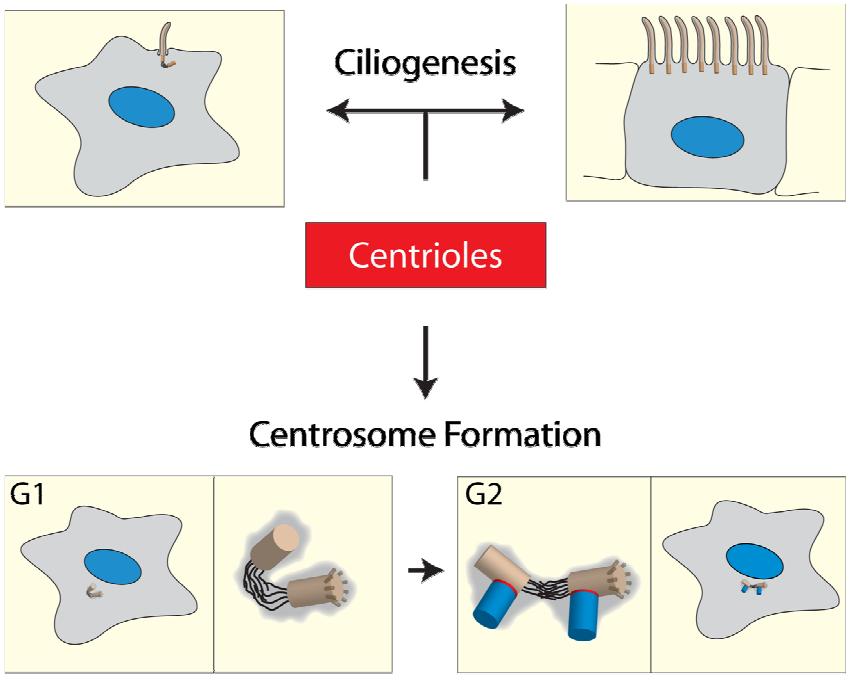

Fig. 2: Functions of centrioles. Centrioles are the core structures for the formation of centrosomes as well as motile and immotile (primary) cilia. Parental centrioles are depicted in light brown and engaged procentrioles in blue. For details, see text.

In preparation for mitotic spindle formation, the MT nucleating capacity of the centrosome dramatically increases, a process referred to as centrosome maturation (Palazzo *et al.*, 2000; Bornens, 2002). The two kinases Plk1 and Aurora A have been implicated in this process, opposed mainly by the phosphatases PP1 and PP4 (reviewed in Blagden & Glover, 2003; Trinkle-Mulcahy & Lamond, 2006). Work in *Drosophila* has shown that Polo (Plk1) activates Abnormal Spindle Protein (ASP) and promotes the increased recruitment of γTuRCs (Gonzalez *et al.*, 1998; do Carmo Avides *et al.*, 2001), while in human cells, Plk1 has been shown to regulate Nlp, a centrosomal protein involved in γTuRC binding and MT nucleation (Casenghi *et al.*, 2003; Casenghi *et al.*, 2005). In addition, Aurora A phosphorylates (and

thereby recruits) the conserved centrosomal protein D-TACC, that in turn together with other factors accelerates the nucleation of MTs (Giet *et al.*, 2002; Barros *et al.*, 2005; Peset *et al.*, 2005; Brittle & Ohkura, 2005; Brouhard *et al.*, 2008).

2.2.2. Centrioles as templates for primary cilium formation

Centrioles are structurally equal to and interconvertible with basal bodies (Dutcher, 2003). Cilia are membrane-bounded, centriole-derived projections protruding from the cell body that contain a MT cytoskeleton, the ciliary axoneme. Mammalian ciliary exonemes are constituted by a cylindrical array of nine doublet MTs that extend from the A and B MTs of each of the nine triplet MT blades of the basal body (Fig. 3) (Satir & Christensen, 2007; Fliegauf *et al.*, 2007). They are formed in two major patterns: 9+2, in which the nine MT doublets surround a central pair of singlet MTs, and 9+0, in which this central pair is missing. Ciliary motility is depended on the structure of the axoneme: While 9+2 cilia usually contain axonemal dyneins (motor proteins) that confer the ability of ciliary beating, 9+0 cilia are lacking these motors and are therefore non-motile (Satir & Christensen, 2007). In addition, non-motile cilia (referred to as primary cilia) are usually solitary and found on virtually all cell types within the mammalian body (except for blood cells), whereas motile cilia often occur in bundles of up to several hundreds, usually on differentiated epithelial cells (Fliegauf *et al.*, 2007).

In contrast to the majority of other organelles, cilia are only assembled when cells exit from the cell cycle into a quiescent and/or differentiated state; *vice versa*, re-entry into the cell cycle from G_0 phase requires a preceding ciliary resorption (Quarmby & Parker, 2005). Proteins localizing to centrosomes/basal bodies may in principle be involved in ciliogenesis, ciliary maintenance and/or resorption. In particular, proteins forming the appendages of the mature centriole are suggested to anchor the centriole at the plasma membrane, as deletion of Odf2, a protein indispensable for the formation of distal and subdistal appendages, also prevented cilia formation in a mouse knock-out model (Ishikawa *et al.*, 2005).

Motile cilia are usually required to move extracellular fluids or particles. For instance, multi-ciliated epithelial cells in the respiratory tract are required for mucociliary clearance, a process in which a thin mucus layer is moved towards the pharynx in order to clear inhaled pathogens and other foreign bodies from the respiratory system (Kollberg *et al.*, 1978; Moller *et al.*, 2006). Furthermore, flagellar mobility is required for sperm cells to propel through the female reproductive system.

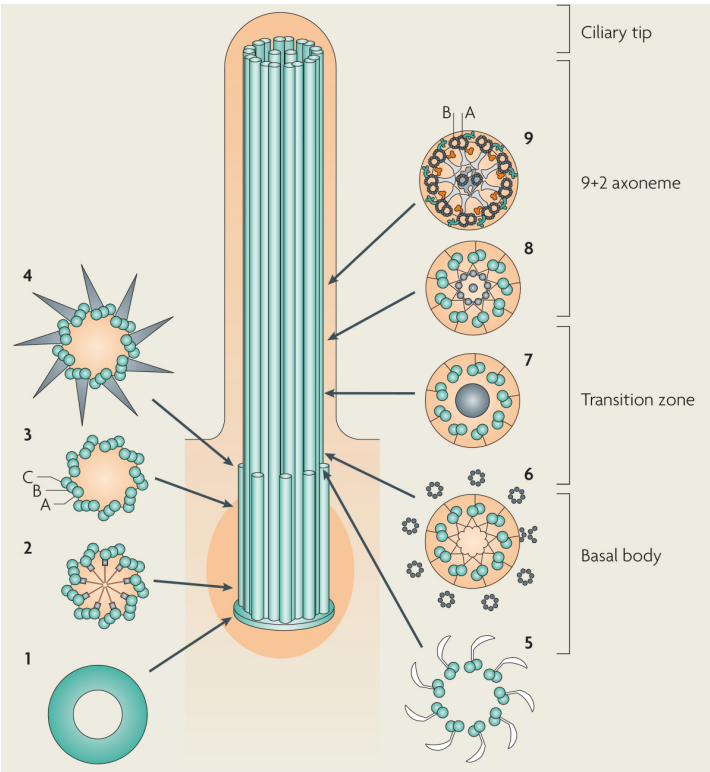

Fig. 3: Structure of a motile cilium with a 9+2 axoneme. MT doublets forming the 9+2 axoneme emanate from the A and B MTs of each of the nine triplet MT blades of the basal body. The remaining PCM is shaded darker orange around the basal body. The ciliary membrane is continuous with the plasma membrane but contains specific signaling molecules. Adapted from Fliegauf *et al.* (2007).

In contrast to these active functions of motile cilia, primary cilia are usually thought to mediate sensing of various environmental cues. They have been shown to play important roles in development, in particular in the establishment of left-right asymmetry (Nonaka *et al.*, 1998), as well as in the adult where the processing of mechanical and chemical signals is required for proper organ and tissue function. For example, flow-induced passive bending of cilia on kidney epithelial cells is required for mechanosensation of fluid flow in the nephron, and perturbance of this mechanosensory function is a cause of polycystic kidney disease (Praetorius & Spring, 2005).

It is therefore not surprising that ciliary defects have been causally linked to several pleiotropic disorders, such as Bardet-Biedl syndrome (BBS), Almstrom syndrome (ALMS), oral-facial-digital syndrome type I (OFD1), and others (Badano *et al.*, 2006; Hildebrandt & Zhou, 2007; Zariwala *et al.*, 2007).

2.3. The centrosome cycle

In many aspects, the canonical centrosome duplication cycle is reminiscent of the DNA replication cycle (Fig. 4). Prior to mitotic cell division, the single centrosome needs to be faithfully duplicated in order to ensure proper bipolar spindle assembly and error-free segregation of chromosomes. With the exception of some specialized cell types and developmental stages in which centrioles are formed *de novo* (Dirksen, 1991; La Terra *et al.*, 2005; Marshall *et al.*, 2001), centriole duplication usually initiates next to a pre-existing centriole, i.e. centrosome duplication occurs in a semi-conservative fashion (Sluder, 2004). Based on morphological changes that have been observed by electron microscopy, the centrosome cycle has been broken down into four distinct steps: centriole disengagement, centriole duplication (with elongation), centrosome maturation and centrosome separation (Sluder, 2004; Chretien *et al.*, 1997; Kuriyama & Borisy, 1981; Alvey, 1985; Kochanski & Borisy, 1990; Paintrand *et al.*, 1992; Vorobjev & Chentsov Yu, 1982) (Fig. 4).

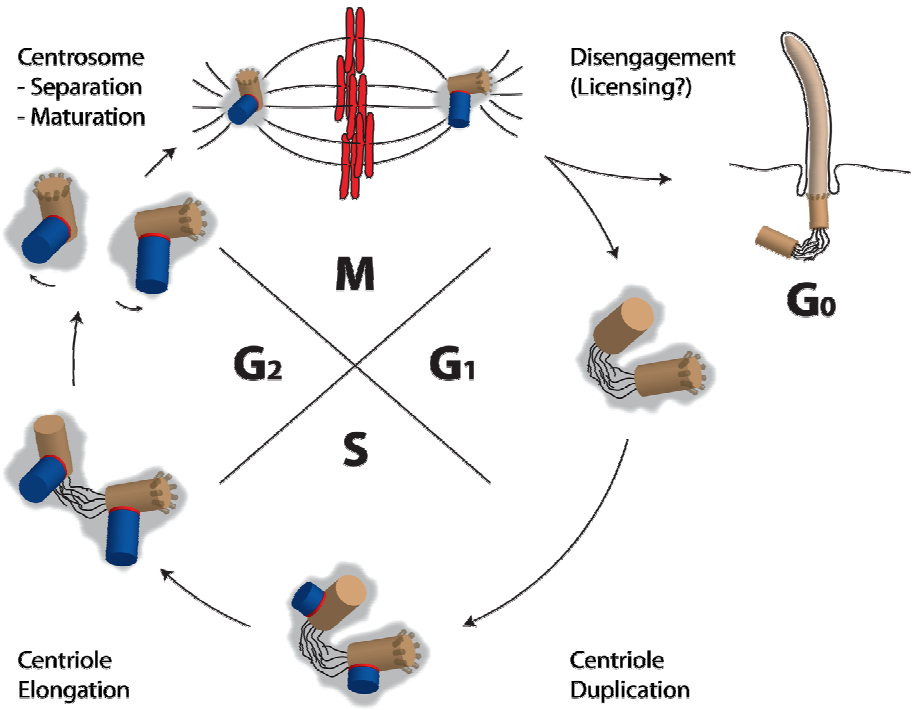

Fig. 4: Schematic view of the centrosome cycle in relation to the cell cycle. Mature centrioles are shown in brown, procentrioles in dark blue, the hypothetical linker protein required for maintenance of engagement in red, and the PCM in gray. Distal and subdistal appendages are represented in darker brown, and the flexible tether connecting parental centrioles until the onset of mitosis is shown as winding black lines.

In cycling somatic cells, centriole duplication is initiated at the G_1/S transition by the formation of a procentriole at the proximal base of each of the two existing (= parental) centrioles. Parental centrioles and their progeny are engaged in an orthogonal manner, with the procentriolar lumen facing the wall of the parental centriole. As cells further progress through S and G_2 phases, these procentrioles elongate to full size, strictly maintaining their intimate orthogonal arrangement. Until late G_2, tethering of the two centriole pairs ensures that the duplicated centrosome still functions as one single MTOC. Centrosome maturation in G_2 is accompanied by a dramatic increase in MT nucleation capacity, the recruitment of additional centrosomal proteins and the acquisition of distal and subdistal appendages by the younger parental centriole (reviewed in Palazzo *et al.*, 2000).

With the onset of mitosis, the flexible tether between the two parental centrioles is severed in response to phosphorylation of linker proteins such as C-Nap1 and rootletin (Bahe *et al.*, 2005; Yang *et al.*, 2006; Mayor *et al.*, 2000); as a consequence, the two engaged centriole pairs separate and initiate the formation of the mitotic spindle.

Upon exit from mitosis, the centrosome duplication cycle closes with the disengagement of the two inherited centrioles and the establishment of the flexible and highly dynamic tether instead.

2.3.1. Centriole biogenesis

A putative templating mechanism holds considerable appeal for explaining how centriole duplication is initiated by coordinated recruitment of centriolar proteins to a specified site at the parental centriole wall (Delattre & Gonczy, 2004). Careful electron microscopic studies in mammalian cells have revealed a filamentous corona forming around the proximal walls of parental centrioles and electron-dense material protruding into the proximal half of the elongating centriole (Anderson & Brenner, 1971; Sorokin, 1968). Moreover, a characteristic fibrous structure displaying ninefold symmetry (termed cartwheel) has been proposed to serve as a scaffold for the assembly of centriolar MTs in some species (Anderson & Brenner, 1971; Beisson & Wright, 2003; Cavalier-Smith, 1974; reviewed in Alvey, 1986). Strikingly, the cartwheel is able to self-assemble *in vitro* in a mixture of solubilized basal body components, strongly suggesting that intrinsic properties of its molecular components dictate the ninefold symmetry of the centriole/basal body (Gavin, 1984).

Interest in this putative scaffolding structure has recently been revived by the identification of the first cartwheel-associated molecule, the coiled-coil protein Bld10p, that

plays a crucial role in centriole/basal body assembly in *Chlamydomonas* (Matsuura *et al.*, 2004).

Another study from the same group identified a second protein of the cartwheel, CrSas6 (Nakazawa *et al.*, 2007). This homologue of the *C. elegans* SAS-6 protein (see below) is part of the central hub. Null mutants fail to assemble this part of the cartwheel, yet occasionally they are able to form basal bodies with aberrant numbers of MT triplet blades, again demonstrating a pivotal role for the cartwheel in the establishment of the centrioles' ninefold symmetry (Nakazawa *et al.*, 2007).

2.3.2. Centriole biogenesis pathways in *C. elegans* and human cells

Genetic studies and RNA interference screens have identified a core module of five centrosomal proteins as being required for centrosome duplication in *C. elegans*: SPD-2, ZYG-1, a complex of SAS-6/SAS-5 and SAS-4 (Kemp *et al.*, 2004; O'Connell *et al.*, 2001; Leidel *et al.*, 2005; Dammermann *et al.*, 2004; Delattre *et al.*, 2004; Leidel & Gonczy, 2003; Pelletier *et al.*, 2006) (Fig. 5a). Upon entry of the sperm, SPD-2 becomes recruited to the paternal centrioles in a Cdk2-dependent manner (Cowan & Hyman, 2006). SPD-2 recruitment itself is required for the subsequent centriolar localization of all other components downstream in the cascade (Delattre *et al.*, 2006; Pelletier *et al.*, 2006). ZYG-1 recruits a complex of the coiled-coil proteins SAS-6 and SAS-5 which in turn are required for the accumulation of SAS-4. In an elegant structural study using electron tomography, the authors revealed that upon recruitment of the SAS-6/SAS-5 complex, the formation of a central tube is initiated. Dependent on the localization of SAS-4 thereafter, centriolar singlet MTs were observed to assemble along the outer wall of this tube (Pelletier *et al.*, 2006).

Studies in other organisms have meanwhile proven that the above described core module of nematode centriole duplication proteins has been conserved through evolution, as orthologues of SPD-2, ZYG-1, SAS-4 and SAS-6 (with the notable exception of SAS-5) have been identified in flies and humans (Bettencourt-Dias & Glover, 2007) (Fig. 5b). Although both *Drosophila* and humans lack an obvious homologue of ZYG-1 in their genomes, two studies independently identified human Plk4 (also known as Sak) and the homologous *Drosophila* Plk4 as likely functional analogues of ZYG-1 (Bettencourt-Dias *et al.*, 2005; Habedanck *et al.*, 2005).

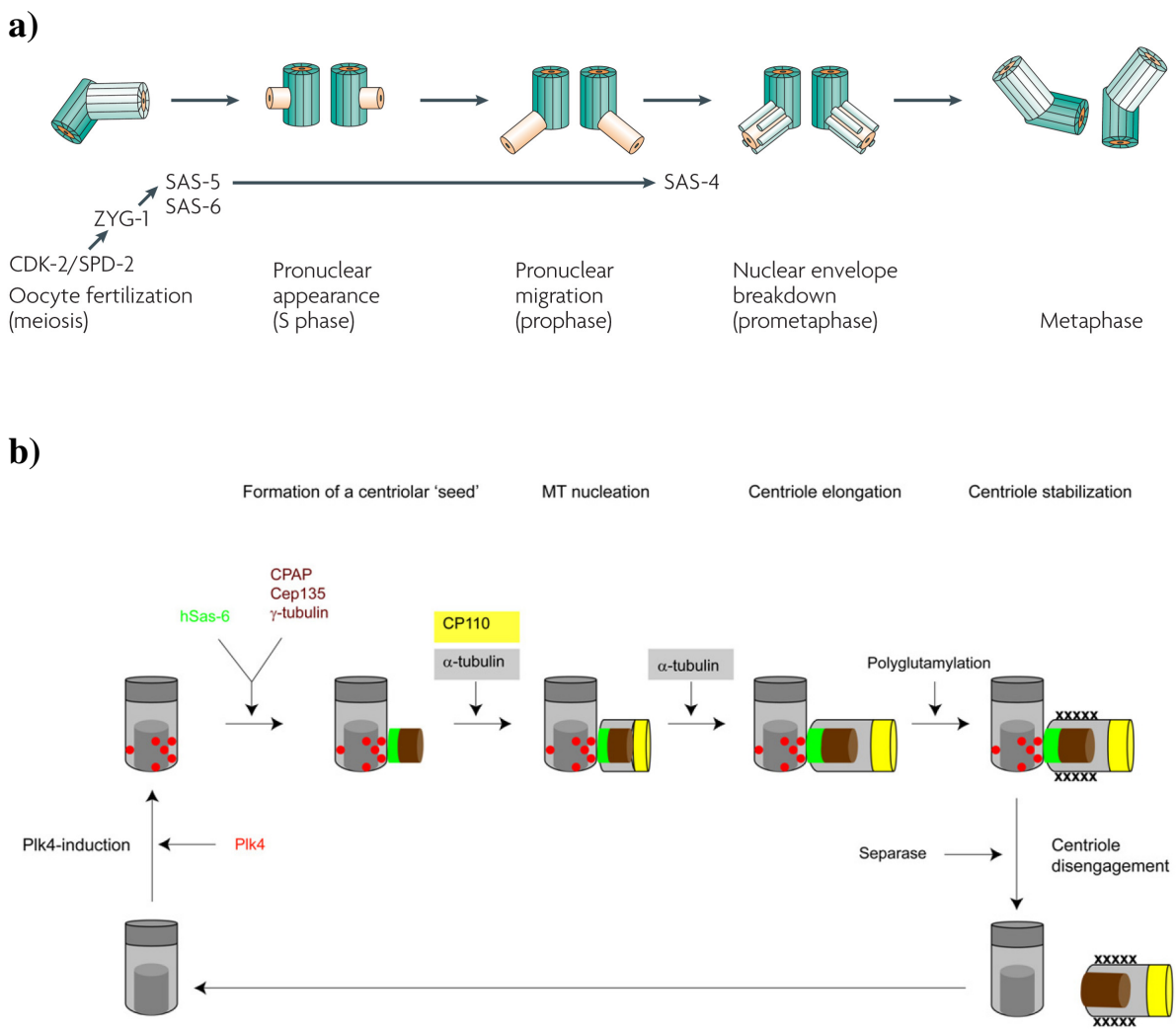

Fig. 5: The entriole biogenesis pathway is highly conserved. **(a)** Centriole biogenesis in *C. elegans*. In S phase, procentrioles start to assemble next to each parental centriole by the formation of a central tube. In a Sas-4-dependent manner, 9 singlet MT are subsequently assembled onto the central tube. **(b)** Centriole biogenesis in human cells. Similarly to *C. elegans*, procentriole formation initiates in S phase dependent on the proteins HsSas-6, CPAP, Cep135 and γ-tubulin. During elongation, tubulin dimers seem to be added underneath a distal cap constituted by CP110. Adapted from Kleylein-Sohn *et al*. (2007).

Subsequently, Plk4-induced overduplication of centrioles has been used as an elegant tool in the delineation of a centriole biogenesis pathway in human cells (Kleylein-Sohn *et al.*, 2007) (Fig. 5b). After induction of Plk4 overexpression, the human proteins HsSas-6, CPAP (the human homologue of SAS-4), Cep135 (the homologue of *Chlamydomonas* Bld10p), and γ-tubulin were rapidly recruited to the centrosome. While HsSas-6 exclusively localized to the nascent procentrioles, CPAP and Cep135 could additionally be detected in the proximal lumen of parental centrioles. Interestingly, three recent studies independently describe a role

for CPAP in the elongation of centrioles, hinting at a conserved function of SAS-4/CPAP in modulating centriolar MTs (Schmidt *et al.*, 2009; Tang *et al.*, 2009; Kohlmaier *et al.*, 2009).
In summary, the protein module originally discovered in *C. elegans* appears to represent a highly conserved centriole assembly pathway (Bettencourt-Dias & Glover, 2007). As the key players in this process have now largely been determined (Kleylein-Sohn *et al.*, 2007), it will be important to unravel their respective functions and interactions on a molecular level.

2.3.3. Regulation of centriole duplication

2.3.3.1. Synchronization of the chromosome and centrosome duplication cycle

It has long been noticed that centriole duplication is strictly limited to S phase of the cell cycle when cells prepare for subsequent cell division by duplicating their genetic content. However, the exact molecular mechanisms of this synchronization remain largely obscure.

Procentriole formation coincides with the rise of Cdk2 activity at the beginning of S phase, and consequently, studies in *Xenopus* egg extracts as well as in mammalian tissue culture cells demonstrated a requirement for Cdk2/Cyclin-E in procentriole biogenesis (Hinchcliffe *et al.*, 2001; Matsumoto *et al.*, 1999; Lacey *et al.*, 1999). Additionally, Cdk2/Cyclin-A has been shown to be essential for the re-duplication of centrioles in S phase-arrested cells (Meraldi *et al.*, 1999). However, although Cdk2 activity seems to be generally required for centriole duplication, a direct requirement at the centrosome seems unlikely in light of the findings that Cdk2 and Cyclin-E knockout mice are viable and show no obvious defects in centriole duplication (Berthet *et al.*, 2003; Geng *et al.*, 2003; Ortega *et al.*, 2003). Thus, a mechanistic explanation for the requirement of Cdk2 activity is still missing, and meanwhile it remains likely that Cdk2 activity is necessary to advance the cell into a certain cell cycle window (i.e. S phase) in which cytoplasmic conditions are permissive for centriole duplication (Sluder, 2004).

2.3.3.2. Once and only once – licensing centrioles for duplication

With the exception of some cancer cell lines that accumulate centrioles by successive rounds of duplication when cell cycle progression is blocked in S phase (Balczon *et al.*, 1995; Meraldi *et al.*, 1999), most cells prevent centriole re-replication in prolonged S phase, including HeLa cells (Loncarek *et al.*, 2008). Obvious similarities between centriole duplication and DNA replication prompted the speculation that centriole re-duplication might normally be prevented through a licensing mechanism in analogy to DNA replication (reviewed in Tsou & Stearns, 2006a; see also Blow & Dutta, 2005; Hook *et al.*, 2007; Diffley,

2001). Here, the licensing step corresponds to the loading of mini chromosome maintenance (MCM) helicases onto DNA in order to unwind the DNA for further replication. This assembly of pre-replicative complexes (preRCs) requires low Cdk activity and thus can take place only in a short window of the cell cycle between the end of mitosis and late G_1 phase. The firing of those preRCs, however, requires the high Cdk activity of the following S phase. As Cdk activity remains high from S phase until the end of mitosis, re-licensing is prevented until the next cell cycle is entered (Hook *et al.*, 2007; Blow & Dutta, 2005; Diffley, 2001).

Wong and Stearns (2003) tested the hypothesis of an analogous mechanism in elegant cell fusion experiments, generating hybrid cells by fusing G_1 and S phase cells or G_1 and G_2 cells, respectively. The authors could show that G_1 (i.e. unduplicated) centrioles readily initiated procentriole formation in S phase cytoplasm, while G_2 (i.e. engaged) centriole pairs did not; this was not due to an inhibitory effect of the cytoplasm as within the same cytoplasm, G_1 centrioles were found to duplicate, and G_2 centrioles did not. These findings led the authors to propose a centriole-intrinsic block to reduplication once the formation of a procentriole had been initiated (Wong & Stearns, 2003).

Supporting experimental evidence could be obtained recently by laser ablation studies in HeLa cells (Loncarek *et al.*, 2008). Although these cells – in contrast to CHO and U2OS cells – possess a stringent control to prevent reduplication in prolonged S phase, parental centrioles depleted for their engaged procentriole by a focused laser beam (repeatedly) initiated a new round of procentriole formation within the S phase block (Loncarek *et al.*, 2008). This finding goes well in line with the above-mentioned hypothesis that centriole engagement imposes an intrinsic block to reduplication.

Recently, the same group proposed a mechanistic explanation for this intrinsic block (Tsou & Stearns, 2006b). Their experiments suggest a role for separase in the disengagement of centrioles upon exit from mitosis, constituting the proposed (temporally separated) licensing step for subsequent centriole duplication in S phase. It has been put forward that separase – directly or indirectly – could catalyze the cleavage of a yet-to-be identified protein that 'glues' the two engaged centrioles together, reminiscent of cohesin functioning in duplicated sister chromatid cohesion (Nigg, 2006).

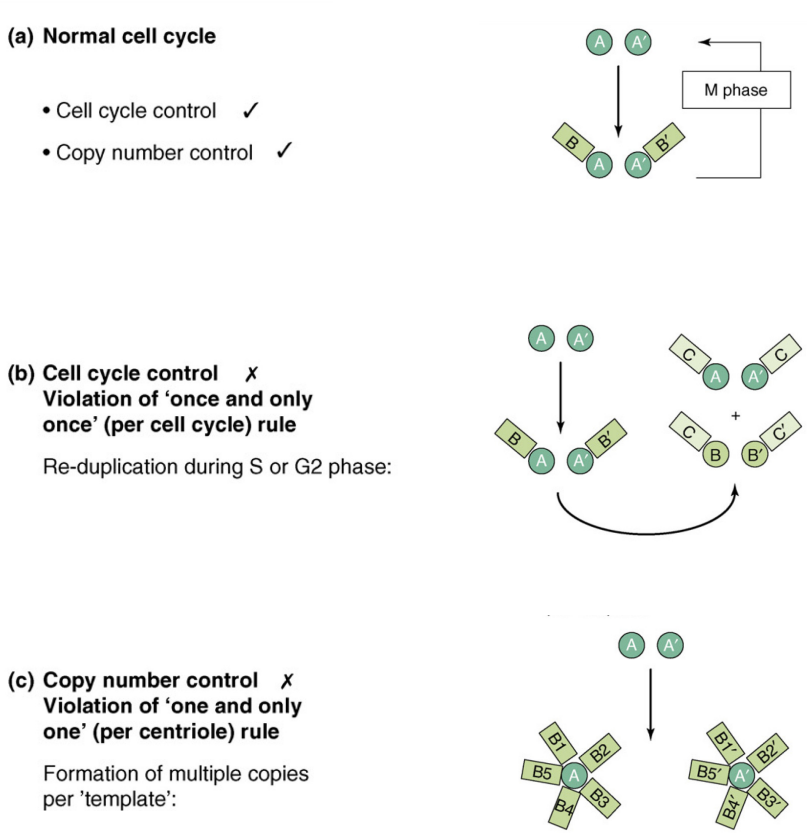

Fig. 6: Controls that govern the centriole duplication cycle. In order to keep centrosome numbers constant, cells adhere to two conceptually different modes of control: cell cycle control and centriole copy number control. While cell cycle control seems to be regulated by a licensing event in analogy to DNA replication (that is, disengagement of duplicated centrioles), copy number control is exerted by the tightly regulated activity of the kinase Plk4. Violation of either rule leads to centrosome amplification, yet via fundamentally different mechanisms. Adapted from Nigg (2007).

Despite the obvious attractiveness of such a scenario, this hypothesis cannot explain certain observations (Nigg, 2007; Loncarek & Khodjakov, 2009): First, in hydroxyurea-induced centriole re-duplication in CHO cells (Balczon *et al.*, 1995), centrioles disengage first before they continue to duplicate another time (Loncarek *et al.*, 2008), yet in S phase separase is kept inactive by securin. Second, during ciliogenesis, procentrioles formed in vicinity of parental centrioles also become disengaged in interphase when separase should not be active (Dirksen, 1991). And third, individual engaged centriole pairs disengage asynchronously in S phase-arrested cells, at least arguing against a global activation of separase at that point (Loncarek *et al.*, 2008). Recent data suggests that Cep76 might serve as a 'sensor' to prospect for the presence of a procentriole at the parental centriole (Tsang *et al.*, 2009).

2.3.3.3. One procentriole per parental centriole – copy number control exerted by Plk4

It appears somewhat counterintuitive that exactly one – and only one – procentriole forms orthogonally to the cylindrical base of a parental centriole. It has been speculated that centrioles carry an intrinsic asymmetry, or that a site at the wall of the cylinder pre-defines the place where a new procentriole emerges (Jones & Winey, 2006; Tsou & Stearns, 2006a). Such a scenario would fit well with the above described licensing model, in that the existing procentriole would simply block the formation of further progeny by occupying the required assembly site. Unfortunately, such an explanation appears too simple and cannot explain apparent deviations from the one-to-one ratio, where two to nine procentrioles were found to assemble on one parental centriole cylinder (Dirksen, 1991; Loncarek *et al.*, 2008).

Considerable progress towards the understanding of the mechanism of centriole copy number control has been achieved with the identification of Polo-like kinase 4 (Plk4) as a key regulator of this process in both human cells (Habedanck *et al.*, 2005) and flies (Bettencourt-Dias *et al.*, 2005). [For a summary of our current knowledge about this kinase, please refer to section 2.5].

Centrosomal localization had first been reported for mouse Plk4 (Hudson *et al.*, 2001). Subsequently, overexpression studies in human cells and flies established that excess Plk4 drives the formation of supernumerary centrioles (Habedanck *et al.*, 2005; Bettencourt-Dias *et al.*, 2005), while the depletion or mutational inactivation of this kinase abolishes centriole duplication, leading to a progressive loss of centrioles in vertebrate and invertebrate cells (Habedanck *et al.*, 2005; Kleylein-Sohn *et al.*, 2007; Bettencourt-Dias *et al.*, 2005). Moreover, the spermatids of *Drosophila plk4* mutants lack basal bodies and are therefore unable to form flagella (Bettencourt-Dias *et al.*, 2005). These observations are reminiscent of the functions that have been assigned to the kinase ZYG-1 in *C. elegans* (O'Connell *et al.*, 2001), and despite the lack of any obvious sequence similarity between these two proteins, it appears plausible that Plk4 represents the functional homologue of ZYG-1 in vertebrate cells (Habedanck *et al.*, 2005). Most strikingly, excess Plk4 can trigger the *de novo* centriole biogenesis pathway in unfertilized *Drosophila* eggs (Peel *et al.*, 2007; Rodrigues-Martins *et al.*, 2007).

Of particular interest in this context was the finding that overexpression of Plk4 in human cells caused the apparent recruitment of 'electron-dense material' around the proximal walls of parental centrioles (Habedanck *et al.*, 2005). In a subsequent study, these electron-dense spots were shown to represent early-stage procentrioles that eventually develop into full centrioles (Kleylein-Sohn *et al.*, 2007; discussed in detail in section 2.3.2). In addition to

Plk4, overexpression of HsSas-6 also leads to the formation of multiple procentrioles around the proximal wall of parental centrioles (Strnad *et al.*, 2007). These observations clearly argue against a pre-defined site of centriole assembly, and rather suggest that, in principle, the maximal number of procentrioles might be dictated only by spatial constraints (Kleylein-Sohn *et al.*, 2007).

Yet, how cells control the formation of just one procentriole per parental centriole remains mysterious. It has been hypothesized that one of the required components might be limiting in the assembly process, such that the rapid outgrowth of one centriole would inhibit the formation of further progeny (Strnad & Gonczy, 2008). Although such mechanisms might indeed be in place, this hypothesis cannot solely explain that Plk4 is able to trigger the formation of multiple procentrioles when all other components are present at endogenous levels (i.e. Plk4 (activity) would be the limiting factor), while also excessive HsSas-6 can initiate this phenotype despite endogenous levels of Plk4 (i.e. HsSas-6 would be the limiting factor).

Another idea (Nigg, 2007) is based on the fact that Plk4 kinase activity at the centrosome is strictly required for the initiation of procentriole assembly (Habedanck *et al.*, 2005), suggesting that Plk4 might phosphorylate one (or more) protein(s) at the assembly site. Such a localized phosphorylation would then trigger the rapid outgrowth of one procentriole, once the cytoplasmic conditions become permissive for centriole assembly. In such a scenario, Plk4 activity is expected to be balanced by a counteracting phosphatase in order to prevent the simultaneous outgrowth of multiple centrioles (Nigg, 2007).

A recent elegant study brought up a new aspect for controlling procentriole numbers (Loncarek *et al.*, 2008). The authors overexpressed pericentrin, a large coiled-coil protein of the PCM, that itself is not involved in centriole duplication (Doxsey *et al.*, 1994), in S phase-arrested CHO cells. As a consequence, the PCM around the parental centrioles was significantly enlarged. Interestingly, this condition also resulted in the formation of numerous procentrioles within the PCM, albeit without the typical orthogonal orientation and in varying distance to the parental centrioles (Loncarek *et al.*, 2008).

Despite this encouraging progress, the molecular mechanisms underlying centriole copy number control still remain obscure. It will be of central importance to unravel Plk4's putative substrate protein(s) at the centrosome and to elucidate if/how its kinase activity is regulated in order to allow the formation of exactly one procentriole per parental centriole.

2.3.3.4. Canonical versus *de novo* centriole formation

While semi-conservative duplication of resident centrioles represents the most common pathway in somatic cells, some specialized cell types are known to assemble centrioles *de novo*. Many ciliated cells, for instance in the vertebrate respiratory tract, assemble 200-300 basal bodies, each of which nucleates a motile cilium. Predominantly, these basal bodies are formed *de novo* around fibrous granules in the cytoplasm, the so-called deuterosomes (Sorokin, 1968). However, a minor fraction of basal bodies is also formed in close vicinity to parental centrioles, and the arrangement of these forming basal bodies appears to be quite similar to procentriole arrangements formed after overexpression of Plk4 or HsSas-6 (Kleylein-Sohn *et al.*, 2007; Strnad *et al.*, 2007). Moreover, the mouse zygote (in contrast to most other mammals) does not receive a paternal centriole pair from the sperm, so that the first embryonic divisions occur acentrosomal. However, during the blastomere stage of embryonic development, each cell assembles the correct number of centrioles apparently *de novo*, and thereafter these centrioles continue to duplicate in the canonical way (Szollosi *et al.*, 1972).

These studies have led to the view that the predominant mechanism of duplication in somatic cells requires pre-existing centrioles as templates, while *de novo* formation was believed to be restricted to specialized cell types only (Beisson & Wright, 2003; Hagiwara *et al.*, 2004). Recent experiments, however, have questioned such a clear distinction between these two pathways. For instance, *de novo* centriole assembly can be induced in vertebrate cycling somatic cells if all resident centrioles are removed by microsurgery (Khodjakov *et al.*, 2002) or ablated by a focused laser microbeam (Uetake *et al.*, 2007), albeit at the expense of a loss over numerical control of newly formed centrioles. Moreover, both pathways seem to rely on common molecular requirements: If progression into S phase is blocked, the *de novo* re-formation of centrioles after ablation is prevented (Uetake *et al.*, 2007), and *de novo* centriole biogenesis has been shown to similarly require the conserved canonical module of centrosomal proteins in *Drosophila* and mammalian cells, namely Plk4, Sas-6 and Sas-4/CPAP (Peel *et al.*, 2007; Rodrigues-Martins *et al.*, 2007). It is noteworthy in this context that driving centriole overduplication by overexpression of Plk4 or HsSas-6 does not initiate the *de novo* pathway in cells with resident centrioles (Kleylein-Sohn *et al.*, 2007), although overexpression of Plk4 in unfertilized (= acentriolar) *Drosophila* eggs is sufficient to assemble large numbers of centrioles *de novo* (Rodrigues-Martins *et al.*, 2007).

As induced *de novo* assembly in somatic cells seems to escape the stringent numerical control characteristic of the canonical pathway, it will be important to clarify how even a

single centriole in the cytoplasm is able to suppress *de novo* centriole assembly (Loncarek & Khodjakov, 2009).

2.4. Proteolysis at the centrosome

2.4.1. The ubiquitin-proteasome system

Virtually all cellular processes are regulated by a complex network involving transcription, translation, posttranslational modifications and degradation of regulatory key proteins. Most regulated protein degradation is carried out by the ubiquitin-proteasome-system which is therefore crucial in the maintenance of cellular homeostasis (Hochstrasser, 1996; Hershko & Ciechanover, 1998).

Ubiquitin-dependent proteolysis occurs following the covalent attachment of a multiubiquitin chain to a specific substrate protein. Such modified proteins are then targeted to the 26S proteasome, a barrel-shaped multi-subunit protease complex that breaks down proteins in an ATP- and ubiquitin-dependent manner (Pickart & Cohen, 2004; Finley, 2009). In order for target proteins to be recognized and degraded by the 26S proteasome, the small 76 amino acid protein ubiquitin becomes activated and covalently attached to the substrate by the sequential action of three enzymes (Fig. 7), termed E1 (ubiquitin-activating enzyme), one of several E2s (ubiquitin-conjugating enzymes), and finally one of many E3s (ubiquitin-ligases) (Hershko & Ciechanover, 1998). Within this cascade, E3 ligases are by far the most diverse and complex group of enzymes (reviewed in Nakayama & Nakayama, 2006).

Ubiquitin contains a C-terminal glycine residue that is capable of forming an isopeptide bond with an acceptor lysine side chain on either the substrate protein or other ubiquitin molecules in order to generate a multiubiquitin chain. It becomes activated in an ATP-dependent reaction to form a thioester bond with a cysteine in the active site of the E1 enzyme. Once activated, the ubiquitin moiety is *trans*-esterified to a cysteine residue within the active center of an E2 enzyme, and this E2 complex in turn is incorporated into a large, multi-subunit protein complex termed E3 ligase (Fig. 7) (Hershko & Ciechanover, 1998). E3 ligases then facilitate the ubiquitination of the target protein, either by coordinating substrate and E2 enzyme to enable ubiquitin transfer, or by actively catalyzing the ubiquitin transfer themselves (Nakayama & Nakayama, 2006) (for further details on E3 ligases, see below).

2.4.2. Ubiquitin-dependent protein degradation regulates cell cycle progression

In order to maintain genetic and functional integrity, cycling cells must progress uni-directionally through the phases of the cell cycle. This is mediated by highly regulated events at each phase transition with a particular emphasis on the irreversibility of each of these transitions (Reed, 2003). In principle, this regulatory network is built of phosphorylation (mainly by Cdks and Plk1) and rapid protein degradation (especially of cyclins E, A and B). The major driving force through the initial events of late G_1, S and M phases largely derives from the activation of the broad-spectrum Cdks by an increasing concentration of their respective cyclin. In this regard, the cell has to deal with an intrinsic problem: An increasing cyclin accumulation would inevitably translate into a (slowly) increasing Cdk activity, being incompatible with a sharp and rapid phase transition (Reed, 2003). To prevent this, Cdk inhibitors keep the activity of Cdk-Cyclin complexes in check, and in most cases, these Cdk inhibitors themselves have to be inactivated via protein degradation in order to allow for a rapid cell cycle phase transition (Nakayama & Nakayama, 2005).

The best-studied example for such an inhibitory release is the protein $p27^{Kip}$. G_0/G_1 pools of Cdk2/Cyclin-E are kept inactive through the formation of the ternary complex Cdk2/Cyclin-E/p^{27Kip} (Coats *et al.*, 1996). However, at the G_1/S transition, $p27^{Kip}$ becomes degraded in an SCF^{Skp2}-dependent manner (a specific E3 ligase, see below), so that rising Cdk2/Cyclin-E activity can promote entry into S phase (Sutterluty *et al.*, 1999; Tsvetkov *et al.*, 1999; reviewed in Chu *et al.*, 2008).

Besides $p27^{Kip}$ as the major inhibitor of Cdk2 at the G_1/S transition, related proteins have been described to be additionally involved (e.g. $p21^{Cip}$, p57, and p130), and data suggest that their SCF^{Skp2}-mediated degradation is also required for proper Cdk2/Cyclin-E activation (Nakayama & Nakayama, 2005). Similarly, the G_2/M transition, which is mainly driven by Cdk1/Cyclin-B, requires controlled proteolysis under normal circumstances. Again, the forming Cdk1/Cyclin-B complexes need to be initially inhibited and then rapidly activated, resulting in a sharp and rapid G_2/M transition (Pomerening *et al.*, 2005). Cdk1/Cyclin-B activity is reversibly inhibited by phosphorylation of the glycine-rich loop (G-loop) of Cdk1/Cyclin-B through the kinases Wee1 and Myt1 (Watanabe *et al.*, 1995; Liu *et al.*, 1997; Booher *et al.*, 1997). Wee1 has subsequently been shown to be a target of the E3 ligase $SCF^{\beta TrCP}$, after phosphorylation by both Plk1 and Cdk1/Cyclin-B, which leads to Wee1 destruction and thereby to an activation of Cdk1/Cyclin-B (Watanabe *et al.*, 2004), aided by a positive feedback loop.

Although the destruction of Wee1 is required to silence the inhibitory phosphorylation of the G-loop of Cdk1/Cyclin-B, also the resident phosphorylation has to be rapidly removed. To this end, the cell activates the phosphatase Cdc25A that dephosphorylates and thereby activates Cdk1/Cyclin-B. This phosphatase itself is also a target of $SCF^{\beta TrCP}$, both in S phase (to prevent premature Cdk1/Cyclin-B activation) and after DNA damage (to halt cell cycle progression for DNA damage repair to occur) (Busino *et al.*, 2003; Jin *et al.*, 2003).

Another prominent example is the required proteolytic destruction of securin in order to liberate and activate the protease separase at anaphase onset (Ciosk *et al.*, 1998). In contrast to the aforementioned degradation of Cdk inhibitors by SCF^{Skp2} or $SCF^{\beta TrCP}$, destruction of securin is mediated by another E3 ligase, the anaphase-promoting complex/cyclosome (APC/C) in its Cdc20-bound form (Cohen-Fix *et al.*, 1996). Upon satisfaction of the spindle assembly checkpoint, the APC/C co-factor Cdc20 associates with the APC/C complex, thereby forming an E3 ligase active towards securin (reviewed in Peters, 2006; Acquaviva & Pines, 2006). Liberated separase, in turn, can then cleave the cohesin subunit Scc1 in order to promote sister chromatid separation and anaphase onset (Nasmyth, 2001).

In addition to securin degradation, the activity of Cdk1/Cyclin-B needs to be abolished upon silencing of the spindle assembly checkpoint at metaphase, in order to allow exit from mitosis and the establishment of G_1 phase. This is achieved by a concerted degradation of Cyclin-B (and similarly Cyclin-A) through APC/C^{Cdc20} and subsequently APC/C^{Cdh1}, as Cdk1 stripped off cyclins is inactive (Murray & Kirschner, 1989). Another cyclin to be timely degraded is Cyclin-E, as dysregulation of Cyclin-E turnover has been shown to induce chromosomal instability (Spruck *et al.*, 1999). Cyclin-E has been found to be degraded in an SCF^{Fbw7}-dependent manner (also known as SCF^{Cdc4}) (Koepp *et al.*, 2001; Moberg *et al.*, 2001; Strohmaier *et al.*, 2001).

These examples, albeit simplified and by no means exhaustive, impressively illustrate the importance of ubiquitin-mediated proteolysis in cell cycle progression.

2.4.3. Structure and function of the E3 ligases SCF and APC/C

In order to carry out the above described functions in the regulation of the cell cycle and the plethora of other cellular functions assigned to E3 ubiquitin ligases, an extraordinary degree of specificity and versatility has to be achieved. This is provided by the existence of 500-1000 different E3 ligases that are at present categorized into four major classes, depending on the presence of specific structural motifs: HECT-type, RING-finger-type, U-box-type, and PHD-finger-type E3 ligases (see Fig. 7) (Nakayama & Nakayama, 2006).

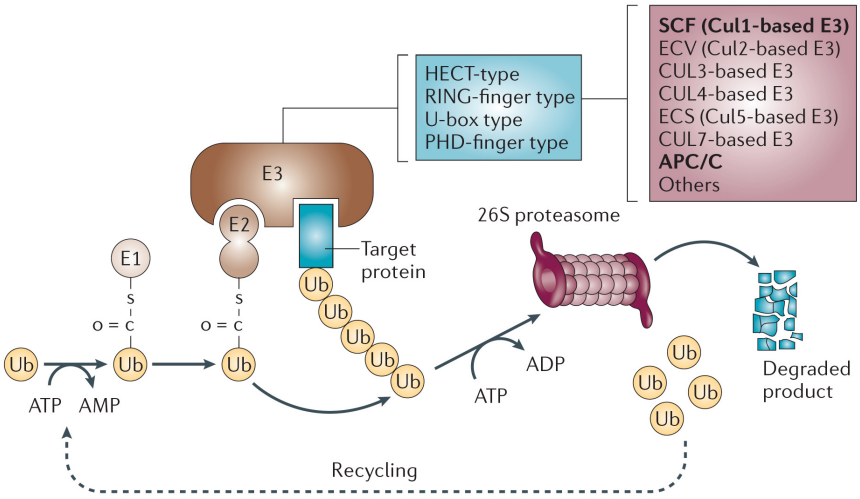

Fig. 7: Overview of the ubiquitin-proteasome-pathway. The small protein ubiquitin is activated in an ATP-dependent manner by the ubiquitin-activating enzyme (E1). From there, ubiquitin is transferred to the ubiquitin-conjugating enzyme (E2), that, in most cases, attaches the ubiquitin moiety to the target protein in a large complex, the ubiquitin ligase (E3). Subsequently, the polyubiquitinated protein is degraded by the 26S proteasome. Depicted in blue are the four major classes of E3 ligases, with the largest subfamily (Cullin-based E3s) therein shown in purple. Adapted from Nakayama & Nakayama (2006).

RING-finger-type E3 ligases comprise the largest group and are further subdivided into families, amongst them the largest subfamily of Cullin-based E3 ligases, including the aforementioned members SCF and APC/C (Fig. 7) (Nakayama & Nakayama, 2006). As a general scheme, Cullin-based E3 ligases are composed of a RING-finger protein, a scaffold protein, an adaptor protein and a receptor protein, the latter conferring most of the substrate specificity to the complex (Fig. 8a). In case of the SCF complex (Skp1-Cul1-F-box protein), the scaffolding function is provided by Cul1 that forms a core complex with Skp1 and Rbx1 (dark blue in Fig. 8b); Rbx1 itself binds the E2 conjugating enzyme with the activated ubiquitin moiety, while Skp1 bridges to the F-box/substrate complex (Fig. 8b) (reviewed in Cardozo & Pagano, 2004).

F-box proteins finally dictate substrate specificity to the SCF complex. The F-box (named after its discovery in Cyclin-F; Bai *et al.*, 1996) is usually found in the N-terminal part of the protein, while in the C-terminus, other protein-protein interaction domains can be found, the most common of which are leucin-rich repeats (LRRs) and tryptophane/aspartate (WD40) repeats (Kipreos & Pagano, 2000). Thus, the common classification distinguishes three classes of F-box proteins: FBXW with a WD40 domain; FBXL with a LLR domain, and

FBXO with either another or no further (identified) domain (Cenciarelli *et al.*, 1999; Winston *et al.*, 1999).

There is a clear conceptual difference between SCF-type and other ligases, such as APC/C, with regard to substrate recognition, namely activation of the ligase (APC/C) versus activation of the substrate (SCF) (Reed, 2003). APC/C activation is thought to occur through a concerted phosphorylation of core subunits by Cdk1/Cyclin-B and Plk1 (Golan *et al.*, 2002; Rudner & Murray, 2000), and is also regulated by the availability of its co-factors Cdh1 and Cdc20 (Kramer *et al.*, 2000). Once activated, APC/C readily recognizes a constitutive degron on its target proteins, usually either a KEN-box or a D-box (Kraft *et al.*, 2005; Glotzer *et al.*, 1991; Pfleger & Kirschner, 2000). In contrast, SCF-type ligases require the prior 'activation' of their substrate proteins, in most cases via phosphorylation of a degron motif (phosphodegron), that in turn is recognized by the substrate-binding domain of the F-box protein (Skowyra *et al.*, 1997). Such a mechanism allows a versatile regulation of substrate degradation, as the required phosphorylation itself might be subject to complex temporal and spatial regulation.

The three best-studied human F-box proteins, βTrCP, Skp2 and FBW7 (Cdc4), catalyze the degradation of various key proteins in cell cycle regulation, as already outlined above (see Fig. 8a). The βTrCP family is highly conserved, including *Drosophila* Slimb (Jiang & Struhl, 1998) and *Xenopus* βTrCP (Spevak *et al.*, 1993). Prominent targets of βTrCP-mediated degradation include Emi1/2 (Erp1), Wee1, and Cdc25A/B, as well as the signaling cascade components β-catenin and IκBα (reviewed in Frescas & Pagano, 2008). It is therefore not surprising that βTrCP has been implicated in cancer biogenesis owing to deregulated proteolysis of its substrates (Frescas & Pagano, 2008).

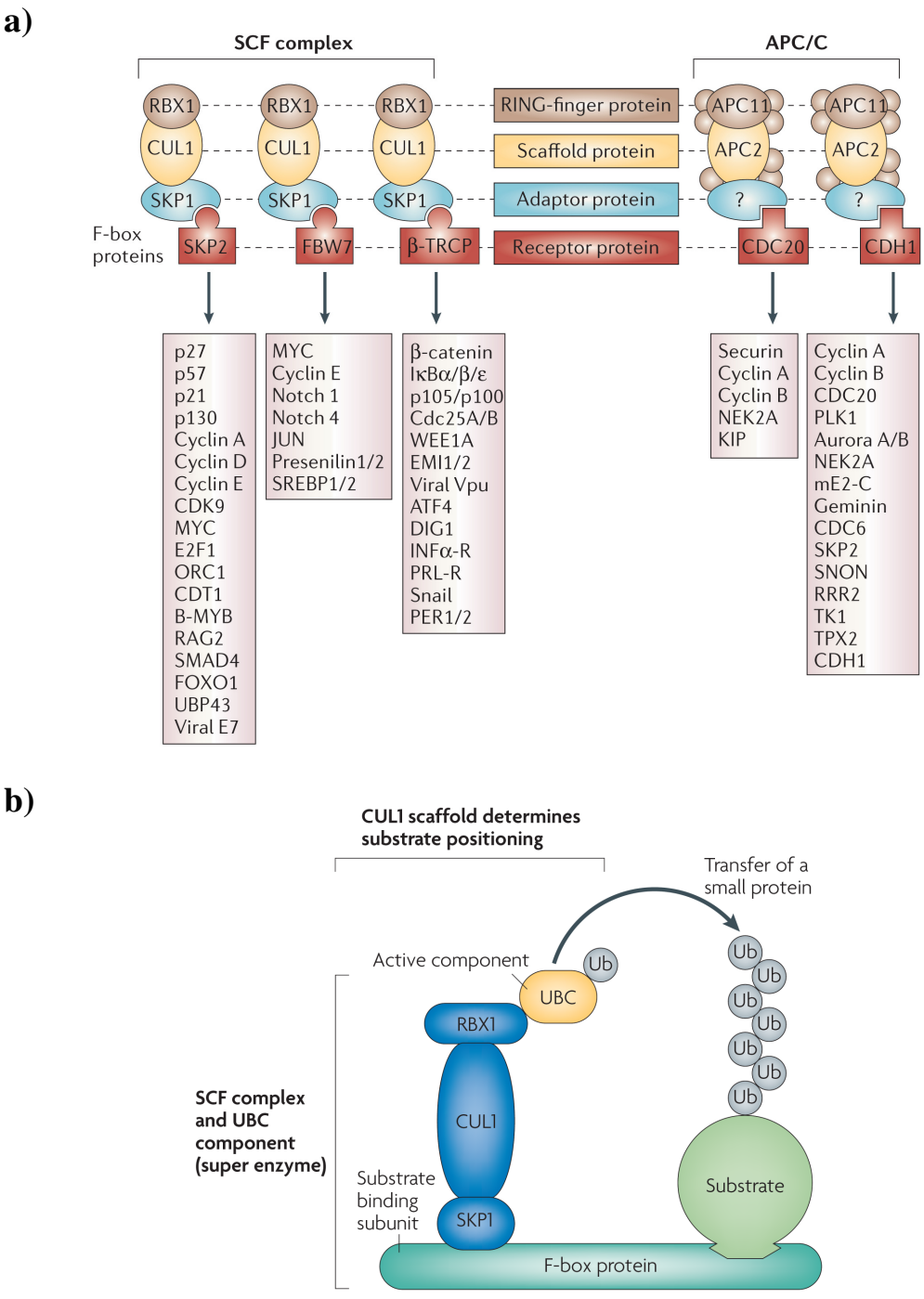

Fig. 8: Detailed schematic of the structure of SCF and APC/C E3 ligases. **(a)** Both SCF and APC/C E3 ligases are composed in a similar manner, with an invariable core of RING-finger-, scaffold- and adaptor proteins, and a more variable receptor protein that confers substrate specificity to the complex. Known targets in the context of cell cycle progression are listed underneath each complex. Adapted from Nakayama & Nakayama (2006). **(b)** Detailed view of an SCF E3 ligase in complex with a substrate protein. The core module (dark blue) brings E2 and substrate protein into close vicinity for the ubiquitination to occur. Adapted from Frescas & Pagano (2008).

2.4.4. Proteolysis at the centrosome

A growing body of evidence suggested SCF-dependent proteolysis to be important for faithful centriole duplication (Freed *et al.*, 1999; Wojcik *et al.*, 2000; Murphy, 2003; Guardavaccaro *et al.*, 2003; Duensing *et al.*, 2007; Piva *et al.*, 2002; Gstaiger *et al.*, 1999; Nakayama *et al.*, 2000). Components of the SCF complex have first been detected at the centrosome of mammalian cells (Freed *et al.*, 1999; Gstaiger *et al.*, 1999). Antibodies to Skp1 as well as to Cul1 stained centrosomes in all phases of the cell cycle, with an increasing recruitment of Skp1 to the mitotic spindle pole. Localization of these SCF components was neither dependent on MT, nor did it require cell cycle progression, as newly formed centrioles in S phase-arrested CHO cells also stained positive for Skp1 (Freed *et al.*, 1999). Moreover, immunoelectron microscopy determined the majority of Skp1 to localize to the PCM, while a minor fraction was also found to be centriolar, presumably at the appendages. Functional studies, according to the experimental system established by Lacey *et al.* (1999), suggested a requirement for Skp1, Cul1 and the proteasome in the initial disorientation of G_2 centrioles that normally precedes the initiation of centriole duplication. Due to this observation, the authors proposed a requirement of SCF-dependent proteolysis for the centriole duplication process (Freed *et al.*, 1999).

Another study identified the F-box protein Slimb (supernumerary limbs) as a negative regulator of centriole duplication in *Drosophila* (Wojcik *et al.*, 2000). Slimb has originally been identified as a regulator of hedgehog signaling in *Drosophila* (Jiang & Struhl, 1998; Theodosiou *et al.*, 1998), and is the homologue of the human F-box protein βTrCP. Slimb mutant flies were found to contain multiple (2-17) centrosomes in diploid neuroblasts, suggesting that division failures, often responsible for supernumerary centrosomes (Nigg, 2002), cannont account for this phenotype. Furthermore, the distribution of the typical centrosomal marker proteins centrosomin (CNN), ASP and CP190 together with an overall intact centrosome morphology led the authors to conclude that Slimb deletion might foster centrosome amplification via the initiation of repeated rounds of centrosome re-duplication (Wojcik *et al.*, 2000). Similarly, the SCF-component SkpA in *Drosophila* (Skp1 in mammals) has been implicated in centrosome duplication, as SkpA mutant flies also show supernumerary centrosomes in a large proportion of diploid neuroblasts (Murphy, 2003). Moreover, the author demonstrated that the centrosome amplification phenotype is independent of Cyclin-E accumulation, which is characteristic of SkpA-deficient cells, and that the extra centrosomes function as nucleation-competent MTOCs during spindle formation (Murphy, 2003).

The analysis of βTrCP$^{-/-}$ null mutant mice revealed a surprisingly mild phenotypic manifestation (Guardavaccaro *et al.*, 2003). However, detailed analysis showed approximately half of the males to be sterile, as a consequence of severely impaired spermatogenesis. Interestingly, FACS analysis of βTrCP$^{-/-}$ MEFs revealed normal progression at G_1/S transition and subsequently through S and G_2 phase, but a prolonged M phase thereafter. This effect is presumably owing to delayed APC/C activation through the persistence of the APC/C inhibitor Emi1, in turn leading to a delay in cyclin-A and -B degradation and thus to a delayed exit from mitosis. Strikingly, 20% of βTrCP$^{-/-}$ MEFs contained supernumerary centrosomes and 10% of cells were found to form multipolar spindles (Guardavaccaro *et al.*, 2003).

Studies on human osteosarcoma cells (U2OS) provided the first insight into the mechanism of how multiple centrosomes might arise in cells deficient for properly regulated protein degradation (Duensing *et al.*, 2007). Cells treated with the proteasome inhibitor Z-L_3VS were shown to contain rosette-like arrangements of procentrioles around parental centrioles, a distinct phenotype reminiscent of that seen after overexpression of either Plk4 (Habedanck *et al.*, 2005) or HsSas-6 (Strnad *et al.*, 2007). As the induction of this *bona fide* centriole overduplication was – expectedly – dependent on Plk4 (see next chapter), this study lent support to the idea that the previously identified SCF-dependent centrosome amplification phenotypes might arise directly from a misregulated centriole biogenesis pathway rather than indirectly from defects in cell cycle progression (Duensing *et al.*, 2007).

Finally, two very recent studies in *Drosophila* deliver an elegant explanation for the above-described phenotypes (Cunha-Ferreira *et al.*, 2009b; Rogers *et al.*, 2009). Slimb mutant flies – known to display supernumerary centrosomes (Wojcik *et al.*, 2000) – were investigated for their mechanism of centriole overduplication by immunoelectron microscopy. Both groups identified rosette-like procentriole arrangements around parental centrioles, the phenotype that had been extensively described previously (Kleylein-Sohn *et al.*, 2007). Consequently, both groups found the levels of endogenous (Cunha-Ferreira *et al.*, 2009b) or overexpressed (Rogers *et al.*, 2009) Plk4 to be elevated in Slimb mutant cells, indicative of defective Plk4 degradation. Moreover, the authors established a direct biochemical interaction between Slimb and Plk4, as was predicted for a direct effect on Plk4 (Cunha-Ferreira *et al.*, 2009b; Rogers *et al.*, 2009). This work for the first time described how – in *Drosophila* – cells prevent excess Plk4 activity. However, important questions remain to be answered in this context. For instance, as Slimb-mediated degradation of Plk4 requires the conserved **DSG**III**T** degron to be doubly phosphorylated, the identity of the kinase(s) responsible remains to be

elucidated; this might lead to the identification of signaling pathways that regulate centrosome duplication. Furthermore, the timing of degradation is still unknown. It will be important to learn whether continuous degradation of Plk4 is required or whether rapid proteolysis at a defined stage in the cell cycle is necessary to prevent excessive centriole formation. And finally, research in vertebrates will have to prove that this mechanism of regulation has been conserved in evolution.

2.5. Plk4 – the most divergent member of the family of Polo-like kinases

Mouse Plk4 was first identified in a screen to search for proteins regulating sialylation in mammalian cells using a murine cDNA library (Fode *et al.*, 1994). The cDNA of the human homologue was separately isolated by a PCR-based search for novel kinases involved in cancer development (Karn *et al.*, 1997). In both cases, primary sequence analysis revealed that Plk4 is the structurally most divergent member of the polo-like kinase family. However, neither of these studies provided any insights into the function of this kinase. The *plk4* gene is located on chromosome 4 in humans and on chromosome 3 in mice (Hammond *et al.*, 1999; Swallow *et al.*, 2005), and the chromosomal region 4q28 has been implicated in frequent rearrangements and loss in human tumor cells, particularly in hepatocellular carcinomas (Hammond *et al.*, 1999).

Like in the other polo-like kinase family members, the kinase domain of Plk4 is found in the N-terminus, spanning residues 12 to 265. It is most closely related to those of other Plk-family members, in particular to Plk2 (Fode *et al.*, 1994), and shares common ancestry with other serine/threonine kinases. However, the catalytic center in subdomain VI-B (according to Hanks & Quinn, 1991) differs significantly from other serine/threonine kinases. Within this subdomain, threonine^{138} in the sequence ^{134}HRDLTLS^{140} is found in a position normally occupied by a lysine in the vast majority of serine/threonine kinases, including all other members of the polo family, and tyrosine kinases carry an alanine (A; receptor tyrosine kinases) or an arginine (R; soluble tyrosine kinases) instead. Hence, this residue is considered a key residue in discriminating genuine serine/threonine from tyrosine kinases (Hanks *et al.*, 1988; Lindberg *et al.*, 1992). Mutation of this lysine in serine/threonine kinases severely diminishes kinase activity (Taylor *et al.*, 1993).

The kinase domain of Plk4 is followed by an extensive C-terminal region of >500 amino acids and a single polo box at the very C-terminal end. The Plk4 polo box is equally related to both polo boxes 1 and 2 of Plk1 (Fode *et al.*, 1994) and, together with the loosely defined cryptic polo box, was described to act as a dimerization domain (Leung *et al.*, 2002;

Habedanck, 2006). It exists as an intermolecular homodimer when crystallized (Leung *et al.*, 2002), while the Plk1 polo boxes 1 and 2 dimerize intramolecularly to form the phosphopeptide binding polo box domain (PBD) (Elia *et al.*, 2003; Cheng *et al.*, 2003). This difference affects the positioning of certain residues, such that the Plk4 polo box dimer structure contains internal amino acids that are located externally on the Plk1 polo box fold. Furthermore, the typical PBD cleft formed by Plk4 lacks a clear positive charge on the surface, and residues directly responsible for the phosphopeptide binding function of the Plk1 PBD are not conserved in the Plk4 primary sequence, suggesting that this functionality might also not be conserved; in fact, no phosphopeptides have been identified to date that would bind to the Plk4 polo box.

Three putative PEST motifs have been identified in Plk4, with one being located close to the kinase domain and the other two further downstream near the polo box (Yamashita *et al.*, 2001). PEST motifs are sequences rich in proline (P), glutamic acid (E), serine (S) and threonine (T) residues that are thought to be responsible for the proteolytic degradation of short-lived proteins (Rogers *et al.*, 1986). Indeed, Plk4 has been reported to have a short half-life of approximately 2-3 h (Fode *et al.*, 1996), and deletion of these sequences was reported to result in increased stability of the corresponding overexpressed Plk4 mutant (Yamashita *et al.*, 2001); furthermore, the involvement of ubiquitination and the anaphase-promoting complex (APC/C) in regulating ectopic Plk4 had been reported early on (Fode *et al.*, 1996), similar in this regard to Plk1 (Lindon & Pines, 2004). However, as discussed above, recent work in *Drosophila* revealed that Plk4 becomes degraded in an SCF^{Slimb}-dependent manner, with Slimb binding to a highly conserved DSGxxT motif downstream of the C-terminal kinase domain (Rogers *et al.*, 2009; Cunha-Ferreira *et al.*, 2009a).

Reports on *plk4* expression indicate that this kinase is cell-cycle regulated at the transcript level in patterns comparable to other Plk family members (Fode *et al.*, 1996). Studies using cultured cells and Northern blot analysis revealed that Plk4 mRNA levels are low in quiescent cells and in early G_1 (Fode *et al.*, 1996), increase from late G_1 to S and G_2, and reach a plateau in M phase. Likewise, when mice were subjected to partial hepatectomy, Plk4 transcripts in regenerating liver tissue increase from late G_1 to S phase, reaching their highest level during G_2/M (Ko *et al.*, 2005). Furthermore, a study on the levels of Plk4 in samples of colorectal cancer (Macmillan *et al.*, 2001) revealed elevated transcript levels in tumor tissue when compared to adjacent normal intestinal cells.

Hints as to the importance of Plk4 in cell proliferation have been gained from mouse knockout experiments (Hudson *et al.*, 2001; Ko *et al.*, 2005). $Plk4^{-/-}$ mouse embryos arrest

shortly after gastrulation, with an increase in mitotic cells containing partially segregated chromosomes. Explants from these embryos also arrested in anaphase and telophase after a few cell divisions, with a concomitant 20-fold increase in apoptotic cells and, consequently, the cellular phenotype of these embryos was described as a late mitotic delay (Hudson *et al.*, 2001). The lethality of Plk4 deficiency revealed that Plk4 is essential to the development of a complete organism, and stands in stark contrast to the viability of $Plk2^{-/-}$ mice (Ma *et al.*, 2003). Analysis of $Plk4^{+/-}$ mice has further revealed a potential role for Plk4 in tumorigenesis (Ko *et al.*, 2005). These mice grew normally to adulthood, but developed tumors over time, most notably in lung and liver tissue. When $Plk4^{+/-}$ mice were subjected to a partial hepatectomy to stimulate growth of tissue, increased numbers of liver cells with aberrant multipolar spindles were observed. Regenerating liver tissue showed altered regulation of cyclins D, E and B and reduced levels of p53 and $p21^{Cip}$, suggesting that cells are subject to a cell cycle delay. In particular, levels of cyclin-B were reduced and extended during prolonged mitosis. Similarly, $Plk4^{+/-}$ MEFs displayed increased numbers of centrosomes, abnormal spindles as well as slower growth. Taken together, these data suggest that Plk4 haploinsufficiency results in abnormal mitotic progression and carcinogenesis.

3. Aims of this thesis

Work from our lab and others has demonstrated that Plk4 is pivotal to the process of centriole duplication. However, despite 15 years of research on this kinase, its precise mode of action at the centrosome still remains incompletely understood. In particular, no physiological substrate has been identified to date, and the regulation of Plk4 kinase activity remains largely unknown. Thus, the aim of this thesis was to identify positive as well as negative regulatory input into Plk4 by upstream signaling pathways in the context of centriole biogenesis.

4. Results

The results of this thesis are grouped into three parts. First, I briefly describe the major tools that I generated in order to address the fundamental question of how Plk4 itself is regulated at the centrosome. Second, I explore if Plk4 is regulated by post-translational modifications (i.e. phosphorylation), as commonly found for many protein kinases. And third, I investigate whether Plk4 activity might be regulated by targeted proteolysis via the human F-box protein βTrCP.

4.1. Generation and characterization of stably transfected U2OS cells

Human Plk4 and its homologues in other species are extremely low abundant enzymes. Despite intensive research, there is currently no antibody available that allows for the detection of the endogenous protein on Western blots, and immunoprecipitations (IPs) have never yielded sufficient amounts of endogenous protein for a thorough and reproducible analysis of posttranslational modifications via mass spectrometry. For this reason, we generated transgenic U2OS cell lines that stably harbor the cDNA of human myc-tagged Plk4 under control of a tetracyclin-inducible CMV promoter.

4.1.1. Generation of stable cell lines

We transfected early-passage U2OS TRex cells (Invitrogen) with either myc-Plk4 wildtype kinase ($Plk4^{WT}$) or the catalytically inactive (kinase-dead) mutant D154A ($Plk4^{D154A}$) (Habedanck *et al.*, 2005). After two weeks of antibiotic selection with geneticin, growing colonies were seperately picked and subsequently examined for their myc-Plk4 expression before and after addition of tetracyclin. Based on minimal basal expression without addition of tetracyclin ('leakiness') and moderate expression after tetracyclin-induction, the clones B6 ($Plk4^{WT}$) and D2 ($Plk4^{D154A}$) were chosen for further analysis.

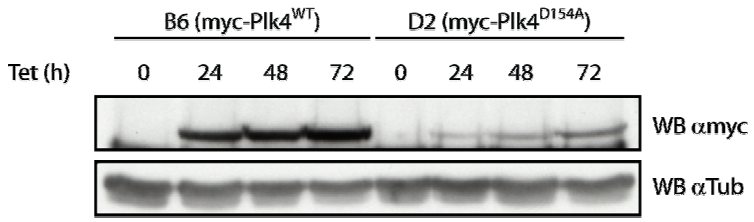

Fig. 9: Stable clones U2OS-TRex B6 and D2 express the myc-tagged protein after addition of tetracyclin. Cells of each clone were grown in the presence of the selection antibiotic geneticin and induced with 1 µg/ml tetracyclin for the indicated times. Cells were lysed and 60 µg of total protein were loaded onto each lane. Presence of myc-Plk4 was probed with αmyc-antibody, equal loading was verified by probing the blot for alpha-tubulin.

As shown in Fig. 9, the tagged protein could be detected after 24 h of induction and accumulated over the next 48 h. While immunofluorescence (IF) microscopy staining against the myc tag revealed that in case of the B6 clone, virtually all cells expressed $Plk4^{WT}$ after induction, only <30% of cells in the D2 population expressed $Plk4^{D154A}$ (not shown), accounting for the differences in protein levels seen in Fig. 9.

4.1.2. Procentriole formation in clones B6 and D2

As excess Plk4 has been shown to promote overduplication of centrioles, B6 or D2 cells were stained with antibodies against the myc tag and the centrosomal protein CP110, an early distal marker of centrioles (Kleylein-Sohn *et al*., 2007), respectively. In contrast to proximal marker proteins, distal CP110 staining allows for the detection of engaged procentrioles early in the centriole biogenesis pathway. After 16 h of induction in an aphidicolin-induced S-phase arrest, about 80% of B6 ($Plk4^{WT}$) cells contained two myc-Plk4-positive dots that were surrounded by either a halo- or a rosette-like staining using the antibody against CP110 (Fig. 10 and Fig. 11b). Extensive subsequent analysis by high-resolution IF and immuno-electron microscopy could show these arrangements to be composed of two central mature centrioles engaged with multiple procentrioles in a configuration resembling petals on a flower (Kleylein-Sohn *et al*., 2007), as had been suggested earlier (Habedanck *et al*., 2005).

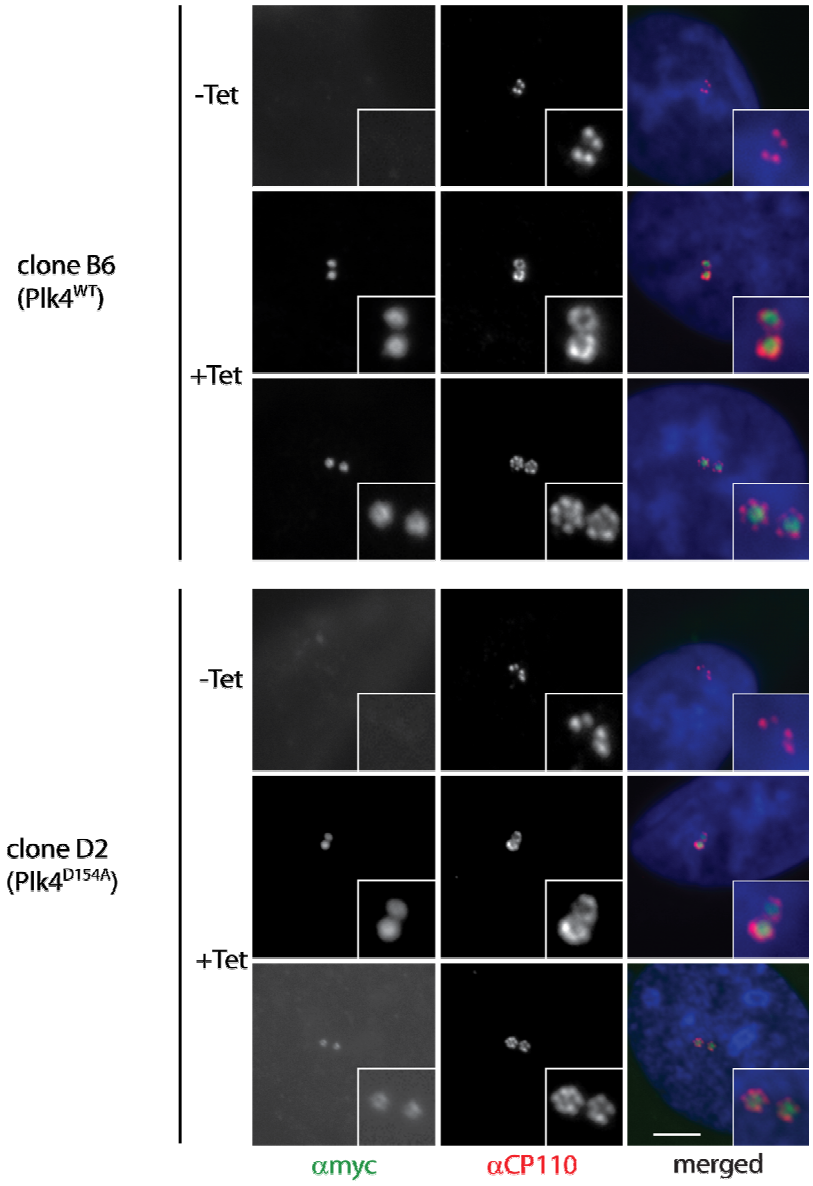

Fig. 10: Induction of both myc-Plk4^{WT} and myc-Plk4^{D154A} causes centriole overduplication. Clones B6 and D2 were arrested in S phase with aphidicolin for 24 h prior to induction with 1 µg/ml tetracyclin for 16 h. Cells were stained with antibodies against the myc tag (green) and CP110 (red) in order to visualize engaged centriole/procentriole arrangements in induced cells. Bar = 5 µm.

In transient overexpression experiments with Plk4, Habedanck and colleagues could show that the evoked centriole overduplication is dependent on Plk4 kinase activity. While the wildtype kinase readily caused overduplication in about 80% of transfected cells, kinase-dead Plk4^{D154A} did so in only 30%, yet significantly above background (<10%) (Habedanck *et al.*, 2005); as this effect could be suppressed by preventing cell cycle progression, the authors hypothesized that Plk4^{D154A} induces supernumerary centrosomes by causing occasional cell division failures. However, to our surprise, we found about 75% of induced cells in the D2 cell line (expressing kinase-dead Plk4^{D154A}) to contain engaged, rosette-like procentriole

arrangements, equal to the B6 cells (Fig. 10). This result was unexpected and could not be explained by the above-mentioned hypothesis.

4.1.3. Plk4^{D154A} cannot rescue the depletion of endogenous Plk4

Since RT-PCR confirmed that indeed the D154A mutation was present in the induced construct (not shown), we decided to perform rescue experiments in order to clarify whether kinase activity is necessary for Plk4-mediated centriole overduplication.

B6 and D2 cells were depleted for 24 h with siRNA duplexes directed against Plk4 (complementary to the 3' untranslated region [3'UTR], so only targeting the endogenous mRNA), HsSas6 as a positive control (Leidel *et al*., 2005), and firefly luciferase (GL2) as a negative control (Elbashir *et al*., 2001). Depleted cells were then arrested in S phase by the DNA polymerase α/δ inhibitor aphidicolin for 8 h, before cells were induced for Plk4^{WT} or Plk4^{D154A} expression, respectively, for 16 h in the continued presence of aphidicolin. Finally, cells were fixed and stained for myc-Plk4 and the distal marker CP110 in order to score induced cells with a halo- or rosette-like procentriole configuration.

As summarized in Fig. 11, both wildtype and kinase-dead Plk4 readily evoked the characteristic centriole overduplication phenotype in the GL2 control. However, while the induced wildtype kinase still caused the same extent of rosette formation in cells depleted for the endogenous protein, kinase-dead Plk4^{D154A} was unable to induce overduplication. And finally, irrespective of Plk4 kinase activity, neither construct was able to induce rosette formation in cells depleted for the protein hSas6, which is an essential key player in the centriole biogenesis pathway downstream of Plk4 (Kleylein-Sohn *et al.,* 2007). Taken together, these data suggest that kinase-dead Plk4^{D154A} is unable to cause centriole overduplication in cells lacking the endogenous kinase. Although the exact molecular mechanism accounting for this effect remains to be clarified, we will discuss a potential explanation in the context of βTrCP-mediated Plk4 degradation later on (see 5.3).

a)

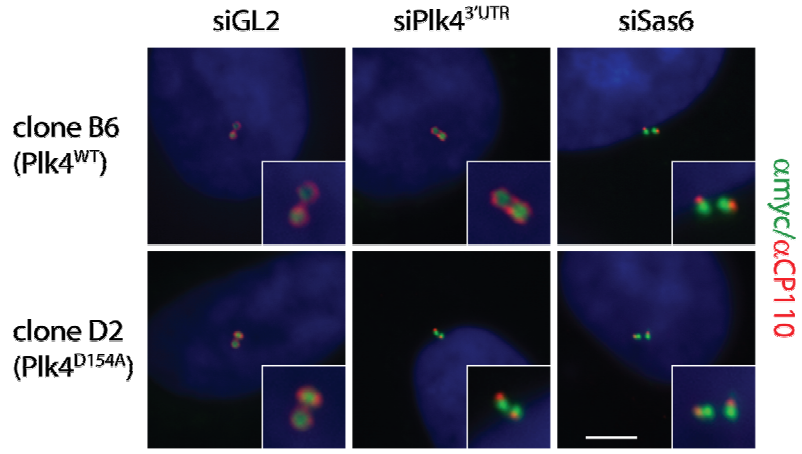

b)

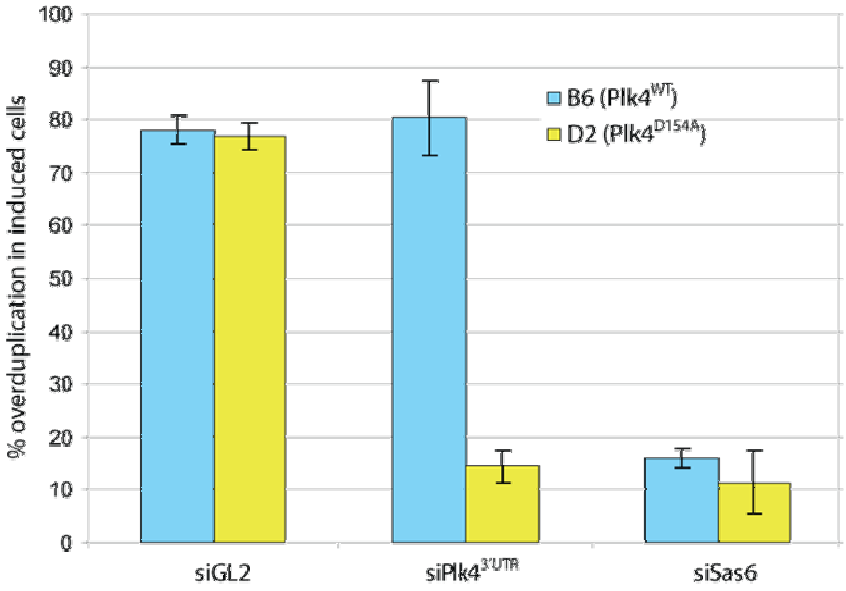

Fig. 11: Plk4^{D154A} cannot rescue the depletion of the endogenous kinase. **(a)** Clones B6 and D2 were transfected for 24 h with siRNA duplexes targeting endogenous Plk4, hSas6 as positive and firefly luciferase (GL2) as negative control. Cells were then arrested in S phase by aphidicolin for 8 h prior to 16 h of induction of protein expression with tetracyclin. IF staining with antibodies against the myc tag (green) and CP110 (red) reveals engaged centrioles in induced cells. Bar = 5 µm. **(b)** Histogram showing the percentage of induced cells containing rosette-like procentriole arrangements. Results are from three independent experiments counting 100 cells for each condition; error bars denote standard deviations.

4.2. Regulation of Plk4 via phosphorylation

As kinases are predominantly regulated via phosphorylation (Newton, 2003; Nolen *et al.*, 2004), we set out to identify phosphorylated residues within Plk4 by means of mass spectrometric (MS) analyses. Subsequent mutational studies were performed to investigate the influence of each posttranslational modification on the known properties of Plk4 – subcellular localization, kinase activity, homodimerization, and its propensity to promote centrosome overduplication.

4.2.1. Identification of phosphorylated residues on Plk4

4.2.1.1. Identification of phosphorylation sites on overexpressed Plk4

In order to identify phosphorylated residues on Plk4, we immunoprecipitated overexpressed myc-tagged Plk4 from human cells (transient overexpression in 293T cells and induced expression in the B6 cell line) that were either growing asynchronously, arrested in S phase by a double thymidine block or arrested in prometaphase by a nocodazole block. Immunoprecipitates were then separated by SDS-PAGE and stained with Coomassie Blue. The band representing myc-Plk4 was excised from the gels and subjected to protease digestion with either trypsin or elastase, respectively. Fig. 12a shows a representative Coomassie Blue staining of immunoprecipitated full-length myc-Plk4.

4.2.1.2. Identification of phosphorylation sites in the recombinant kinase

In parallel, bacterially expressed Plk4 was analyzed. As the full-length protein was completely insoluble as a GST- or 6xHis-tagged fusion protein, we generated various C-terminal truncations fused to GST in order to yield sufficient amounts of recombinant protein. The following fragments all contain the kinase domain plus varying C-terminal extensions:

aa 1-430: This fragment represents an extended form of the kinase domain (aa 1-265), encompassing all of the highly homologous sequences further downstream (i.e. N-terminal of the highly variable linker region of Plk4 (Habedanck, 2006)).

aa 1-608: This fragment lacks the C-terminal polobox including the 'cryptic polobox' (Leung *et al.*, 2002) of human Plk4, which, based on secondary structure prediction algorithms (PsiPred server, www.expasy.ch; McGuffin *et al.*, 2001), encompasses aa 609-970.

aa 1-889: Our attempt at purifying GST-fusions of Plk4 revealed that deleting the very C-terminal single polobox (aa 890-970) was sufficient to yield a soluble GST-fusion protein.

These truncations were affinity purified, allowed to autophosphorylate *in vitro* in presence of ATP, and finally separated by SDS-PAGE as described above (Fig. 12b). Prior to mass spectrometry analysis, phosphorylated peptides were enriched via metal ion affinity chromatography on TiO_2 columns.

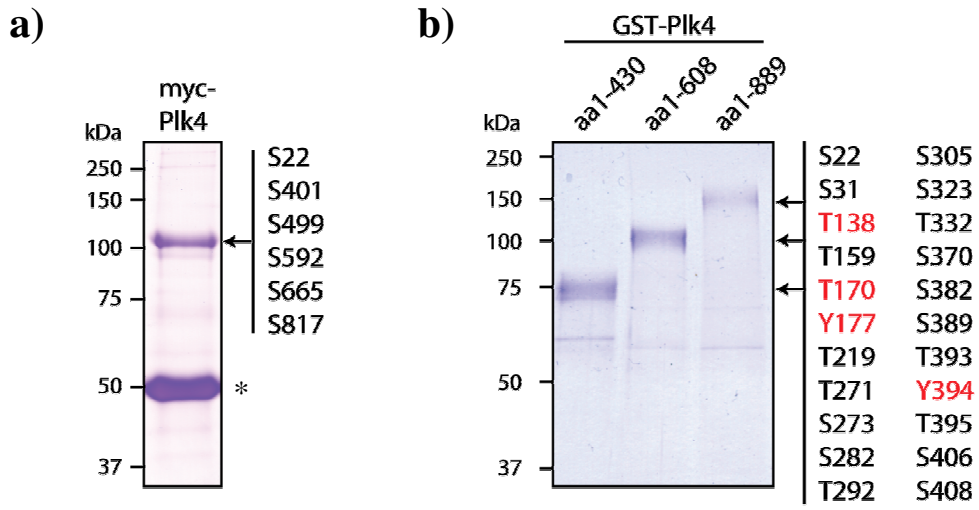

Fig. 12: Representative experiments for mass spectrometric analysis of Plk4 phosphorylation. **(a)** myc-Plk4 was immunoprecipitated from asynchronously growing 293T cells and separated via SDS-PAGE. The band containing myc-Plk4 was excised and digested with trypsin or elastase, before phosphorylated peptides were enriched on TiO_2 metal ion affinity columns. Subsequently identified phosphorylation sites are depicted next to the gel. *immunoglobulin heavy chain. **(b)** GST-Plk4 fusion proteins of different lengths were purified from *E. coli*, allowed to autophosphorylate *in vitro* and subsequently analyzed as described above. Identified sites are listed on the right, with sites chosen for further analysis (see below) depicted in red.

While only a limited set of phosphorylation sites could be repeatedly identified on the immunoprecipitated protein (see below), the bacterially expressed C-terminal truncations of Plk4 were phosphorylated to a surprisingly high extent (Fig. 12).

4.2.2. Analysis of phosphorylation sites from the recombinant kinase

4.2.2.1. Tyrosine phosphorylation

With tyrosines Y177 and Y394, not only serines and threonines were identified among the phosphorylated residues. As tyrosine phosphorylation does not occur in bacteria, these residues must reflect Plk4 autophosphorylation, identifying Plk4 as dual specificity kinase, at least *in vitro*.

To investigate this aspect in more detail, we subjected the above-shown truncations, this time including aa 1-430 in its kinase-inactive form (D154A), together with hMPS1 and Plk1 for comparison, to an *in vitro* kinase assay in presence of (γ-^{32}P)ATP.

Autophosphorylation activity was monitored via autoradiography; in parallel, $^{1}/_{10}$ of the reaction mixture was immunoblotted with an antibody specific for the phosphorylated form of tyrosines (4G10). As seen in Fig. 13a, all active Plk4 fusions were strongly phosphorylated on tyrosines, as expected from the previous MS analysis. In contrast, Plk4^{D154A} showed no reactivity to this antibody, clearly demonstrating that phosphorylated tyrosines were generated by Plk4 autophosphorylation. Mutational analyses of recombinant Plk4 aa 1-265 revealed that within this fragment, Y177 is the only phosphorylated tyrosine, as Plk4^{Y177F} – although it retained autophosphorylation activity – does not show any signal with the 4G10 antibody (Fig. 14, lower panel). We also noted that despite substantial tyrosine autophosphorylation, no substrate tyrosine phosphorylation was detected when using Cep135 as an exogenous substrate. It should be pointed out that hMPS1 kinase reacted weakly with the 4G10 antibody, although it had been shown previously that hMPS1 is a dual specificity kinase *in vitro* (Mills *et al.*, 1992). Plk1, in contrast, did not display any tyrosine phosphorylation.

In stark contrast to the above results, myc-Plk4 immunoprecipitated from asynchronously growing 293T cells did not display detectable tyrosine phosphorylation (Fig. 13b), questioning the prediction that endogenous Plk4 acts as a dual specificity kinase *in vivo*.

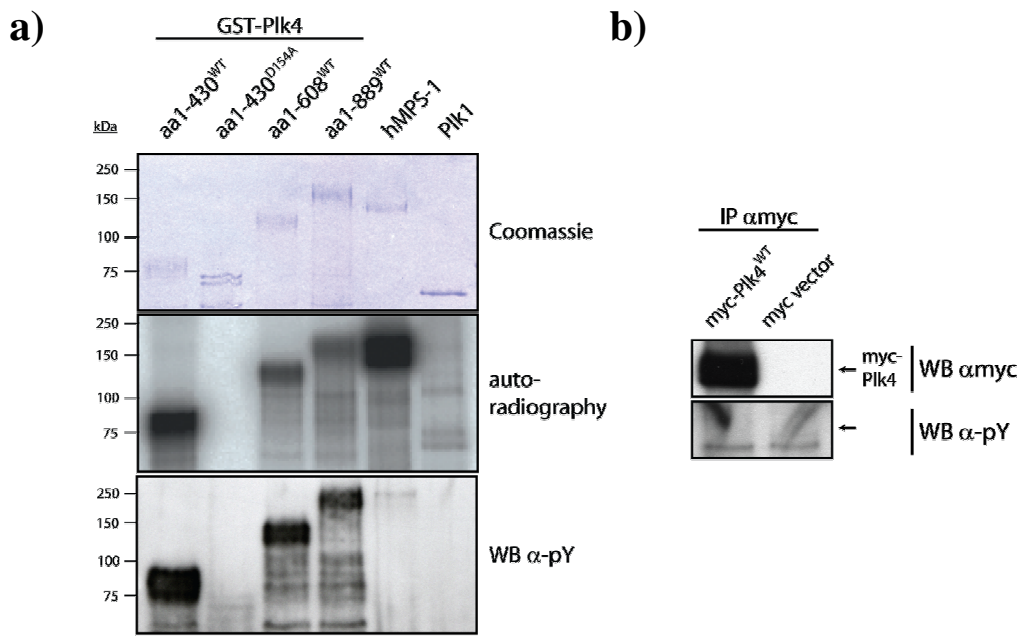

Fig. 13: Plk4 autophosphorylates on tyrosines *in vitro* but not *in vivo*. **(a)** Recombinant GST-Plk4 fusion constructs, GST-hMPS1 and His-Plk1 were allowed to autophosphorylate *in vitro* in the presence of (γ-^{32}P)ATP. The reaction mixtures were separated by SDS-PAGE, stained with Coomassie Blue, dried and exposed to film. $^{1}/_{10}$ of the reaction mixture was immunoblotted with α-phospho-tyrosine antibody (4G10) to visualize tyrosine autophosphorylation. Kinase-dead Plk4^{D154A} (aa 1-430) serves as negative control. See also Fig. 14 for further details. **(b)** Myc-Plk4 was immunoprecipitated from asynchronously growing 293T cells and probed for phosphorylated tyrosines (lower panel). pY, phosphotyrosine.

4.2.2.2. Mutational analyses of identified residues within the kinase domain

The following list summarizes the major properties of the phosphorylation sites chosen for mutational analyses, based on homology to well-defined sites of other protein kinases.

T138: This residue lies in the catalytic center of Plk4's kinase domain, close to the catalytic base aspartate[136] (D136). Virtually all serine/threonine kinases carry an invariant lysine (K) at this position (including Plks 1-3), while tyrosine kinases carry an alanine (A; receptor tyrosine kinases) or an arginine (R; cytoplasmic tyrosine kinases) instead. Hence, this residue is considered a key residue in discriminating genuine serine/threonine from tyrosine kinases (Hanks *et al.*, 1988; Lindberg *et al.*, 1992). Mutation of this lysine in serine/threonine kinases severely diminishes kinase activity (Taylor *et al.*, 1993). Interestingly, the atypical feature of Plk4 (in contrast to Plks 1-3) of carrying a phosphorylatable threonine at this position is conserved in all Plk4s examined and can even be found in the kinase ZYG-1 in *C. elegans*, which is only considered a *functional* homologue of Plk4, due to a lack of significant sequence homology and due to the lack of a detectable polobox.

T170: Based on homology to Plk1 threonine^{210}, this residue is expected to be the main phosphate acceptor in the activaton loop of Plk4. Phosphorylation of T210 in the activation loop increases Plk1 activity and is thought, by analogy to other protein kinases, to result in stabilization of the activation loop in a conformation in which important active site residues are properly positioned for substrate binding and catalytic activity (Nolen *et al.*, 2004).

Y177: Tyrosine^{177} is – in addition to T170 – another residue in the activation loop (i.e. N-terminal of the highly conserved APE motif of protein kinases) found to be phosphorylated. For the group of mitogen activated protein kinases (MAPKs), it is well established that a double phosphorylation of a threonine and tyrosine (TXY motif) within their activation loop is required for full activity; hence, the upstream activators of these kinases belong to the growing class of kinases with a proven dual specificity *in vivo* (Dhanasekaran & Premkumar Reddy, 1998).

We mutated the above-listed residues to either alanine or aspartate (or phenylalanine and glutamate), in order to generate non-phosphorylatable or phosphomimetic mutants, respectively. The mutated, GST-fused kinase domains were purified from bacteria and subjected to an *in vitro* kinase assay in presence of (γ-^{32}P)ATP. As an exogenous substrate, we used GST-Cep135 aa 648-1145 that had been purified in two steps, with the second involving a denaturing gel purification (whether or not Cep135 is also a *bona fide* Plk4 substrate *in vivo* was not further addressed in the context of this thesis, but will be of considerable interest in the future).

As shown in Fig. 14, the wildtype kinase domain phosphorylated itself as well as the substrate Cep135, albeit showing a less prominent retarded mobility compared to larger wildtype truncations (compare to Fig. 13). In contrast, the D154A mutant appeared completely inactive. Surprisingly, the T170V unphosphorylatable mutant appeared to be active, while its supposedly phosphomimetic counterpart T170D displayed no enhanced activity. This finding suggests that Plk4 might not be activated in analogy to Plk1, going in line with the notion that phosphorylated T170 has never been detected on the immunoprecipitated protein (see below).

Mutating the residue Y177 in the activation loop to phenylalanine (F) slightly enhanced kinase activity, while the phosphomimetic glutamate (E) mutation rendered the kinase domain completely inactive. The phosphotyrosine Western blot clearly demonstrates that within aa 1-265 this tyrosine is the only one to be phosphorylated, as all active mutants except for Y177F react with the α-phosphotyrosine antibody. Together with the finding that

on the immunoprecipitated kinase from 293T cells, no phosphotyrosine could be detected (Fig. 13b), it therefore appears questionable whether tyrosine autophosphorylation of Plk4 exists *in vivo*.

Finally – and most surprisingly – mutating T138 to alanine significantly enhanced kinase activity compared to the other active mutants. In contrast, introduction of the phosphomimetic negative charge was not tolerated at this position with regard to substrate phosphorylation, and autophosphorylation was also reduced. In case of the well-studied serine/threonine kinase PKA, mutating the corresponding invariant lysine to an alanine completely abolished kinase activity, as has been found for many other kinases as well (Gibbs & Zoller, 1991).

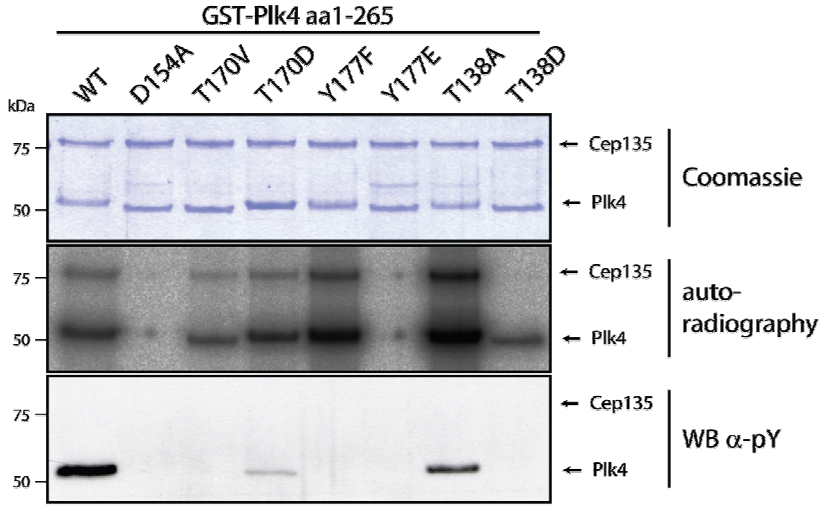

Fig. 14: Mutational analysis of putative phosphorylation sites in the kinase domain of Plk4. GST-fused Plk4 kinase domains (aa 1-265) carrying the indicated mutations were purified from bacteria and eluted from beads. 1 µg of each kinase domain was then subjected to an *in vitro* kinase assay with GST-Cep135 (aa 648-1145) as substrate. Substrate- and autophosphorylation was monitored by autoradiography (middle panel). In parallel, crude bacterial lysates were immuno-blotted with α-phosphotyrosine antibody (4G10) to visualize tyrosine autophosphorylation (lower panel). Kinase-dead Plk4^{D154A} serves as negative control.

4.2.3. Functional characterization of phosphorylation sites from overexpressed Plk4

Fig. 15 summarizes all repeatedly identified phosphorylation sites and depicts their position relative to the functional domains within Plk4.

a)

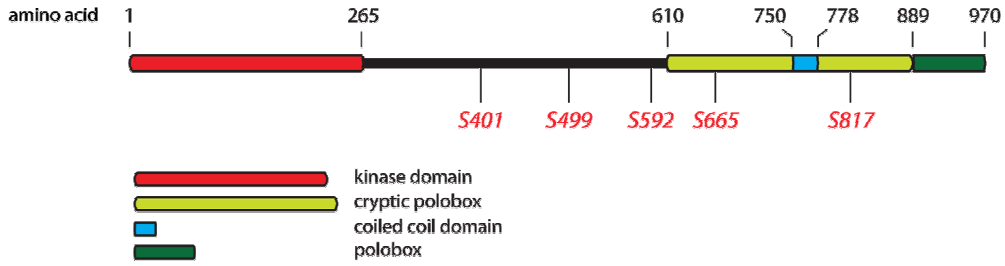

b)

site	tryptic peptide	possible consensus	within domain	regulation*	
				S/G_1	M/S
S22	KGSFAGVYR	Plk4	G-loop of kinase domain	n.d.	n.d.
S401	KTYTMERCHSAEMLSVSK	CamKII, Chk	-	n.d.	n.d.
S499	KTTEYDSISPNR	Cdk1/2	-	1.4	5.3
S592	RSITSPLVAHR	Ck1	-	1.7	4.2
S665	RPPSPTDNISR	MAPK	'cryptic' polobox	3	1
S817	KALSPPPSVDSNYPTR	GSK3β	'cryptic' polobox	2.6	1.25

Fig. 15: Summary of all repeatedly identified phophorylation sites of immunoprecipitated Plk4. **(a)** The schematic depicts all sites (red) and their position relative to the functional domains within Plk4. Schematic drawn to scale. **(b)** The table summarizes the major properties of all sites. The residues found to be phosphorylated are underlined in the tryptic peptides. Abbreviations: CamKII, Calmodulin-dependent kinase II. Chk, checkpoint kinase. Cdk, Cyclin-dependent kinase. Ck, Casein kinase. MAPK, Mitogen activated protein kinase. GSK3β, Glycogen synthase kinase 3β.
* for details, see text (section 4.2.3.1).

Interestingly, only one phosphorylation site has been identified in the kinase domain of Plk4 immunoprecipitated from 293T cells. Based on homology to Plk1 threonine^{210}, we expected to find threonine^{170} (T170) within the activation loop of the kinase domain among the phosphorylated residues, as phosphorylation within this loop is required for full activity of a plethora of kinases (Nolen *et al.*, 2004). However, although the unphosphorylated peptide could be detected and although this residue was found to be phosphorylated in the recombinant kinase, we never found this residue to be phosphorylated in the immunoprecipitated protein. Instead, we found serine^{22} among the phosphorylated peptides, which is located within the G-loop of the small lobe of the kinase domain. This loop is responsible for proper ATP positioning and the actual phosphotransfer (Hanks & Hunter,

1995). At a similar position, double phosphorylation of a threonine and tyrosine residue of the cell cycle master regulator Cdk1 by the kinases Wee1 and Myt1 abolishes activity in G_2 in order to prevent premature entry into mitosis (Watanabe *et al.*, 1995; Liu *et al.*, 1997; Booher *et al.*, 1997).

4.2.3.1. Regulation of the phosphorylation sites over the cell cycle

Having identified a set of phosphorylation sites on the immunoprecipitated protein, we asked whether these sites could be regulated in accordance to the cell cycle. To address this question, we used the technique of **S**table **I**sotope **L**abeling of **A**minoacids in **C**ell Culture (SILAC) combined with mass spectrometry analysis. In this setup, cells are grown in media containing the amino acids lysine (K) and arginine (R) in either their normal form ('light'), or isotope-labelled with $^{13}C/^{15}N$ ('heavy'). As in each case the corresponding other form of the amino acids is not present in the culture medium, cells incorporate arginine-U-$^{13}C_6$-$^{15}N_4$ and lysine-U-$^{13}C_6$-$^{15}N_2$ to virtually 100% into their proteins. Subsequent mass spectrometry analysis can distinguish the origin of a peptide based on its different molecular mass. Most strikingly, this technique also allows for a relative quantification of the peptides, setting the stage for quantitative analyses of post-translational modifications under various conditions.

We grew three different cultures of HeLa S3 cells, all of which were equally transfected with myc-Plk4 (two cultures labeled with 'light' amino acids, one culture labeled with the 'heavy' counterparts). The 'heavy' culture was then synchronized in S phase by a double thymidine block, while the other two sets were synchronized in G_1 phase (release from a noscapine block) or mitosis (treatment with noscapine), respectively. Efficiency of synchronization was monitored by immunoblotting total cell extracts with antibodies against Cyclin-B1 (mitosis) or Cyclin-E (S phase), respectively (Fig. 16a). Subsequently, equal amounts of total cell extracts were mixed ([G_1 + S phase] or [S phase + mitosis]) prior to immunoprecipitation of myc-Plk4 with αmyc antibody (Fig. 16b). Myc-Plk4 was excised from the gel and processed for mass spectrometry analysis as described above (section 4.2.1.1).

The analysis identified the sites S499, S592, S665 and S817 in both immunoprecipitations, allowing for a relative quantification. As noted in the table of Fig. 15b, sites S499 and S592 appeared to be upregulated upon entry into mitosis by 5.3-fold and 4.2-fold, respectively, fitting well with their sequence matching the consensus sequence of cyclin-dependent kinases. In contrast, S665 phosphorylation was upregulated 3-fold upon entry into S phase, but remained unchanged throughout the following mitosis.

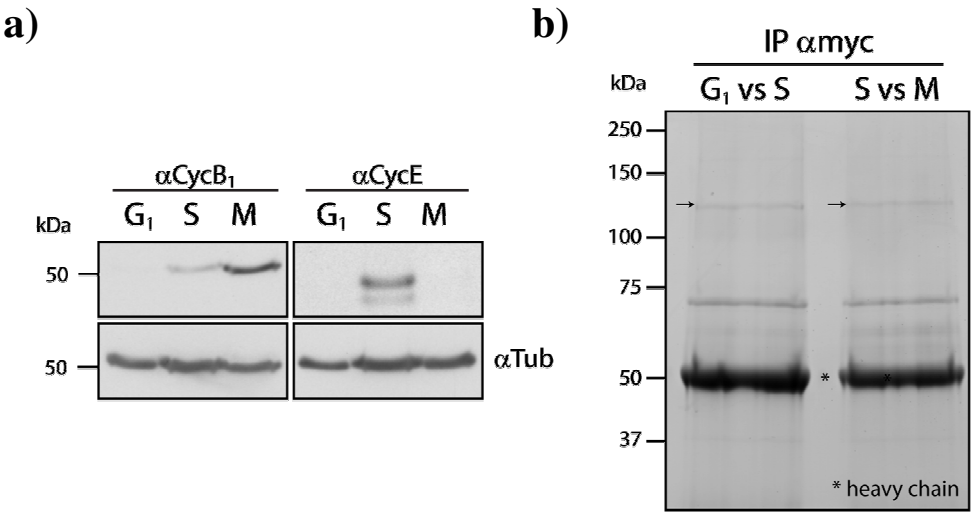

Figure 16. Mass spectrometric SILAC analysis of Plk4 phosphorylation. (a) 293T cells were grown in cell culture media containing 'heavy' or 'light' amino acids lysine and arginine, respectively. Cells were transfected with myc-Plk4 and subsequently synchronized in G_1 phase, S phase, or mitosis. Successful synchronization was verified by immunoblotting the extracts for the cell cycle markers cyclin B_1 and E. **(b)** Equal amounts of total cell extracts were mixed (G_1 + S or S + M) and subjected to immunoprecipitation with αmyc-antibody. Immunoprecipitated Plk4 (arrows) was analyzed for the presence of phosphorylated residues as described earlier (section 4.2.1.1). See table (Fig. 15b) for the regulation of the identified phosphorylation sites.

4.2.3.2. All phosphorylation site mutants localize to the centrosome

The identified residues were mutated to either alanine (A) or aspartate (D), in order to generate non-phosphorylatable or phosphomimetic mutants, respectively. As a first step, these mutants were transiently overexpressed in U2OS cells and analyzed for their subcellular localization. Fig. 17 documents the correct centrosomal localization of all myc-tagged mutants in the presence of the endogenous kinase, including $Plk4^{WT}$ for comparison. Similar results were obtained when the endogenous protein was depleted by siRNA duplexes targeting the 3'UTR of the cellular Plk4 mRNA, and when the mutants were expressed as FLAG-tagged fusion proteins (not shown).

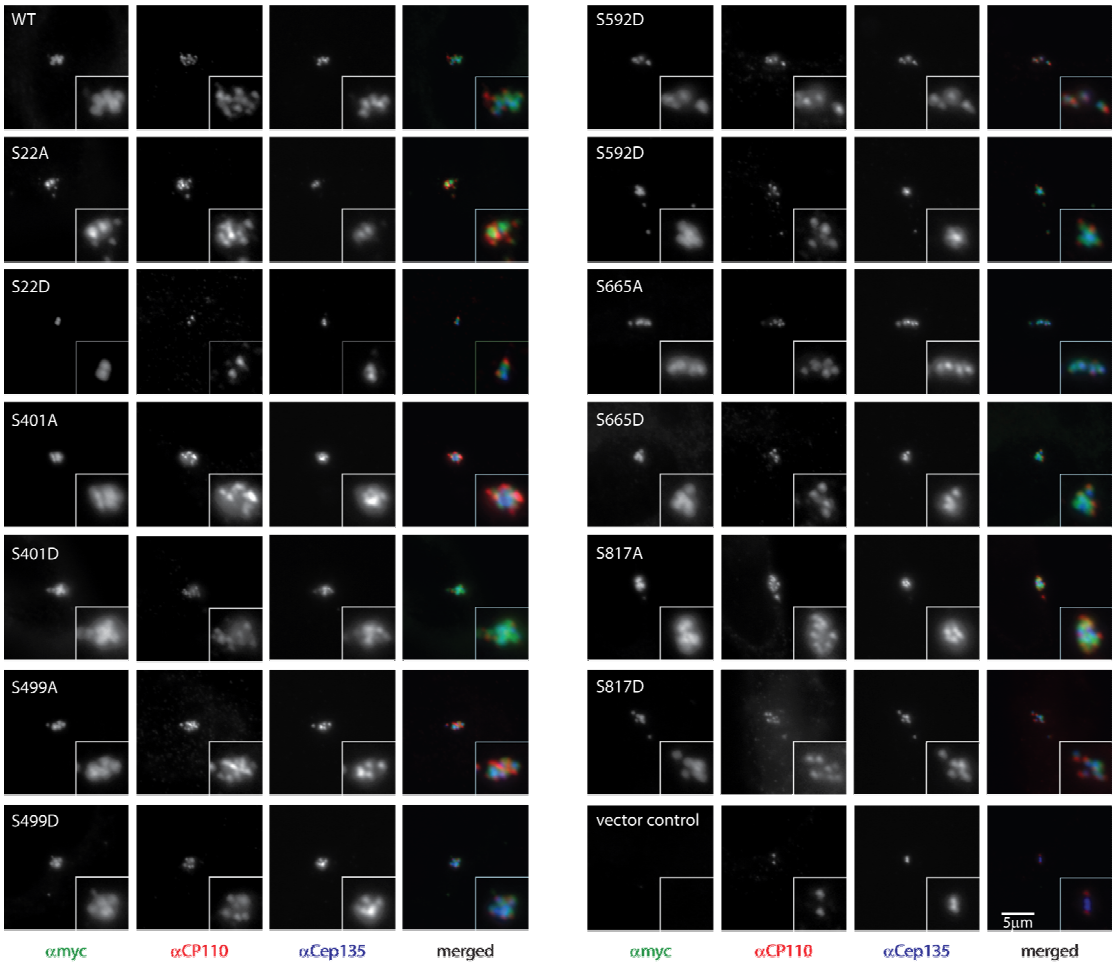

Fig. 17: All phosphorylation site mutants localize to the centrosome. U2OS cells were transfected with the indicated Plk4 mutants in order to assess their ability to localize to the centrosome. As visualized by co-staining with centrosomal markers CP110 (distal) and Cep135 (proximal), all phosphorylation site mutants of Plk4 localize to the centrosome. See also section 4.2.3.5 on centriole overduplication. Bar: 5 µm.

4.2.3.3. Kinase activity of phosphorylation site mutants

Next, we asked whether kinase activity was influenced by the diverse mutations. To this end, we expressed the myc-tagged Plk4 mutants in 293T cells for 24 h, immunoprecipitated them with αmyc ProteinG beads, washed the beads extensively and subjected them to an *in vitro* kinase reaction in presence of (γ-^{32}P)ATP. As no genuine substrates for Plk4 have been identified so far, and as the commonly used model substrates MBP, casein and histone H1 were not phosphorylated above background (Habedanck, 2006), autophosphorylation was used as a readout for Plk4 kinase activity. As shown in Fig. 18, all mutants but Plk4^{S22D} (and Plk4^{D154A} as negative control) displayed autophosphorylation activity to an extent indistinguishable from the WT protein. As predicted from the position of S22 in the G-loop of Plk4's kinase domain, the phosphomimetic Plk4^{S22D} mutation almost completely abolished

kinase activity as judged by autophosphorylation, while the unphosphorylatable Plk4^{S22A} mutation appeared indistinguishable from the WT protein.

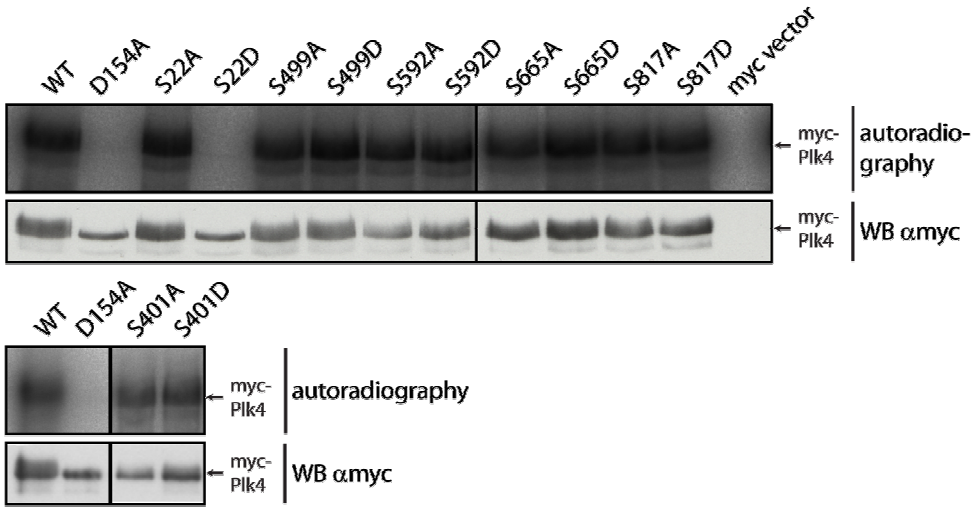

Fig. 18: **Kinase activity of all phosphorylation site mutants.** *In vitro* autophosphorylation assay with immunoprecipitated Plk4. 293T cells were transfected with the respective mutant forms of myc-Plk4 and the appropriate empty vector for 16 h. After immunoprecipitation, myc-Plk4 bound to αmyc-ProtG beads was assayed for autophosphorylation in a conventional *in vitro* kinase assay in presence of (γ-^{32}P)ATP. Autophosphorylation activity was detected by autoradiography, while successful immunoprecipitation was monitored by immunoblotting the exposed membrane with αmyc-antibody. Kinase-dead Plk4^{D154A} and empty vector transfection serve as negative control.

4.2.3.4. Homodimerization of phosphorylation site mutants

Previously, it had been shown that mouse Plk4 is capable of self-association, with the C-terminal polo-box domain being required and sufficient for dimerization (Leung *et al*., 2002). Work in our lab could further specify that the polo box alone (aa 889-970) is dispensable for this process, while upstream residues between aa 610-888 (of human Plk4) mediate homodimerization (Habedanck, 2006). Yet, the functional significance of Plk4 homodimerization remains unclear.

We asked whether the identified phosphorylation sites might be involved in the dimerization process. To this end, we co-transfected 293T cells with FLAG- and myc-tagged phosphorylation site mutants, performed IPs with αFLAG agarose beads and tested the FLAG immunoprecipitates for the presence of co-immunoprecipitated myc-tagged mutants. In contrast to the investigated kinase activities, no difference to the WT protein could be detected for any of the phosphorylation site mutants (Fig. 19). This finding demonstrates that

neither kinase activity nor one of the identified phosphorylation sites is required for homodimerization.

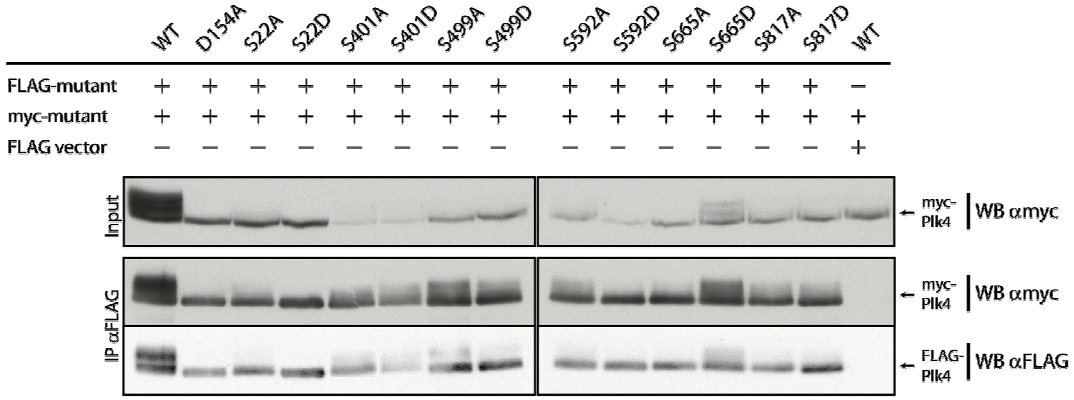

Fig. 19: Mutation of the identified phosphorylation sites does not interfere with homodimerization. FLAG- and myc-tagged Plk4 phosphorylation site mutants were co-overexpressed in 293T cells. Subsequently, FLAG immunoprecipitates were tested for the presence of co-immunoprecipitated myc-tagged mutants.

4.2.3.5. Centriole overduplication evoked by Plk4 phosphorylation site mutants

Finally, we investigated the mutants' propensities to cause centriole overduplication in U2OS cells. We transfected the myc-tagged phosphorylation site mutants into asynchronously growing U2OS cells for 48 h, fixed the cells and stained them with antibodies against the myc tag, the distal end capping protein CP110, and the proximal centriolar protein Cep135 for immunofluorescence analysis (Fig. 17). As predicted from their subcellular localization and kinase activities (Figs. 17, 18), all mutants but Plk4^{S22D} caused centriole overduplication to an extent comparable to Plk4^{WT} (Fig. 20). The kinase-inactive mutant Plk4^{S22D} only promoted overduplication in about 30% of transfected cells, significantly above background but similar to the kinase-dead Plk4^{D154A} control.

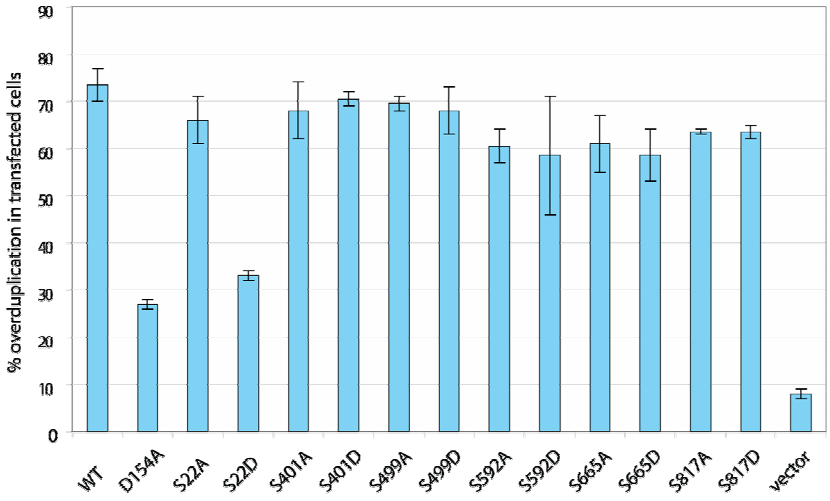

Fig. 20: Centriole overduplication evoked by Plk4 phosphorylation site mutants. Myc-tagged Plk4 phosphorylation site mutants were transfected into asynchronously growing U2OS cells for 48 h. Overduplication of centrioles in transfected cells was scored by IF microscopy analysis with αmyc- and αCP110-antibodies. Blue bars indicate percentage of cells with more than 4 centrioles. Data from three independent experiments, n = 100 cells each; error bars denote standard deviations.

As the overexpressed Plk4 mutants are likely to form heterodimers with the endogenous protein, we set out to test their propensity to promote overduplication in cells depleted of the endogenous kinase. Unfortunately, in all conditions tested, it was not possible to achieve a reasonable degree of depletion together with a satisfying transfection efficiency. Further studies into this direction will therefore require the generation of inducible stable cell lines (see Fig. 11), ideally making use of a predefined single genomic integration site in order to circumvent clonal variations between the different stable cell lines (e.g. FlpIn system, Invitrogen).

In summary, none of the identified phosphorylation sites, except for S22, seem to be of major importance for either localization, kinase activity, homodimerization, or Plk4's propensity to promote centriole overduplication. However, as S22 phosphorylation negatively influences kinase activity and hence reduces centriole overduplication to a level similar to the kinase-dead control, this residue requires further investigation. It will be important to see whether its phosphorylated form also exists on the endogenous kinase and, if so, to learn about its precise regulation.

4.3. βTrCP-mediated degradation of Plk4

Recently, two studies reported that *Drosophila* Plk4 is bound by the ubiquitin ligase SCF^{Slimb}, leading to its degradation by the 26S proteasome (Cunha-Ferreira *et al.*, 2009b; Rogers *et al.*, 2009). As a key finding, both studies demonstrated that controlled destruction of Plk4 is necessary to prevent the formation of supernumerary centrioles, for the first time unraveling one way of how a cell prevents excess Plk4 activity to arise. However, several important questions remain unanswered in this context. For instance, as SCF^{Slimb}-mediated degradation of Plk4 requires the conserved DSGIIT phosphodegron to be doubly phosphorylated, the identity of the responsible kinase(s) remains to be elucidated. Furthermore, the timing of degradation is still unknown. It will be important to learn whether continuous degradation of Plk4 is required or whether rapid proteolysis at a defined stage in the cell cycle is necessary to prevent centriole formation. And finally, research in vertebrates will have to prove that this mechanism of regulation has been conserved in evolution.

4.3.1. βTrCP downregulation causes centriole overduplication

Since in our group we established that excessive Plk4 evokes a readily detectable rosette-like procentriole arrangement (Habedanck *et al*., 2005; Kleylein-Sohn *et al*., 2007), we decided to make use of this assay in testing whether human Plk4 might be regulated similar to *Drosophila* Plk4.

First, we explored the effect of downregulating the human homologue of the *Drosophila* F-box protein Slimb, βTrCP, on centrosome duplication. As shown in Fig. 21a, siRNA duplexes targeting βTrCP1/2, but not the unspecific control siRNAs, significantly increased the proportion of cells with overduplicated centrioles, from <10% to about 40% of all cells. Moreover, staining with an antibody against the distal centriolar marker protein CP110 revealed a significant number of cells containing a halo- or rosette-like configuration of procentrioles typically seen after Plk4 overexpression (Fig. 21b), strongly suggesting that depletion of βTrCP1/2 generates excess Plk4 activity at the centrosome, rather than fostering multiple rounds of centriole re-duplication.

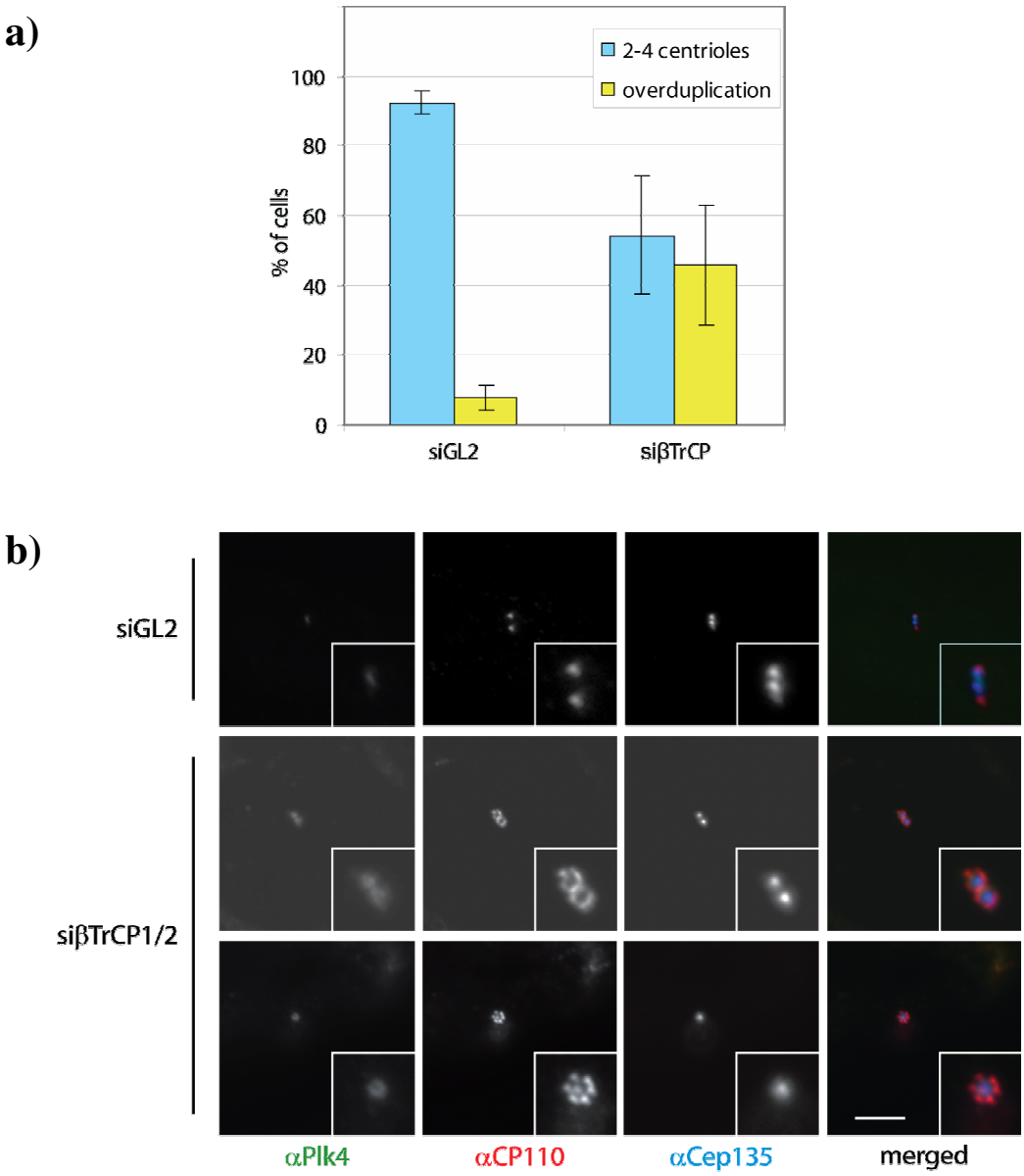

Fig. 21: Downregulation of βTrCP by RNAi causes *bona fide* centriole overduplication via a rosette-like procentriole arrangement. **(a)** Asynchronous U2OS cells were treated for 72 h with siRNA duplexes against βTrCP1/2 or an unspecific control (GL2). IF microscopy analysis of centriole numbers was performed by staining against Plk4 (green), CP110 (red), and Cep135 (blue). Data from three independent experiments, n = 100 cells for each condition. Error bars denote standard deviations. **(b)** Representative pictures of cells treated as described above. Note the halo- and rosette-like procentriole arrangement revealed by CP110 staining (middle and bottom row). Compare to Fig. 10. Bar = 5µm.

Next, we explored whether this observation might be due to the stabilization of Plk4 itself. To this end, we depleted βTrCP1/2 for 72 h in HeLa cells or in the U2OS-B6 cell line inducible for myc-Plk4^{WT} expression (see section 4.1); in the latter case, we induced myc-Plk4^{WT} expression for the last 24 h of the experiment. As shown in Fig. 22a, downregulation

of βTrCP1/2 stabilized induced myc-Plk4^{WT} in the U2OS-B6 cell line; however, no signal for endogenous Plk4 could be detected in HeLa lysates.

Vice versa, simultaneous overexpression of myc-Plk4^{WT} with either FLAG-βTrCP or the empty FLAG vector as control clearly demonstrated that the Plk4 kinase was degraded in the presence of this F-box protein (Fig. 22b).

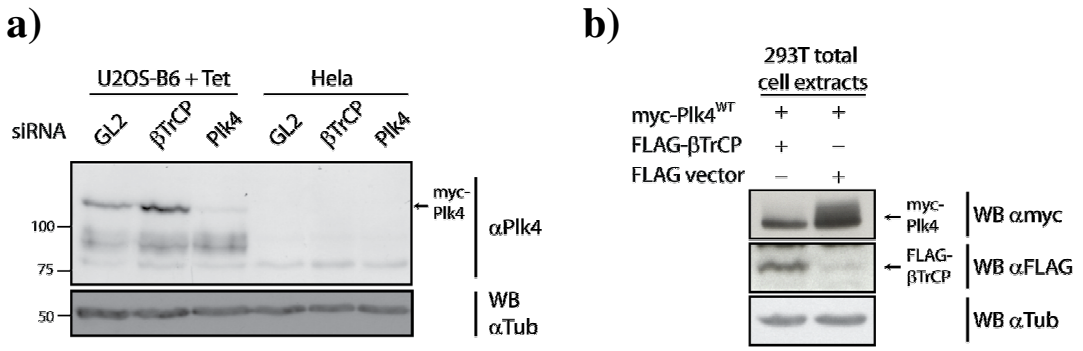

Fig. 22: βTrCP levels regulate Plk4 protein stability. **(a)** U2OS-B6 cells (see section 4.1) and HeLa cells were transfected with siRNA duplexes against βTrCP, Plk4 as a positive control or an unspecific sequence (GL2) as negative control for 72 h. In case of the B6 cell line, myc-Plk4^{WT} expression was induced during the last 24 h of the experiment. Total cell extracts were then immunoblotted with a polyclonal antibody against Plk4. Note that no signal for endogenous Plk4 could be detected in HeLa lysates. **(b)** Myc-Plk4^{WT} and FLAG-βTrCP or empty FLAG vector were co-transfected into 293T cells for 24 h; total cell extracts were then immunoblotted to monitor myc-Plk4^{WT} levels and FLAG-βTrCP expression.

4.3.2. Biochemical interaction between Plk4 and βTrCP

4.3.2.1. Plk4 and βTrCP interact directly in co-immunoprecipitation assays

To further establish that the observed effect is a direct consequence of βTrCP-mediated Plk4 degradation, we examined whether these two proteins are able to interact biochemically. We co-transfected either FLAG-βTrCP with myc-Plk4^{WT} or FLAG-Plk4^{WT} with myc-βTrCP, immunoprecipitated with αFLAG agarose beads and probed the extensively washed immunocomplexes for the presence of myc-tagged protein (Fig. 23).

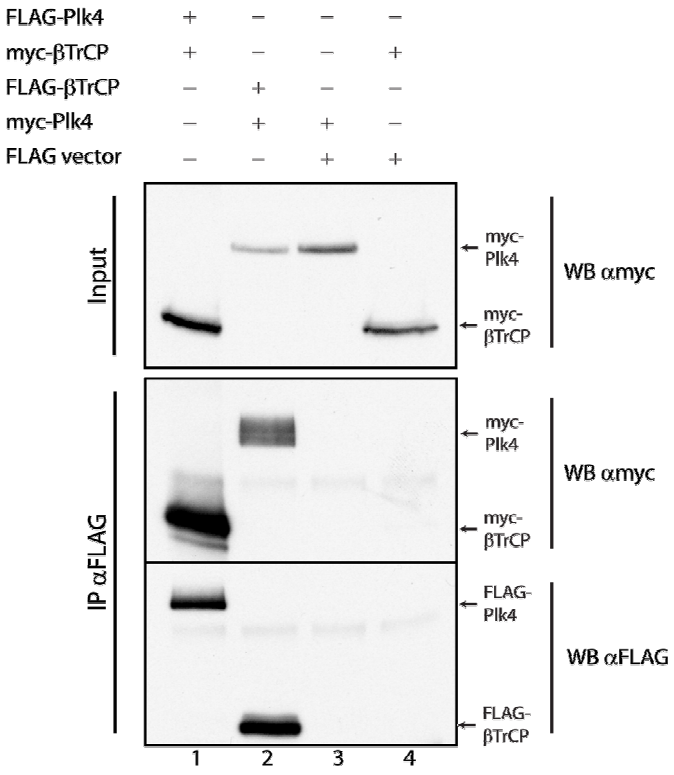

Fig. 23: βTrCP binds directly to Plk4. 293T cells were co-transfected with Plk4 and βTrCP as indicated, and immunoprecipitations were performed using αFLAG antibody. Immunocomplexes were probed for the presence of co-immunoprecipitated myc-tagged protein (middle panel).

As expected, both proteins strongly associated *in vivo*. Interestingly, βTrCP seemed to preferentially bind the highly phosphorylated fraction of Plk4 (Fig. 23, middle panel, lane 2), consistent with the idea that βTrCP binding requires double phosphorylation of the DSGxxT motif (Cardozo & Pagano, 2004). Whether or not this putative phosphorylation is (solely) responsible for the remarkable retardation of the band will be addressed below (Fig. 26).

4.3.2.2. Interaction between Plk4 and βTrCP is dependent on phosphorylation

Having established that βTrCP interacts with a subfraction of Plk4 that is presumably highly phosphorylated, we set out to prove that this interaction is indeed phosphorylation-dependent. As summarized in Fig. 24, we co-overexpressed myc-Plk4^{WT} together with FLAG-βTrCP and subsequently immunoprecipitated this complex from total cell extracts that had been incubated with or without lambda phosphatase in order to globally remove protein phosphorylation. Probing the immunocomplexes with an antibody against the myc-tag revealed that the characteristic retarded mobility of myc-Plk4^{WT} had been abolished (Fig. 24, top panel, lanes 5 and 6), consistent with our earlier findings that active Plk4 is a highly phosphorylated protein *in vitro* and *in vivo* (Fig. 15). Clearly, dephosphorylation of myc-Plk4

prevented efficient association with βTrCP *in vivo* (Fig. 24, bottom panel, lanes 5 and 6), in line with the concept that βTrCP's substrate-binding WD40 domain is specific for a phosphorylated form of a binding motif.

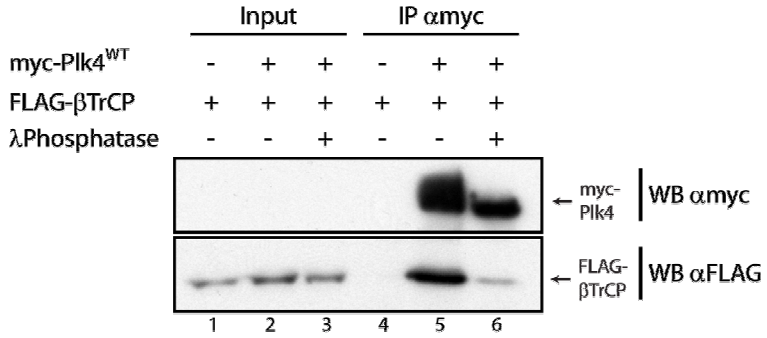

Fig. 24: Interaction of βTrCP and Plk4 is dependent on phosphorylation. 293T cells were transfected with myc-Plk4^{WT} and FLAG-βTrCP or empty FLAG vector for 24 h. Total cell extracts were incubated with or without lambda phosphatase prior to immunoprecipitation of myc-Plk4^{WT} using αmyc-antibody. FLAG-βTrCP co-immunoprecipitation was monitored by immunoblotting with αFLAG antibody (lower panel).

4.3.2.3. Interaction between Plk4 and βTrCP is dependent on the DSGHAT motif

Next, we asked whether this interaction is mediated through binding to the conserved ^{284}DSGHAT^{289} motif in the N-terminal part of Plk4. To this end, we mutated serine^{285} and threonine^{289} to either alanines or aspartates in order to generate an unphosphorylatable or phosphomimetic mutant, respectively. As revealed by co-overexpression and co-immunoprecipitation studies performed as described above, neither Plk4$^{S285A/T289A}$ nor Plk4$^{S285D/T289D}$ associated with FLAG-βTrCP (Fig. 25, middle panel, lanes 1-3). Interestingly, mutation of these residues had no visible effect on Plk4's retarded mobility, indicating that other sites also contribute to this physical property. Together with the previous finding that the interaction is phosphorylation-dependent (Fig. 24), we conclude that (double) phosphorylation of the conserved DSGHAT motif is required for proper βTrCP-mediated degradation of Plk4. The fact that the phosphomimetic Plk4$^{S285D/T289D}$ mutant did not bind βTrCP might reflect that in this context the serine-to-aspartate mutation does not mimic the structural requirements close enough to allow βTrCP binding – thus, in our further experiments we decided to work only with the unphosphorylatable Plk4$^{S285A/T289A}$ mutant.

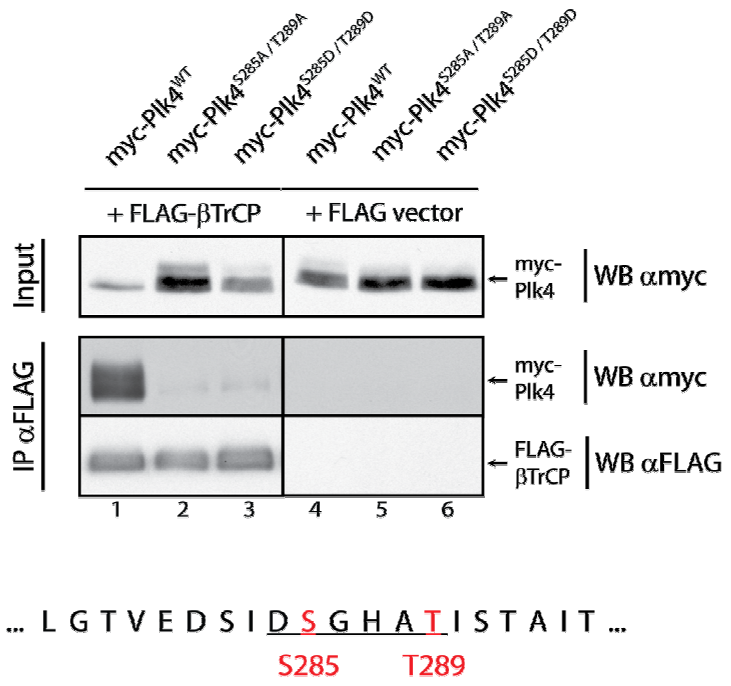

Fig. 25: Interaction of βTrCP and Plk4 is dependent on the conserved DSGHAT motif. 293T cells were co-transfected for 24 h with the respective myc-Plk4 constructs and FLAG-βTrCP or empty FLAG vector as indicated. FLAG-βTrCP was immunoprecipitated from total cell extracts with αFLAG antibody, and immunocomplexes were tested for the presence of myc-tagged proteins by immunoblotting with αmyc-antibody.

4.3.3. Mass spectrometric analysis of Plk4 co-immunoprecipitated with βTrCP

As the previous results suggested that βTrCP-bound Plk4 is highly phosphorylated (Fig. 23, lane 1), we decided to analyze this Plk4 subfraction via mass spectrometry for the presence of phosphorylated residues. From 293T cells co-transfected with myc-Plk4^{WT} and FLAG-βTrCP, the latter was immunoprecipitated and, after extensive washing, immunocomplexes were separated by SDS-PAGE. The band representing co-immunoprecipitated myc-Plk4^{WT} was excised and digested with either trypsin or elastase, in order to enhance peptide coverage. To our surprise, in addition to the well-known sites S22, S401, S499, S592, S665, and S817 (Fig. 15), we identified another 13 sites to be phosphorylated (Fig. 26a). However, no peptide revealing the phosphorylation state of the DSGHAT motif could be detected (see paragraph below).

Among those additional 13 sites, serine^{282} lies remarkably close to the DSGHAT motif. In another study, the authors identified a serine residue at a similar position in the βTrCP substrate protein REST to be phosphorylated (Westbrook *et al.*, 2008). The authors demonstrate that the S1027A mutation of this residue weakens the interaction between REST

and βTrCP, concluding an active involvement of this phosphorylation into controlled REST degradation.

Thus, we decided to test a potential involvement of serine^{282} into βTrCP binding by a functional analysis of Plk4^{S282A} and Plk4^{S282D} mutants. Not only the unphosphorylatable S282A mutation seemed to significantly weaken the interaction between Plk4 and βTrCP (Fig. 26b), but also the supposedly phosphomimetic S282D mutant bound βTrCP to a lesser extent. The latter suggests that, again, the serine-to-aspartate mutation does not mimic a phosphorylation close enough to restore functionality. This analysis indicates that phosphorylation of S282 is likely to be involved in the process of Plk4 degradation. However, compared to the mutation of the canonical phosphodegron, the substitution of this site did not show the same drastic effect; it remains to be elucidated whether this site might therefore be involved in fine tuning of the degradation process.

Since no peptide spanning the DSGHAT motif could be detected in this mass spectrometric analysis, we decided to mutate residues glycine^{277} and isoleucine^{294} to arginine and lysine, respectively. Tryptic digest of Plk4$^{G277R/I294K}$ was expected to yield a peptide spanning the DSGHAT motif that is of suitable molecular mass for detection by mass spectrometry. Unfortunately, although the unphosphorylated peptide was found in the corresponding analysis (not shown), the (singly or doubly) phosphorylated phosphodegron peptide could still not be identified.

a)

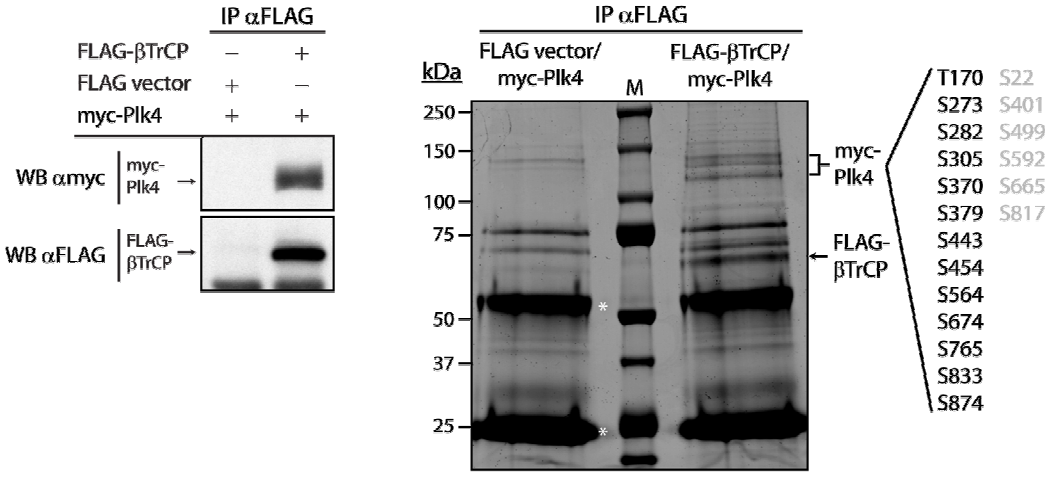

b)

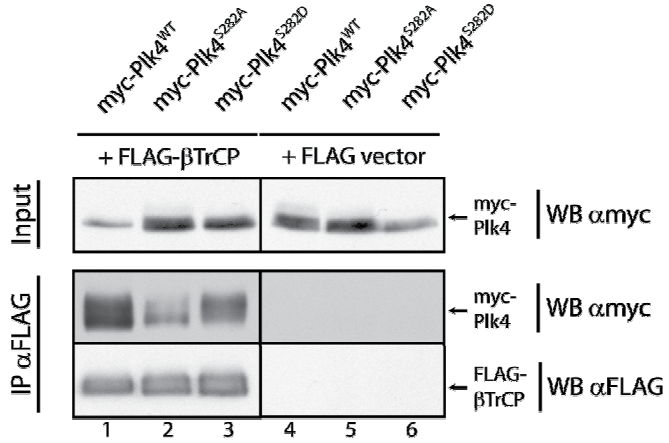

... L G T V E D S I D S G H A T I S T A I T ...

S282

Fig. 26: Mass spectrometric analysis of myc-Plk4^{WT} co-immunoprecipitated with βTrCP. **(a)** 293T cells were co-transfected with myc-Plk4^{WT} and FLAG-βTrCP for 24 h. FLAG-βTrCP was immunoprecipitated from total cell extracts, and successful co-immunoprecipitation was verified by Western blotting (left panel). Immunocomplexes were separated by SDS-PAGE and stained with Coomassie Blue (right panel). Co-immunoprecipitated myc-Plk4^{WT} was excised from the gel and processed for mass spectrometric analysis of phosphorylation sites as described earlier (see 4.2.1.1). Identified sites are depicted to the right, with previously characterized phosphorylation sites shown in light grey. **(b)** Myc-Plk4^{S282A} and myc-Plk4^{S282D} were co-transfected with FLAG-βTrCP as described above and tested for their ability to associate with FLAG-βTrCP. The position of S282 relative to the DSGHAT motif is shown below. White asterisks denote immunoglobulin light and heavy chains.

4.3.4. Plk4 kinase activity is required for its own βTrCP-mediated degradation

4.3.4.1. Kinase-dead Plk4^{D154A} and Plk4^{S22D} fail to bind to βTrCP

Plk4 has been placed on top of a highly conserved assembly pathway leading to the formation of new centrioles (Bettencourt-Dias *et al*., 2005; Habedanck *et al*., 2005; Kleylein-Sohn *et al*., 2007). Despite this recent progress, the molecular details still remain mysterious. As the identification of βTrCP-mediated Plk4 degradation shed first light on the upstream regulation of this kinase (Cunha-Ferreira *et al.*, 2009b; Rogers *et al.*, 2009), the stage is now set for the identification of the kinase(s) responsible for the phosphorylation of Plk4's DSGHAT motif.

In order to obtain first indications, we decided to test all generated phosphorylation site mutants identified in the first part of this thesis (Fig. 15) for their capability to interact with βTrCP. We performed co-immunoprecipitation studies according to the previous experiments, by immunoprecipitating FLAG-βTrCP and probing the complexes for the presence of myc-Plk4 phosphorylation site mutants (Fig. 27a). Surprisingly, all of the tested mutants were unaffected in βTrCP binding, except for the kinase-dead Plk4^{D154A} and the similarly inactive Plk4^{S22D} mutant. To further confirm that catalytic activity of Plk4 is required for proper association with βTrCP, we repeated the co-immunoprecipitation experiment by switching FLAG and myc tag on the two proteins. Fig. 27b confirms that Plk4 catalytic activity is indeed required for proper Plk4 degradation.

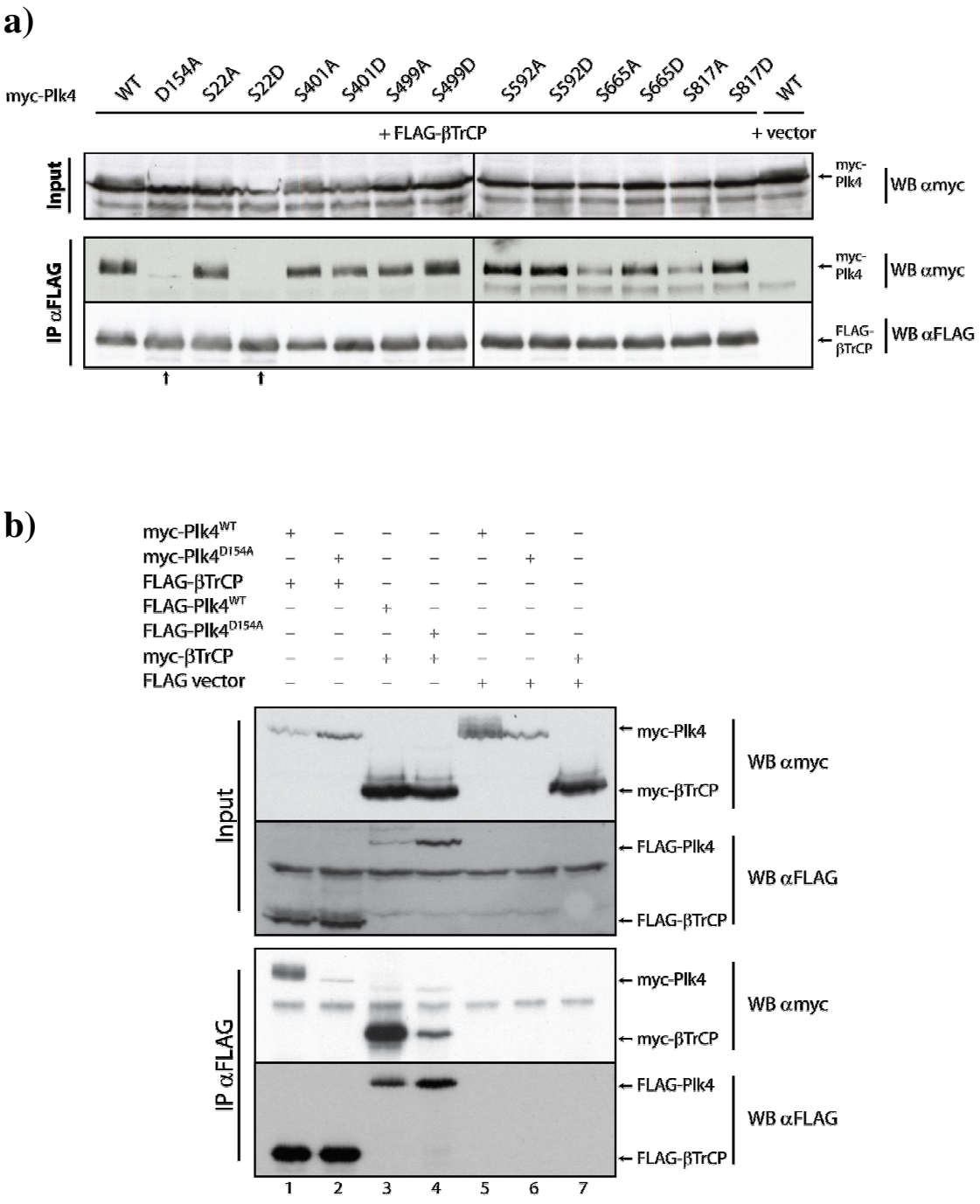

Fig. 27: Plk4 phosphorylation site mutants reveal a requirement of Plk4 kinase activity for βTrCP binding. **(a)** Myc-tagged Plk4 phosphorylation site mutants were co-overexpressed with FLAG-βTrCP in 293T cells for 24 h. FLAG-immunoprecipitates were then tested for the presence of co-immunoprecipitated myc-tagged mutants by immunoblotting with αmyc-antibody. **(b)** 293T cells were co-transfected with Plk4 and βTrCP as indicated, and immunoprecipitations were performed using αFLAG antibody. Immunocomplexes were probed for the presence of co-immunoprecipitated myc-tagged protein.

4.3.4.2. Kinase-dead Plk4^{D154A} is stabilized equally to the Plk4$^{S285A/T289A}$ degron mutant

As a consequence of βTrCP binding, Plk4 is supposed to be degraded by the 26S proteasome (Cunha-Ferreira *et al.*, 2009b; Rogers *et al.*, 2009). Since the previous experiments demonstrated the requirement of Plk4 catalytic activity for association with βTrCP, the kinase-dead Plk4^{D154A} mutant would be predicted to have a prolonged half-life in comparison to Plk4^{WT}, similar to the unphosphorylatable Plk4$^{S285A/T289A}$ degron mutant. To test this prediction, we transfected FLAG-tagged Plk4^{WT}, Plk4^{D154A} or Plk4$^{S285A/T289A}$ into 293T cells for 16 h, blocked translation at timepoint 0 h by the addition of 25 µg/ml cycloheximide, and monitored the decay of Plk4 over the following 8 h by Western detection. Fig. 28 clearly shows that Plk4^{WT} becomes rapidly degraded during the first 4 h, consistent with a previous report that determined its half-life to be 2-3 h (Fode *et al*., 1996). In contrast, both Plk4^{D154A} as well as Plk4$^{S285A/T289A}$ displayed no detectable decay over this time course, clearly demonstrating that Plk4 kinase activity is pivotal to its own targeted proteolysis.

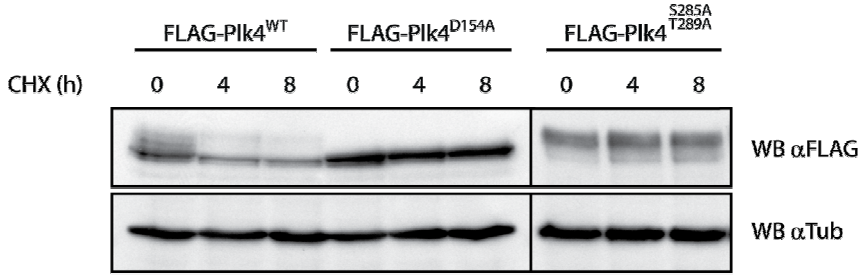

Fig. 28: Kinase-dead Plk4^{D154A} is stabilized equally to the Plk4$^{S285A/T289A}$ degron mutant. FLAG-tagged Plk4^{WT}, Plk4^{D154A} or Plk4$^{S285A/T289A}$ were transfected into 293T cells for 16 h prior to blocking further translation with 25 µg/ml cycloheximide (CHX) at timepoint t = 0 h. Four and eight hours later, cells were lysed and total cell extracts were probed for FLAG-tagged proteins with αFLAG-antibody.

4.3.4.3. Binding deficiency of kinase-dead Plk4^{D154A} can be rescued by active Plk4 *in vivo*

Having established that Plk4 catalytic activity is *required* for controlled Plk4 proteolysis, the fundamental question arises if it is also *sufficient* for this process. First, we tried to address this question *in vivo*. We overexpressed myc-Plk4^{WT} or myc-Plk4^{D154A} - or the degron mutant myc-Plk4$^{S285A/T289A}$ as control - in 293T cells, and captured the overexpressed protein by αmyc ProteinG beads. After extensive washing, the immunocomplexes were incubated with *in vitro*-translated, ^{35}S-labelled FLAG-βTrCP, washed again extensively and finally separated by SDS-PAGE (Fig 29). Successful binding of ^{35}S-FLAG-βTrCP was monitored via

autoradiography, while efficient immunoprecipitation was controlled by Western blot detection of myc-tagged proteins. Lanes 8-10 recapitulate our previous findings: Plk4^{WT} efficiently bound ^{35}S-FLAG-βTrCP, while neither the degron mutant Plk4$^{S285A/T289A}$ nor kinase-dead Plk4^{D154A} were able to pull down ^{35}S-FLAG-βTrCP. In contrast, when myc-Plk4^{D154A} was overexpressed together with a FLAG-tagged, active mutant of Plk4, that itself cannot bind to βTrCP (FLAG-Plk4$^{S285A/T289A}$), the binding deficiency of Plk4^{D154A} could be fully restored. This finding demonstrates that – in cells – overexpression of an active form of Plk4 is sufficient to render the binding-deficient Plk4^{D154A} binding-competent. However, it cannot be excluded at this point that an additional kinase might be involved whose function in degrading Plk4 is in turn dependent on Plk4 autophosphorylation. *In vitro* experiments will ultimately be required to distinguish between these two scenarios.

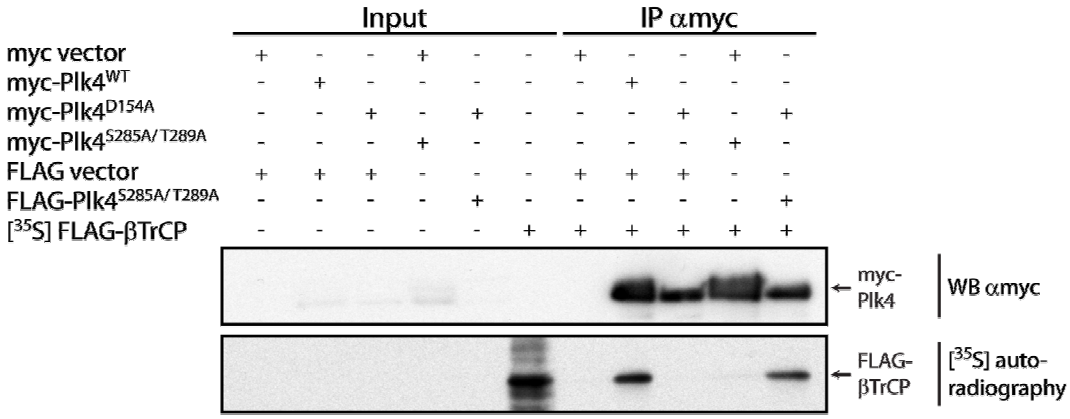

Fig. 29: Binding deficiency of kinase-dead Plk4^{D154A} can be rescued by active Plk4 *in vivo*. FLAG- and myc-tagged constructs were overexpressed in 293T cells as indicated above. Immunoprecipitated myc-Plk4 – still bound to the beads – was then incubated with *in vitro*-translated ^{35}S-FLAG-βTrCP to allow protein association. Subsequently, immunocomplexes were separated by SDS-PAGE; successful immunoprecipitation was verified by immunoblotting with αmyc-antibody (upper panel), and presence of ^{35}S-FLAG-βTrCP was detected via autoradiography (middle panel).

4.3.5. N-terminal truncations of Plk4 cause centriole overduplication as visualized by rosette-like procentriole arrangements

In the previous section, we provided evidence that *trans*-autophosphorylation of Plk4 represents a key step in the βTrCP-mediated proteolytic degradation of Plk4. To corroborate this finding, we asked whether preventing *trans*-autophosphorylation of endogenous Plk4 would interfere with its degradation. To this end, we first transfected different truncation mutants of Plk4 (Fig. 30a) into 293T cells and determined their capability to dimerize with the full-length protein (as described in section 4.3.2.4) (Fig. 30b). It has been shown earlier that the C-terminal region of Plk4 contains the sequences that mediate the homodimerization with the full-length protein (Habedanck, 2006; Leung *et al.*, 2002). Consistent with this, we observed that Plk4$^{aa1\text{-}889}$, Plk4$^{aa265\text{-}970}$, and Plk4$^{aa609\text{-}970}$ all readily bound to full-length FLAG-Plk4, while the N-terminal part Plk4$^{aa1\text{-}608}$ failed to do so (Fig. 30b). We then transfected Plk4$^{aa1\text{-}608}$, Plk4$^{aa609\text{-}970}$, and Plk4$^{aa265\text{-}970}$ into U2OS cells and stained them with antibodies against the myc tag and the centriolar proteins CP110 and Cep135/ CAP350. As summarized in Fig. 30c, Plk4$^{aa265\text{-}970}$ and Plk4$^{aa609\text{-}970}$ were able to cause centriole overduplication, as visualized by the formation of a rosette-like procentriole arrangement, albeit to a low degree. Of note, the C-terminus Plk4$^{aa609\text{-}970}$ was only weakly detectable at the centrosome, yet it evoked the distinct phenotype of rosette-like procentriole arrangements. In contrast, the N-terminal part of Plk4 did not localize to the centrosome and did not cause centriole overduplication.

We therefore conclude that the truncation mutants Plk4$^{aa609\text{-}970}$ and Plk4$^{aa265\text{-}970}$ bind to endogenous Plk4 and prevent its *trans*-autophosphorylation, in turn leading to a stabilization of the endogenous kinase and to centriole overduplication.

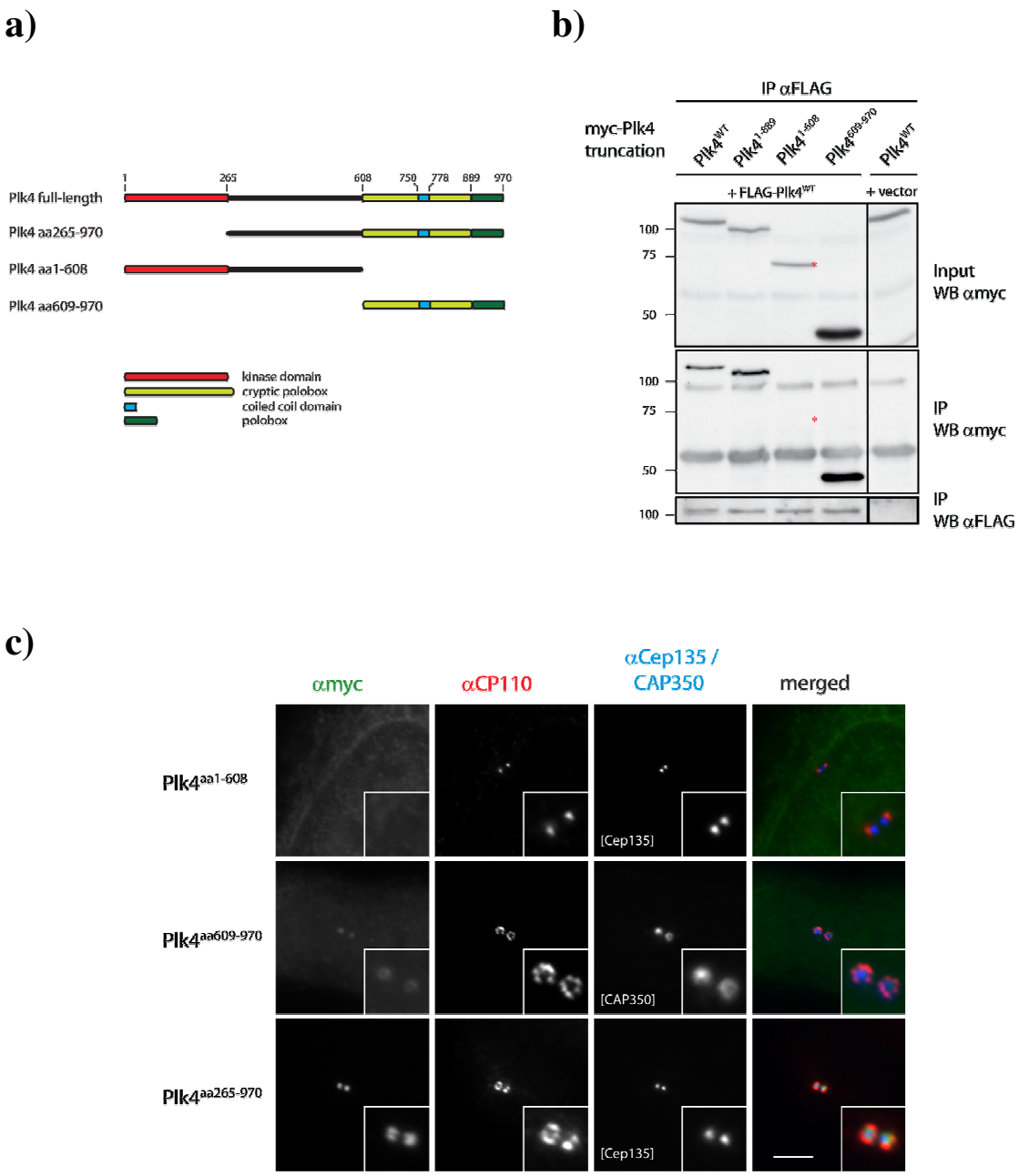

Fig. 30: N-terminal truncations of Plk4 are able to cause centriole overduplication as visualized by the formation of rosette-like procentriole arrangements. **(a)** Schematic depicting the truncation mutants of Plk4 that were used in this experiment. Drawn to scale. **(b)** Dimerization assay of Plk4 truncation mutants. Full-length FLAG-Plk4 and myc-tagged Plk4 truncation mutants were co-overexpressed in 293T cells. Subsequently, FLAG immunoprecipitates were tested for the presence of co-immunoprecipitated myc-tagged truncation mutants. Red asterisks indicate that myc-Plk4$^{aa1-608}$ cannot be detected in the immunoprecipitates. **(c)** U2OS cells were transfected with myc-Plk4$^{aa1-608}$, myc-Plk4$^{aa609-970}$ and myc-Plk4$^{aa265-970}$ for 48 h. Cells were fixed and stained with α-myc-antibody to identify transfected cells, for CP110 to detect centrioles with engaged pro-centrioles, and for Cep135 or CAP350 as proximal centriolar markers. Bar: 5 µm.

5. Discussion

Plk4's cellular functions have long remained mysterious, and only recent studies demonstrate that this kinase is pivotal in the process of centriole biogenesis (Cunha-Ferreira *et al.*, 2009a; Bettencourt-Dias & Glover, 2009). However, no physiological substrate of Plk4 has yet been identified, and with the regulation of *Drosophila* Plk4 being dependent on its degradation, the first and only hint towards upstream regulatory mechanisms has been proposed very recently (Cunha-Ferreira *et al.*, 2009b). We therefore set out to investigate, first, whether Plk4 might be regulated by phosphorylation. We identified numerous phosphorylation sites on overexpressed Plk4 and analyzed whether they are implicated in any of Plk4's centrosome-associated functions. As a second approach, we investigated whether Plk4 might be regulated, in analogy to *Drosophila* Plk4, via regulated proteolysis.

5.1. Kinase activity of endogenous Plk4 is strictly required for centriole biogenesis

When Plk4 was first shown to be a master regulator of centriole biogenesis (Habedanck *et al.*, 2005; Bettencourt-Dias *et al.*, 2005), the experiments revealed a requirement for Plk4 kinase activity to exert its functions in this process (Habedanck *et al.*, 2005). However, it was noticed that transiently overexpressed kinase-inactive $Plk4^{D154A}$ caused about 30% of centriole overduplication, compared to 80% in case of the wildtype protein but only 5% in untransfected control samples (Habedanck *et al.*, 2005).

In principle, supernumerary centrosomes might arise via different routes (Meraldi *et al.*, 2002; Nigg, 2002; Sluder, 2004; Nigg, 2007), namely aborted mitosis or cytokinesis, cell fusion, centrosome fragmentation, centriole re-duplication during prolonged S phase, and finally *bona fide* centriole overduplication by generating more than one procentriole adjacent to each mother centriole. To investigate this further, Habedanck *et al*. (2005) suppressed cell cycle progression by an aphidicolin-induced S phase block. While the wildtype kinase still caused excessive overduplication, the $Plk4^{D154A}$-induced overduplication was suppressed to the levels of the untransfected control. This led the authors to conclude that $Plk4^{D154A}$ might cause occasional division failures by a dominant-negative mode of action, fitting well with the observation that reduced Plk4 levels in heterozygous $Plk4^{+/-}$ mice also showed centrosome amplification (Ko *et al.*, 2005).

Staining of induced B6 (WT) and D2 (D154A) cells, however, argue against the explanation that kinase-dead Plk4 evokes overduplication solely via division failures. D2 cells were found to contain a high degree of parental centrioles surrounded by the typical halo- or

rosette-like arrangement of procentrioles. These structures have extensively been characterized in the corresponding B6 cell line and shown to constitute near-simultaneously formed procentrioles around parental centrioles, notably in an engaged configuration (Kleylein-Sohn *et al.*, 2007). In fact, this phenotypic manifestation of Plk4 overexpression proved invaluable in the delineation of the centriole assembly pathway in human cells, unraveling that the *C. elegans* core module identified before (reviewed in Strnad & Gonczy, 2008) is conserved also in humans (Kleylein-Sohn *et al.*, 2007). We therefore believe that centriolar rosettes induced by the expression of Plk4^{D154A} represent *bona fide* centriole overduplication. In order to assess whether this effect depends on the endogenous wildtype kinase, we depleted the endogenous protein by RNAi and induced overexpression thereafter. Strikingly, expression of the wildtype kinase in B6 cells caused centriole overduplication irrespective of the presence or absence of endogenous Plk4, while Plk4^{D154A}-induced rosette formation was completely abolished when endogenous Plk4 was missing. As expected, neither construct induced overduplication in HsSas-6-depleted cells, recapitulating the established requirement of this protein in the assembly pathway downstream of Plk4 (Dammermann *et al.*, 2004; Habedanck *et al.*, 2005; Kleylein-Sohn *et al.*, 2007). We therefore conclude that Plk4^{D154A} modulates endogenous Plk4 in a yet-to-be-identified way; one hypothesis will be discussed later in the context of ßTrCP-mediated Plk4 degradation. The notion that Plk4^{D154A} influences endogenous Plk4 goes in line with the observation that Plk4 is a homodimer (or oligomer) *in vivo* (Habedanck, 2006) and that homodimerization does not depend on kinase activity (Fig. 19).

Another potential explanation is based on the fact that an enlargement of the PCM is sufficient to induce centriole overduplication in vertebrate cells (Loncarek *et al.*, 2008); of note, the formation of extra centrioles upon overexpression of pericentrin (i.e. PCM enlargement) appears to be similar to the *de novo* pathway in that centriole biogenesis is initiated in local densities throughout the PCM rather than orthogonally to the proximal base of a pre-existing centriole (Loncarek *et al.*, 2008). Along the same lines, Song and colleagues reported that the *C. elegans* proteins SZY-20 and ZYG-1 have opposing effects on centrosome size (Song *et al.*, 2008a), extending on the intimate relationship between centrioles and their surrounding PCM (Bobinnec *et al.*, 1998; Dammermann *et al.*, 2004). The authors propose that ZYG-1 functions in PCM recruitment and thus positively influences centrosome size, while SZY-20 antagonizes the recruitment of centrosomal proteins, including ZYG-1, SPD-2 and SPD-5 (Song *et al.*, 2008a). Thus, albeit clearly speculative, we cannot rule out the possibility that the pronounced accumulation of Plk4^{D154A} to the

centrosome influences centrosome duplication via increasing centrosome size. Yet, as in all scenarios investigated Plk4 is required for centriole biogenesis (Habedanck *et al.*, 2005; Bettencourt-Dias *et al.*, 2005; Rodrigues-Martins *et al.*, 2007), such an effect of Plk4^{D154A} would still require the endogenous Plk4 to be present.

5.2. Phosphorylation site analysis

As most kinases are predominantly regulated via phosphorylation/dephosphorylation (Hunter, 2000; Shi *et al.*, 2006), we asked whether Plk4 could be regulated in an analogous way. An unbiased approach of mutating all conserved serine/threonine/tyrosine residues within Plk4 was not feasible, because the 970 aa protein Plk4 contains too many residues that are highly conserved. Thus, we set out to determine phosphorylation sites present on Plk4 in different stages of the cell cycle, followed by mutational analyses. Endogenous Plk4 is an extremely low abundant enzyme within the cell (Habedanck *et al.*, 2005; Bettencourt-Dias *et al.*, 2005), reflected by the fact that despite more than 15 years of research, there is no antibody available to date that would allow for the detection of endogenous Plk4 on Western blots, or immunoprecipitation of appropriate amounts of kinase for efficient mass spectrometric analysis of post-translational modifications. Thus, we were dependent on the analysis of over-expressed Plk4 immunoprecipitated from human cells and included an analysis of putative autophosphorylation sites on the *in vitro* autophosphorylated, recombinant kinase.

5.2.1. Phosphorylation sites from the recombinant kinase

GST-Plk4 isolated from *E. coli* was phosphorylated to a surprisingly high extent (Fig. 12b). Therefore, we chose conserved sites within the kinase domain for further analysis, based on the well-defined general architecture of protein kinases. Most surprisingly, we detected tyrosine autophosphorylation of Plk4 upon expression in bacteria. Tyrosine phosphorylation upon expression of apparent serine/threonine kinases in bacteria has been the foundation for the identification of so-called dual specificity kinases (Lindberg *et al.*, 1992), however, this behaviour does not necessarily reflect an actual dual specificity *in vivo*. Although recombinant Plk4 was substantially tyrosine-autophosphorylated *in vitro*, we did not detect any tyrosine phosphorylation in its exogenous substrate protein Cep135 (Fig. 14), nor could we confirm tyrosine autophosphorylation to be present on the overexpressed kinase immuno-precipitated from human cells. We therefore conclude that Plk4 might not act as a dual specificity kinase in mammalian cells. However, as tyrosine autophosphorylation could not be detected on Plk1 and has never been reported for any Plk-family member, we emphasize that

Plk4 in this regard behaves significantly differently from Plks 1-3. This notion substantiates the finding that the preferred substrate consensus sequence of Plk4 is significantly different from Plk1 (Leung *et al.*, 2007), and that despite partially overlapping localizations, the set of substrates is likely to be distinct (Barr *et al.*, 2004).

In vitro dual specificity of Plk4 might be explained by an atypical feature within the kinase domain, namely the substitution of a near-invariant lysine with a threonine (T138) close to the catalytic base. While virtually all serine/threonine kinases carry this near-invariant lysine, only tyrosine kinases differ from this scheme by showing either an alanine or an arginine substitution (Taylor *et al.*, 1993); hence, this residue is considered to be fundamental in the determination of the preferred phospho-acceptor residue. Intriguingly, and in marked contrast to Plks 1-3, this rare and atypical feature within Plk4's kinase domain is conserved in all homologues examined, and can also be found in *C. elegans* ZYG-1. Moreover, mutation of T138 to an alanine in Plk4 did not interfere with kinase activity. In light of these findings, it will be important to learn more about the architecture of Plk4's kinase domain from a crystal structure, and to determine endogenous substrate phosphorylation sites in order to refine its proposed consensus sequence.

5.2.2. Phosphorylation sites from the overexpressed protein

In contrast to the recombinant protein, overexpressed Plk4 showed only a limited set of repeatedly identified phosphorylation sites. Unfortunately, all identified sites were present in all phases of the cell cycle, as SILAC-mediated quantification could only show moderate up- and downregulations upon cell cycle transitions (table in Figs. 15, 16). Interestingly, during the course of this work another study surveyed the global changes of protein kinase phosphorylation upon S/M transition (Daub *et al.*, 2008). The authors determined an overlapping set of phosphorylation sites to the ones presented here – notably on the endogenous Plk4 protein – and revealed an upregulation of all sites but S401 upon entry into mitosis. These data fit well with the regulation determined in the context of this thesis, and further validate that overexpressed Plk4 seems to be regulated similarly to the endogenous protein. Upregulation of sites in mitosis might reflect increasing regulatory input into Plk4, however, as outlined below, these sites do not seem to be major regulatory sites in the context of centriole biogenesis.

We mutated the identified sites to either alanine or aspartate, in order to mimic unphosphorylated or phosphorylated residues, respectively, and analyzed the mutants for

Plk4's known centrosomal properties, namely centrosomal localization, homodimerization, (auto)phosphorylation activity, and its propensity to promote centriole overduplication.

As a general mechanism, phosphorylation is well known to be required for the proper subcellular localization of numerous proteins. For instance, the human kinesin-related motor protein Eg5 needs to be phosphorylated at T927 by Cdk1/Cyclin-B in order to be properly targeted to the centrosome via binding to the dynactin subunit $p150^{Glued}$ (Blangy *et al.*, 1995; Blangy *et al.*, 1998). A non-phosphorylatable T927A mutant does not associate with centrosomes, and as a consequence of impaired localization, the duplicated centrosome does not separate in prophase and causes the formation of a monopolar spindle (Blangy *et al.*, 1995; Blangy *et al.*, 1998). Moreover, centrosome cohesion is regulated by the timely dissociation of the proximal centriolar proteins C-Nap1 and its interactor Rootletin (Mayor *et al.*, 2002; Bahe *et al.*, 2005). Both proteins are phosphorylated by the centrosomal kinase Nek2, and data suggest Ned2-dependent phosphorylation is required for timely dissociation prior to centrosome separation at the beginning of mitosis.

In order to investigate whether one of the identified phosphorylation sites could be involved in subcellular localization of Plk4, we overexpressed all myc-tagged mutants in U2OS cells. Unfortunately, all mutants readily localized to the centrosome as apparent from immunofluorescence stainings against the myc tag and the centrosomal proteins CP110 and Cep135 (Fig. 17). As Plk4 is known to dimerize (or oligomerize) *in vivo* (Leung *et al.*, 2002; Habedanck, 2006), we repeated the experiments in cells that were depleted of endogenous Plk4 prior to overexpression (see also below). As a consequence of depletion, many cells appeared to contain only a single centriole (Habedanck *et al.*, 2005), yet all mutants were found to readily localize to these single centrioles shortly after transfection (not shown). We therefore conclude that none of the phosphorylation sites is involved in Plk4's subcellular localization, even in the absence of the endogenous protein. Of note, it has been reported previously that mouse Plk4, in addition to the centrosome, localizes to the nucleoli and the cleavage furrow (Hudson *et al.*, 2001; Martindill *et al.*, 2007); however, subsequent studies did not confirm such a localization in human cells or *Drosophila* (Habedanck *et al.*, 2005; Bettencourt-Dias *et al.*, 2005). In line with this, none of the phosphorylation site mutants were ever observed at either the nucleoli or the cleavage furrow/midbody in the context of this work.

As mentioned above, Plk4 is known to dimerize *in vivo* (Leung *et al.*, 2002; Habedanck, 2006). To investigate a possible interference of the mutations with Plk4's dimerization abilities, we co-overexpressed FLAG- and myc-tagged mutants in 293T cells,

immunoprecipitated via the FLAG tag and tested the immunocomplexes for dimerized Plk4. The experiment revealed that all mutants dimerized with each other (Fig. 19) and also with co-overexpressed $Plk4^{WT}$ (not shown). Notably, the kinase-dead $Plk4^{D154A}$ mutant (and also inactive $Plk4^{S22D}$, see below) were equally capable of self-association despite their lack of activity, demonstrating that autophosphorylation is not required for this process.

We next asked whether one of the phosphorylation sites could be regulatory to Plk4's kinase activity. Predominantly, kinases are activated by (auto)phosphorylation within their activation loop (Nolen *et al.*, 2004). Usually, activation loop phosphorylation leads to a structural rearrangement, stabilizing the activation segment in a conformation that allows proper substrate positioning and phosphate transfer (Nolen *et al.*, 2004). However, some kinases are known to be active independently of such a phosphorylation (Nolen *et al.*, 2004), and data presented in this thesis indicate that Plk4 might belong to the latter group (Fig. 14). In addition to activation loop phosphorylation, other structural rearrangements dependent on phosphorylation have been reported to affect kinase activity. For instance, Calcium/Calmodulin-dependent kinase II (CamKII) exists in an autoinhibited state, where a C-terminal regulatory domain blocks substrate and ATP binding sites. Release from autoinhibition through binding of Ca^{2+}/Calmodulin induces catalytic activity, resulting in an immediate regulatory *trans*-autophosphorylation that renders the Ca^{2+}/Calmodulin off-rates to be magnitudes lower and thus positively feeds back on further kinase activation (Griffith, 2004).

In lack of a *bona fide* endogenous substrate to test the activity of immunoprecipitated Plk4 from human cells (Habedanck, 2006), we used the extent of autophosphorylation as a readout for kinase activity (Fig. 18). While the WT kinase and all phosphorylation site mutants, except for $Plk4^{S22D}$, displayed strong autophosphorylation activity and a correspondingly pronounced retarded mobility in SDS-PAGE, $Plk4^{D154A}$ and $Plk4^{S22D}$ appeared to be completely inactive. D154 is a residue of the critical and highly conserved DFG motif within protein kinase activation segments that aids in the proper positioning of Mg^{2+}-ATP for phosphate transfer (Nolen *et al.*, 2004). Mutation of this residue is widely used to render kinases inactive as a proper control in the elucidation of biological functions. In contrast, S22 is positioned within the G-loop of the small lobe of the kinase domain. With a following phenylalanine in the +1 position (see table in Fig. 15b), it minimally corresponds to the consensus motif proposed by Leung *et al.* (2007), and indeed S22 has also been detected as phosphorylated residue in the recombinant kinase, suggesting that it may represent an autophosphorylation site.

Finally, we tested the Plk4 phosphorylation site mutants for their ability to promote centriole overduplication. When transiently overexpressed in U2OS cells, myc-Plk4^{WT} caused centriole overduplication in about 80% of all transfected cells (Habedanck *et al.*, 2005), and similarly, overexpression of *Drosophila* Plk4 induced supernumerary centrosomes, even *de novo* in the unfertilized egg (Peel *et al.*, 2007; Rodrigues-Martins *et al.*, 2007). As predicted from their subcellular localizations and kinase activities, all mutants, except for Plk4^{D154A} and Plk4^{S22D}, readily caused centriole overduplication to an extent similar to the wildtype kinase. Plk4^{S22D} was expected to behave like the kinase-dead Plk4^{D154A} control, owing to its abolished kinase activity, and indeed both proteins caused overduplication in only about 30% of transfected cells (Fig. 20). A putative mechanism for this elevated background overduplication will be discussed below (see section 5.3).

Taken together, we conclude that none of the phosphorylation sites identified in this study is significantly involved in the known centrosomal processes catalyzed by Plk4. However, we emphasize at this point that, for technical reasons, no classical rescue experiments could be conducted. The reason for this is that levels of endogenous Plk4 are extremely low (Habedanck *et al.*, 2005; Bettencourt-Dias *et al.*, 2005), so that any detectable overexpression is likely to deliver a multiple of the endogenous protein. Furthermore, Plk4 levels within the cell are well balanced and fine-tuned, reflected by the fact that Plk$^{+/-}$ mice are haploinsufficient for tumor suppression (Ko *et al.*, 2005) and that centriole numbers are tightly correlated with Plk4 activity (Habedanck *et al.*, 2005; Kleylein-Sohn *et al.*, 2007; Bettencourt-Dias *et al.*, 2005; Cunha-Ferreira *et al.*, 2009b; Rogers *et al.*, 2009). In conjunction with different kinetics of the RNAi-mediated depletion and the CMV-driven expression of the transfected mutant, it appears impossible to restore physiological levels of mutant proteins at the depleted centrosome. For this reason, we cannot exclude that we might have missed a subtle role of one of the phosphorylation sites in the regulation of Plk4.

5.3. βTrCP-mediated degradation of Plk4

Protein kinases, once activated, can be downregulated through a variety of mechanisms, including phosphorylation/dephosphorylation and regulated proteolysis (Hunter, 2007). In fact, the activation-dependent degradation of protein kinases is an emerging theme (comprehensively reviewed in Lu & Hunter, 2009). This has been shown for the first time with regard to protein kinase C (PKC) degradation, as inhibition of PKC activity abolished its polyubiquitination and subsequent proteolysis (Lu *et al.*, 1998).

Long-standing evidence suggested that SCF-dependent proteolysis is involved in the regulation of the centriole duplication cycle, as Skp1 and Cul1 were found to localize to the centrosome (Freed *et al.*, 1999) and the SCF components Skp2, *Drosophila* SkpA and *Drosophila* Slimb/human βTrCP appeared to regulate centrosome numbers (Nakayama *et al.*, 2000; Murphy, 2003; Wojcik *et al.*, 2000; Guardavaccaro *et al.*, 2003). With the identification of Plk4 as a centrosomal target of the F-box protein *Drosophila* Slimb, a mechanism has been presented that for the first time establishes a direct link between SCF-dependent proteolysis and the centriole duplication cycle (Rogers *et al.*, 2009; Cunha-Ferreira *et al.*, 2009b). The core centriole duplication machinery has been well conserved throughout evolution (Bettencourt-Dias & Glover, 2007), but despite this conservation, some regulatory mechanisms are likely to be different between evolutionary distant organisms like *C. elegans*, *Drosophila* and humans. Accordingly, different roles have been proposed for certain key proteins, e.g. for SPD-2/Cep192. While SPD-2 in *C. elegans* is clearly involved in the biogenesis cascade upstream of ZYG-1 (Kemp *et al.*, 2004; Dammermann *et al.*, 2004), *Drosophila* SPD-2 is not required for centriole duplication (Dix & Raff, 2007), and for humans, evidence has been reported for both scenarios (Zhu *et al.*, 2008; Gomez-Ferreria *et al.*, 2007).

We therefore set out to determine whether human Plk4 might be regulated via proteolytic degradation in analogy to *Drosophila* Plk4. We first depleted the mammalian homologue of Slimb, βTrCP, via RNAi. In mammals, two distinct paralogues of βTrCP are expressed, but these two forms are indistuinguishable in their biochemical properties (Frescas & Pagano, 2008). Although preferences towards βTrCP1 or 2 have been reported for some substrates (e.g. Seo *et al.*, 2009), in most cases βTrCP1 and 2 are considered redundant (Frescas & Pagano, 2008). We therefore targeted βTrCP with siRNA duplexes that recognize both paralogues (Guardavaccaro *et al.*, 2003) in order to circumvent βTrCP redundancy (Fig. 21). In the further course of this discussion, we will thus only refer to βTrCP. We detected centriole overduplication in about 45% of all βTrCP-depleted cells, consistent with previous studies that reported centrosome overduplication in $\beta TrCP^{-/-}$ mouse embryonic fibroblasts (MEFs) and in *Drosophila* Slimb-mutant neuroblasts (Guardavaccaro *et al.*, 2003; Wojcik *et al.*, 2000). Most strikingly, we detected rosette-like procentriole arrangements around parental centrioles when we stained cells with antibodies to CP110, a distal centriolar cap protein. This phenotype was equal to cells overexpressing Plk4 (compare Figs. 10 and 21), and has been shown previously to represent multiple procentrioles engaged with a parental centriole (Kleylein-Sohn *et al.*, 2007). In *Drosophila*, Slimb RNAi has been shown

by immunoelectron microscopy to induce a similar phenotype, and here the authors reported a dependency on Plk4 (Cunha-Ferreira *et al.*, 2009b). Overexpression of the coiled-coil duplication protein HsSas-6 has also been shown to cause a similar phenotype (Strnad *et al.*, 2007). However, HsSas-6 proteolytic regulation was found to depend on APC/C^{Cdh1} (Strnad *et al.*, 2007), and Slimb RNAi in *Drosophila* did not interfere with DSas-6 levels (Cunha-Ferreira *et al.*, 2009b). We also noted that in βTrCP-depleted cells that formed a halo- or rosette-like procentriole arrangement, the IF signal for endogenous Plk4 was consistently elevated compared to control cells (Fig. 21b). Similarly, Cunha-Ferreira *et al*. (2009b) and Rogers *et al*. (2009) reported an increase of IF staining intensity for endogenous Plk4 levels at the centrosome. Exploiting the total levels of overexpressed Plk4 protein revealed a slight increase in protein levels in the absence of βTrCP (Fig. 22a); conversely, levels of overexpressed Plk4 were markedly decreased when βTrCP was co-overexpressed (Fig. 22b). Together, we conclude that βTrCP depletion causes a stabilization of endogenous Plk4, in turn leading to the near-simultaneous formation of multiple procentrioles around parental centrioles.

As Plk4 contains a conserved binding motif for βTrCP just C-terminal of its kinase domain, we asked whether Plk4 is a direct target of the F-box protein βTrCP. In retrospect, the majority of so-called PEST instability sequences (stretches rich in prolin, aspartate, serin and threonine, bounded by basic residues; Rogers *et al.*, 1986) in reality represents phosphodegrons (Hunter, 2007). An earlier study demonstrated a PEST sequence C-terminal to Plk4's kinase domain, that contains the conserved DSGHAT motif investigated here, to be involved in Plk4 turnover (Yamashita *et al.*, 2001). Our co-immunoprecipitation assays (Fig. 23) go well in line with the two studies on the interaction of these two proteins in *Drosophila* (Rogers *et al.*, 2009; Cunha-Ferreira *et al.*, 2009b), establishing that human βTrCP binds Plk4 directly in order to target it for degradation. This result provides a mechanistic explanation for the finding that proteasome inhibition evokes a procentriole overduplication phenotype similar to the one observed here, in line with the notion that the described effect was dependent on Plk4 (Duensing *et al.*, 2007).

βTrCP is known to bind its targets through a conserved DSGxxS/T motif (Skowyra *et al.*, 1997), although exceptions from this scheme have been reported, e.g. for Wee1 (Watanabe *et al.*, 2004). We therefore assessed whether βTrCP binding to Plk4 occurs solely via its conserved DSGHAT motif, and whether the interaction is dependent on phosphorylation of Plk4. Mutation of the two conserved phosphoacceptor residues in the phosphodegron completely abolished the interaction of the two proteins. However, as the

supposedly phosphomimetic S285D/T289D mutation did not restore binding to βTrCP, we confirmed the requirement of prior degron phosphorylation by phosphatase treatment. Here, substantial dephosphorylation of Plk4, as apparent from its abolished retarded mobility, also prevented association of βTrCP, clearly indicating that targeting Plk4 for $SCF^{\beta TrCP}$-mediated proteolysis requires the conserved phosphodegron to be phosphorylated, similar to what has been reported in *Drosophila* (Cunha-Ferreira *et al.*, 2009b; Rogers *et al.*, 2009).

Moreover, we identified another phosphorylated residue (S282) in the pool of Plk4 complexed with βTrCP (Fig. 26). Two independent studies reported the βTrCP-mediated degradation of the transcription factor REST (Westbrook *et al.*, 2008; Guardavaccaro *et al.*, 2008), yet with conflicting data on the identity of the involved phosphodegron. Westbrook and colleagues determined a phosphorylation site similarly upstream of the phosphodegron as S282 presented here, and mutational analyses suggested this site to be involved in βTrCP binding. Here, the identified residue S282 also appeared to be involved in binding, yet the mutation only weakened the interaction in contrast to the classical phosphodegron double-mutation. Of note, S282 was also found as autophosphorylation site in the analysis of the recombinant protein (Fig. 22b), raising the possibility that an autophosphorylation event might be involved in Plk4's degradation process (see below).

We have firmly established that human Plk4 is degraded in an $SCF^{\beta TrCP}$-dependent manner, and our findings thus highlight the remarkable degree of conservation within the centriole biogenesis pathway between such distant organisms as humans and flies. The fact that all investigated Plk4 homologues, including ZYG-1, contain the DSGxxT motif lends support to the assumption that this mechanism of Plk4 regulation has been preserved in evolution. Yet, with the identification of βTrCP-mediated degradation, we just know *how* regulatory input impinges upon Plk4 activity, but we still lack information on the signaling pathways that control this process. Thus, the stage is now set for the identification of the kinase(s) responsible for degron phosphorylation.

When we tested all generated Plk4 phosphorylation site mutants (Fig. 15) for their ability to be recognized by βTrCP, we discovered that both $Plk4^{D154A}$ and $Plk4^{S22D}$ failed to bind (Fig. 27). This is unlikely to arise from a general misfolding of the kinase domain, as these mutations are expected to alter significantly different structures within the kinase domain. We therefore conclude that an autophosphorylation event might be necessary for proper degradation of Plk4. In support of this, kinase-dead $Plk4^{D154A}$ was stabilized equally to the phosphodegron mutant $Plk4^{S285A/T289A}$ (Fig. 28).

Having established that autophosphorylation of Plk4 is required for its proper degradation, we additionally could show that this defect could be rescued by simultaneous co-overexpression of active $Plk4^{WT}$ *in vivo* (Fig. 29). Thus, our data strongly argue in favor of an important autophosphorylation site to be missing on $Plk4^{D154A}$ for βTrCP recognition, and suggest that this putative site is likely to be autophosphorylated *in trans*. Similar to our findings, the degradation of PKCη was also found to depend on *trans*-autophosphorylation (Kang *et al.*, 2000). The inactive PKCη wildtype kinase exists in an autoinhibited state where a C-terminal pseudosubstrate sequence folds back and blocks the kinase domain. While in this conformation PKCη was not degraded, activation of the kinase or mutation of the pseudosubstrate sequence resulted in rapid proteolytic degradation. Interestingly, a pseudo-substrate mutant that additionally carried a kinase-inactivating mutation (i.e. that adopted the same open conformation as the activated wildtype kinase) was not degraded, suggesting that after activation an autophosphorylation event has to occur. Moreover, simultaneous overexpression of active PKCη restored the degradation of the mutant.

So far, we have not been able to experimentally determine whether or not this proposed autophosphorylation event is also sufficient for Plk4 degradation. Further experiments will have to address whether active, *de*phosphorylated $Plk4^{WT}$ (that looses its phosphodegron for βTrCP binding, see Fig. 24) can restore its own phosphodegron *in vitro*, or whether the activity of another kinase is additionally required for this process. In most cases investigated, the double phosphorylation of a DSGxxT degron is carried out by two different kinases, providing an elegant 'AND logic gate' for the integration of different signaling pathways (Hunter, 2007). Taken together, we hypothesize that (continuous?) *trans*-auto-phosphorylation of active Plk4 initiates its own degradation, either dependent or independent of another kinase (Fig. 31).

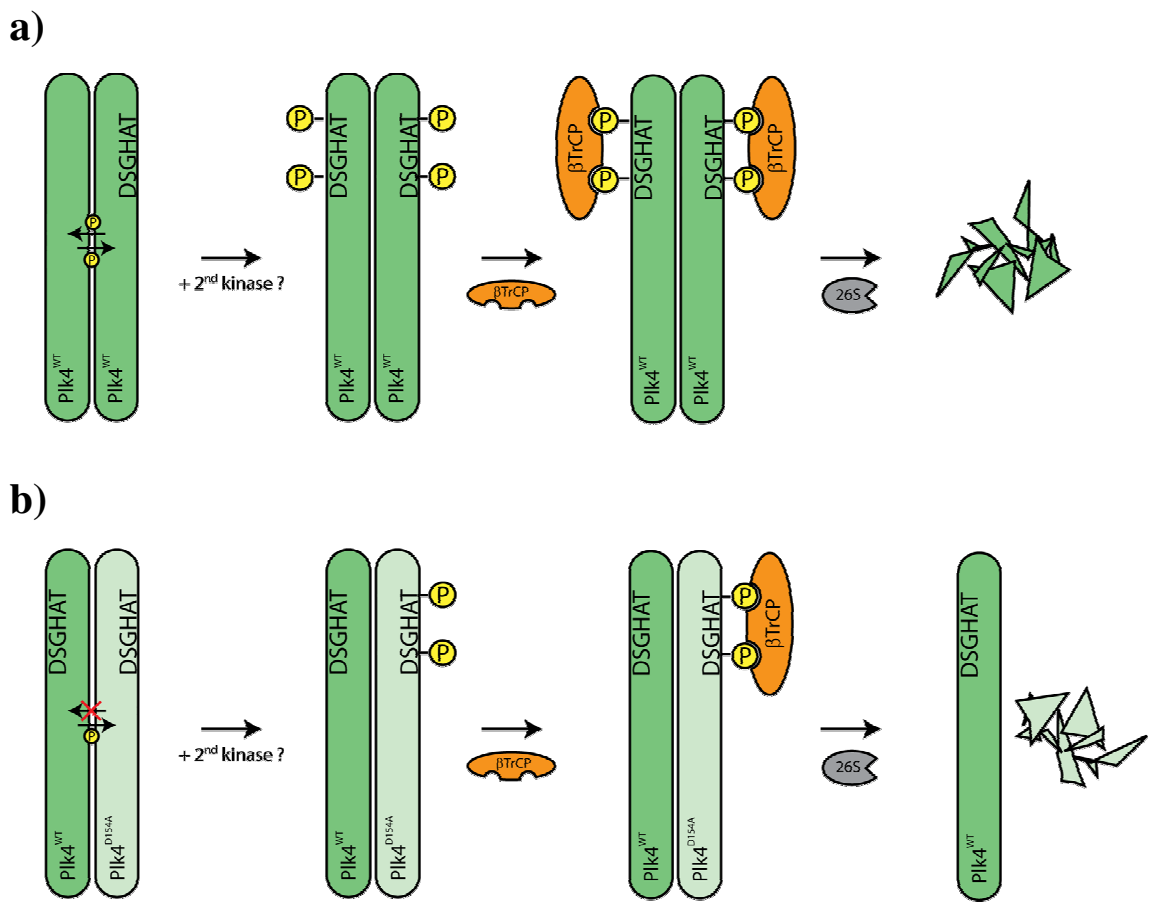

Fig. 31: Model for the autophosphorylation-dependent proteolytic degradation of Plk4.
(a) In normal cells, homodimers of active endogenous Plk4 (constantly?) autophosphorylate *in trans*. This leads to the phosphorylation of the DSGHAT phosphodegron of Plk4, either dependent or independent of a second kinase, and finally to the proteolytic destruction of active Plk4 through the 26S proteasome. **(b)** In cells overexpressing a kinase-dead mutant of Plk4 (e.g. Plk4^{D154A}, depicted in light green), heterodimers with the endogenous kinase (dark green) are expected to form. In this scenario, *trans*-autophosphorylation of the endogenous kinase is blocked and βTrCP fails to bind. As a consequence, endogenous Plk4 is stabilized and accumulates to levels sufficient to induce *bona fide* centriole overduplication.

This model elegantly reconciles the strict requirement for Plk4 kinase activity for centriole duplication (see Fig. 11b) with the unexpected finding that kinase-dead Plk4^{D154A} (Fig. 10) as well as N-terminal Plk4 truncations (Fig. 30) are able to trigger *bona fide* centriole overduplication. As dimerization of Plk4 is independent of its kinase activity (see Figs. 19 and 30b), a subfraction of overexpressed Plk4^{D154A} (or Plk4$^{aa265-970}$ or Plk4$^{aa609-970}$) is expected to form heterodimers with the endogenous kinase. In such heterodimers, endogenous Plk4 is not autophosphorylated *in trans* and consequently not recognized by βTrCP. Thus, the stabilized endogenous Plk4 eventually accumulates and triggers the formation of rosette-like procentriole arrangements (schematically summarized in Fig. 31).

According to this scheme, we further propose that Plk4 degradation takes place in early S phase (or continuously), as no cell cycle progression through late S, G_2 and M phases is required for $Plk4^{D154A}$ to induce overduplication (Fig. 11).

In summary, these data pave the way towards the beginning of a mechanistic understanding of Plk4 regulation by controlled proteolysis. It will be of central importance to determine whether Plk4 autophosphorylation is not only required but sufficient for degradation, and to identify further players (notably a potential second kinase) in the process. In light of the emerging view that supernumerary centrosomes are not only a consequence but potentially also a cause of tumorigenesis (Nigg, 2002; Castellanos *et al.*, 2008; Basto *et al.*, 2008; Ganem *et al.*, 2009), the necessity to unravel the complex regulation of centrosome biology may also contribute to a better understanding of cancerogenesis.

6. Materials and Methods

Chemicals and materials

All chemicals were purchased from Merck, Sigma-Aldrich Chemical Company (St Louis, MO), Fluka-Biochemika (Switzerland), or Roth, unless otherwise stated. Growth media components for *E. coli* were from Difco Laboratories or Merck. The Minigel system was purchased from Bio-Rad and the Hoefer SemiPHor Blotting system from Pharmacia-Biotech. Tabletop centrifuges were from Eppendorf.

Plasmid construction

All cloning procedures were performed according to standard techniques as described in Molecular Cloning, A Laboratory Manual, 2nd editition, Sambrook, J., Fritsch, E.F., Maniatis, T., Cold Spring Harbor Laboratory Press 1989 and Current Protocols in Molecular Biology, Wiley, 1999. Restriction enzyme reactions were carried out as specified by the supplier (Fermentas) and ligation reactions were done using T4 DNA Ligase (NEB). Extraction of DNA from agarose gels and preparation of plasmid DNA was performed using kits from QIAGEN according to the manufacturer's instructions. For PCR reactions, the Pfu DNA polymerase PCR System was used as recommended by the manufacturer (Promega) and reactions were carried out in a RoboCycler Gradient 96 (Stratagene). All PCR products were checked by sequencing at Medigenomix (Martinsried, Germany).

Human Plk4 cDNA was constructed by Dr. Robert Habedanck (Habedanck, 2006). Sequence mutations were inserted by using the Stratagene QuickChange site-directed mutagenesis kit according to the manufacturer's instructions (for primers, see below).

Antibody Production

A Plk4 fragment spanning residues 888-970 was expressed as a GST-tagged fusion protein in *E. coli* and purified under denaturing conditions. Polyclonal antibodies were raised at Charles River Laboratories (Romans, France). Antibodies were affinity-purified using GST-tagged antigen bound to Affigel (Biorad) according to standard protocols.

Cell culture and transfections

All cells were grown at 37°C in a 5% CO_2 atmosphere. HeLa, U2OS or HEK293T cells were cultured in Dulbecco's modified Eagle's medium (DMEM), supplemented with 10% heat-inactivated fetal calf serum and penicillin-streptomycin (100 µg/ml, Gibco-BRL, Karlsruhe, Germany).

Cells adherent on acid treated glass coverslips were transiently transfected using FuGene (Roche Diagnostics, Mannheim, Germany) according to the manufacturer's protocol.

Tetracycline-inducible cell lines expressing myc-tagged $Plk4^{WT}$ and $Plk4^{D154A}$ were generated by transfection of U2OS-TRex cells (Invitrogen). Stable transformants were established by selection for

two weeks with 1 mg/ml G418 (Invitrogen, Carlsbad, CA) and 50 µg/ml hygromycin (Merck, Darmstadt, Germany) after which colonies were picked and tested for Plk4 expression by immunofluorescence and by Western blot analysis. Cell lines were induced to express Plk4 by adding 1 µg/ml tetracycline to the growth medium.

siRNA-mediated protein depletion

Proteins were depleted using siRNA duplex oligonucleotides (Dharmacon Research Inc, Lafayette, CO and Qiagen, Hilden, Germany). siRNA target sequences are listed below. Oligoduplexes targeting luciferase were used as control (GL2, Elbashir *et al.*, 2001). Transfections were performed using Oligofectamin (Invitrogen, Carlsbad, CA) according to the manufacturer's protocol; in case of rescue experiments (see below), the transfection mix was replaced with fresh medium after 6h in order to improve cell viability.

RNAi rescue experiments were performed using the inducible stable cell lines U2OS-B6 ($Plk4^{WT}$), U2OS-D2 ($Plk4^{D154A}$) and U2OS-B3 ($Plk4^{D154A}$, not shown). Cells were depleted for endogenous Plk4 or HsSas6 (as positive control) for 24h as described above. Cells were then arrested in S phase by the addition of 1.6 µg/ml aphidicolin for 8h prior to induction of protein expression for 16h.

Cell extracts, immunoprecipitations and immunoblotting

For immunoprecipitations of epitope-tagged overexpressed proteins, HEK293T cells were plated to approx. 50% confluency in 10 cm cell culture dishes. 24h later, cells were transfected as described above with 5 µg of plasmid DNA. For co-immunoprecipitations, 3 µg of plasmid encoding FLAG-tagged protein and 2 µg of plasmid encoding myc-tagged protein were mixed and transfected as described above. After transfection, cells were trypsinized and collected, washed with PBS and lysed on ice for 20 min in lysis buffer (50mM Tris-HCl pH 7.4, 0.5% NP40, 150mM NaCl, 1mM DTT, 5% glycerol, 50mM NaF, 1mM PMSF, 25mM β-glycerophosphate, 1mM vanadate, Complete Mini protease inhibitor cocktail (Roche Diagnostics, Mannheim, Germany)). Lysates were cleared by centrifugation for 15 min at 16,000 g, 4°C, and incubated with proteinG beads bearing epitope-tag targeting antibodies (mouse monoclonal 9E10 αmyc; mouse monoclonal M2 αFLAG affigel (Sigma, Steinheim, Germany)) for 2h at 4°C. Immunocomplexes bound to beads were washed three times with (Co-)IP wash buffer (50mM Tris-HCl pH 7.4, 0.5% NP40, 300mM NaCl, 1mM DTT, 5% glycerol, 50mM NaF, 1mM PMSF, 25mM β-glycerophosphate, 1mM vanadate). Beads carrying bound proteins for use in *in vitro* kinase assays were treated as described below. Otherwise, immunoprecipitated proteins were eluted into Laemmli buffer, separated by SDS-PAGE and transferred to PVDF membranes using a Hoefer semi-dry blotting apparatus (Amersham Biosciences, Little Chalfont, UK). For Western blot analysis, membranes were incubated for 30 min in blocking buffer (5% low-fat dry milk in PBS, 0.1% Tween-20). All antibody incubations were carried out in blocking buffer overnight at 4°C. Membranes were probed with indicated antibodies in blocking buffer, followed by incubation

with HRP conjugated goat anti-mouse or anti-rabbit antibodies (Jackson Immunoresearch). Signals were detected by enhanced chemoluminescence using ECL reagents (Amersham Biosciences, Little Chalfont, UK).

To assay protein degradation kinetics, 293T cells were transfected with the respective plasmids for 16h. In order to globally shut off translation, 25 µg/ml cycloheximide was added to the cells (t = 0 h). At timepoints 0h, 4h, and 8h, one plate of transfected cells was lysed and total cell extracts were immunoblotted for the overexpressed protein as described above.

Purification of the recombinant Plk4$^{aa1-265}$ kinase domain

The GST-tagged WT and D154A mutant of Plk4$^{aa1-265}$ was expressed in *E. coli* BL 21 RIL codon + (Invitrogen). To express the protein, a starter culture of transformed bacteria was grown overnight under ampicillin selection and diluted 1:10 with fresh medium in the morning. The culture was grown to OD_{600} = 0.6 and expression of the recombinant protein was induced with 1mM IPTG at 30°C for 3h. Cells were then pelleted by centrifugation, lysed in buffer (20mM Tris-HCl pH7.4, 0.5% NP40, 150mM NaCl, 1mM DTT, 5% glycerol, 5mM PMSF) by sonication and centrifuged to remove debris. The lysate was then incubated with glutathione coated beads (Amersham) for 1h to allow binding of expressed protein. After three washing steps with lysis buffer and one washing with elution buffer without glutathione, GST-tagged Plk4$^{aa1-265}$ was then eluted by incubating beads in elution buffer (50mM HEPES pH 7.5, 100mM NaCl, 10mM $MgCl_2$, 10mM glutathione, 5% glycerol, 1mM DTT).

In vitro kinase assays

Following immunoprecipitation, tagged Plk4 immunocomplexes were washed three times with lysis buffer and once with Plk4 kinase buffer (50mM HEPES pH 7.0, 100mM NaCl, 10mM $MgCl_2$, 5% glycerol, 1mM DTT). Alternatively, 1 µg of recombinant GST-tagged Plk4$^{aa1-265}$ kinase domain was used as enzyme. Kinase reactions were carried out for 30min at 30°C in Plk4 kinase buffer supplemented with 10µM ATP and 2µCi of (γ-^{32}P)-ATP (Hartmann). Kinase reactions were stopped by addition of sample buffer and heating at 95°C for 5 minutes. Proteins were then separated by SDS-PAGE and transferred to PVDF membranes in the case of immunoprecipitated kinase. Alternatively, when recombinant proteins were used, SDS-PAGE gels were stained by Coomassie Blue followed by drying on filter paper. ^{32}P incorporation was visualized by autoradiography.

Microscopic techniques

Immunofluorescence microscopy was carried out as described (Meraldi *et al*., 1999). Briefly, cells were fixed on coverslips in -20°C methanol for at least 5 minutes before incubation in blocking buffer (2% BSA in PBS). After rehydration in PBS, cells were incubated with primary antibodies in blocking buffer for 1 hour at room temperature, followed by staining with Alexa-Fluor conjugated goat secondary antibodies (Molecular probes). DNA was visualized by staining with DAPI (200 ng/ml).

Coverslips were mounted onto glass slides using mounting medium (phenylenediamine in 90% glycerol). Slides were analyzed using a Zeiss Axioplan II microscope with Apochromat 63x and 100x/1.4 n.a. oil immersion objectives and images were taken using a CoolSNAP HQ CCD camera (Photometrics, Tuczon, AZ) and Metaview (Visitron Systems GmbH, Puchheim, Germany) software followed by processing with Adobe Photoshop CS2 (Adobe Systems, Mountain View, CA).

Mass spectrometry

Proteins isolated by (co-)immunoprecipitation were prepared for mass spectrometric analysis as previously described. Briefly, for 1D-gel electrophoresis, proteins were separated on a NuPAGE Bis-Tris gel (4-12%) from which the spacers between the lanes had been removed to achieve maximal loading capacity. The separated proteins were stained with Coomassie Blue and bands were excised and in-gel digested using trypsin or elastase (Promega, sequencing-grade). Peptides were desalted and concentrated using C18 extraction tips.

All analyses were kindly performed by Dr. Roman Körner and his group (Max-Planck Institute of Biochemistry, Martinsried, Germany).

SILAC media

DMEM high glucose medium deficient in amino acids arginine and lysine was supplemented with 5% dialyzed FCS, penicillin-streptomycin (100µg/mL), and either unlabeled L-arginine.HCl and L-lysine.HCl (*SILAC light*), L-arginine-U-$^{13}C_6$HCl and L-lysine-$^{2}H_4$.2HCl (*SILAC medium*), or L-arginine-U-$^{13}C_6$-$^{15}N_4$.HCl and L-lysine-U-$^{13}C_6$-$^{15}N_2$.HCl (*SILAC heavy*) at concentrations of 42 µg/mL (arginine) and 72 µg/mL (lysine). Supplemented amino acids were from Cambridge Isotope Laboratories. Media were kept at 37°C before use.

Titansphere enrichment of phosphopeptides

Phosphopeptides were enriched using TiO_2 columns as described previously with minor modifications. Approximately 3 µl of Titansphere (GL Sciences, Japan) suspension (100 mg/ml re-suspended in 80% acetonitrile in Milli-Q water/2% TFA) were placed on top of home-made C8 (Empore, 3M) STAGE Tips in 200 µl GELoader (Eppendorf) pipette-tips. The columns were washed twice with 40 µl of LA1 solution (80% acetonitrile/0.2% TFA + 300 mg/ml of lactic acid as a modifier). Dried samples were reconstituted in LA2 solution (80% acetonitrile/2% TFA + 300 mg/ml of lactic acid as a modifier), loaded on TiO_2 columns, and slowly passed through twice. The TiO_2 columns were washed with the following solutions: 40 µl of LA1 solution, 40 µl of 80% acetonitrile/0.2% TFA and 40 µl of water. Flow-through fractions were collected and analyzed separately for the determination of protein ratios. Phosphorylated peptides bound on the TiO_2 were eluted slowly with 60 µl of freshly prepared 0.6% ammonium hydroxide and 30 µl of 80% acetonitrile/0.2% TFA. Phosphopeptide enriched eluates were immediately acidified with 12 µl of 5% formic acid (FA) and dried in a SpeedVac concentrator. The

phosphopeptide samples and the flow-through samples were desalted and purified on C18 STAGE columns and resuspended in 5 µl of 0.5% FA for online nanoLC-Orbitrap analysis.

Mass spectrometry analysis

Desalted Titansphere-eluates (enriched for phosphopeptides) and flow-through fractions (non-phosphorylated peptides) were analyzed by online C18 reversed-phase nanoscale liquid chromatography tandem mass spectrometry on a NanoAcquity UPLC system (Waters) connected to an Orbitrap (Thermo Electron) equipped with a nanoelectrospray ion source (Proxeon). The mass spectrometer was operated in data-dependent mode for software controlled switching between MS survey and MS/MS fragmentation.

Desalted samples were loaded by the NanoAcquity autosampler directly onto a 13-cm pulled fused-silica capillary packed with ReproSil-Pur C18-AQ (Dr. Maisch GmbH) 3-µm reversed-phase material at a flow of 350 nl/minute for 30 minutes. This fritless capillary column had an internal diameter of 75 µm and a tip opening of 8 µm (NewObjective). Peptides were then separated by a stepwise 90-minutes gradient of 0–100% between buffer A (2% ACN, 0.5% formic acid) and buffer B (80% ACN, 0.5% formic acid) at a flow rate of 200 nL/minutes. Orbitrap full scan MS spectra (from m/z 350-1500) were acquired by the Orbitrap at a resolution of 60,000 and the five most intensive ions were fragmented in the linear ion trap using collision-induced dissociation. Fragmented target ions selected for MS/MS were dynamically excluded for 60s. The total cycle time was approximately 1.5 s. Other Orbitrap parameters were: spray voltage, 2.3 kV; no sheath and auxiliary gas flow; ion transfer tube temperature, 170 °C; normalized collision energy using wide band activation mode and multistage activation mode, on; collision energy for MS2, 35%; MS2 selection threshold, 250 counts; activation q, 0.25; activation time, 30 ms.

Data analysis

MaxQuant (version 1.0.12.5) was used for identification and quantitation of phosphopeptides. A peptide false discovery rate (FDR) specification of 0.01 was used, whereas the precursor mass tolerance was set to 7 ppm, and refined during MaxQuant processing as described(Cox & Mann, 2008). To account for differences in protein levels, all determined phosphopeptide ratios were normalized by the measured ratios of the corresponding proteins. For the determination of protein levels, at least two unmodified peptides were required. Otherwise, MaxQuant default parameters were used. Data were searched against IPI_human (version 3.48) using MASCOT (version 2.204). Results were filtered using Mascot Score ≥ 12 and phosphorylation site localization probabilities ≥ 75% as criteria.

Table 1: siRNA duplexes used in this study.

Gene	Target sequence	Internal oligo#
hSas-6	5'-CTAGATGATGCTACTAAGCAA-3'	295
Plk4	5'-CTGGTAGTACTAGTTCACCTA-3'	302
Plk4 3'UTR	5'-NNCTCCTTTCAGACATATAAG-3'	141/142
βTrCP1/2*	5'-AAGTGGAATTTGTGGAACATC-3'	488

*Guardavaccaro *et al.* (2003)

Table 2: Antibodies used in this study. a.p., affinity-purified.

Number	Antigen	Made in	Dilution	Comment	Distributor/reference
738	human Cep135	rabbit	1:2000	a.p.	Kleylein-Sohn *et al*., 2007
689	human Plk4	rabbit	1:500	a.p.	this work; Kleylein-Sohn *et al*., 2007
DM1A	α-tubulin	mouse	1:5000	a.p.	Sigma
36-298-4	human Plk1	mouse	1:3	hybridoma supernatant	(Yamaguchi *et al.*, 2005)
9E10	myc tag	mouse	1:6	hybridoma supernatant	(Evan *et al.*, 1985)
M2	FLAG tag	mouse	1:1000	a.p.	Sigma
HE-12	human cyclin-E	mouse	undiluted	hybridoma supernatant	Kindly provided by J. Bartek (Danish Cancer Society, Copenhagen
V152	human cyclin-B1	mouse	1:1000	a.p.	Millipore
766.2	human CP110	rabbit	1:1000	a.p.	Schmidt *et al.* (2009)
4G10	phophotyrosine	mouse	1:1000	a.p.	Sigma

Table 3: Primers used for mutagenesis of Plk4.

Name	Dept number	Purpose	sequence (5' > 3')
oJW2	3920	mutagenesis S22A	CTTGGTAAAGGAGCATTTGCTGGTGTCTACAGAGC
oJW3	3921		GCTCTGTAGACACCAGCAAATGCTCCTTTACCAAG
oJW4	3922	mutagenesis S22D	CTTGGTAAAGGAGACTTTGCTGGTGTCTACAGAGC
oJW5	3923		GCTCTGTAGACACCAGCAAAGTCTCCTTTACCAAG
oJW6	3924	mutagenesis S401A	GAACGATGTCACGCAGCAGAAATGCTTTCAGTGTCC
oJW7	3925		GGACACTGAAAGCATTTCTGCTGCGTGACATCGTTC
oJW8	3926	mutagenesis S401D	GAACGATGTCACGACGCAGAAATGCTTTCAGTGTCC
oJW9	3927		GGACACTGAAAGCATTTCTGCGTCGTGACATCGTTC
oJW10	3928		TTAAGAAGCATTACAGCTCCGTTGGTTGCTCACAGG

oJW11	3929		CCTGTGAGCAACCAACGGAGCTGTAATGCTTCTTAA
oJW12	3930	mutagenesis S592D	TTAAGAAGCATTACAGATCCGTTGGTTGCTCACAGG
oJW13	3931		CCTGTGAGCAACCAACGGATCTGTAATGCTTCTTAA
oJW14	3932	mutagenesis S665A	GATAGACCACCCGCACCTACTGACAACATC
oJW15	3933		GATGTTGTCAGTAGGTGCGGGTGGTCTATC
oJW16	3934	mutagenesis S665D	GATAGACCACCCGACCCTACTGACAACATC
oJW17	3935		GATGTTGTCAGTAGGGTCGGGTGGTCTATC
oJW18	3936	mutagenesis S817A	CCTAAGGCCTTAGCACCTCCTCCTTCTGTGG
oJW19	3937		CCACAGAAGGAGGAGGTGCTAAGGCCTTAGG
oJW20	3938	mutagenesis S817D	CCTAAGGCCTTAGACCCTCCTCCTTCTGTGG
oJW21	3939		CCACAGAAGGAGGAGGGTCTAAGGCCTTAGG
oJW26	5181	muatgenesis S499A	GAATATGACAGCATCGCCCCAAACCGGGACTTCCAGGG
oJW27	5182		CCCTGGAAGTCCCGGTTTGGGGCGATGCTGTCATATTC
oJW28	5183	muatgenesis S499D	GAATATGACAGCATCGACCCAAACCGGGACTTCCAGGG
oJW29	5184		CCCTGGAAGTCCCGGTTTGGGTCGATGCTGTCATATTC
oJW30	4353	mutagenesis S22E	CTTGGTAAAGGAGAATTTGCTGGTGTCTACAGAGC
oJW31	4354		GCTCTGTAGACACCAGCAAATTCTCCTTTACCAAG
oJW37	4809	mutagenesis Y177E	TGTGGAACTCCTAACGAAATTTCACCAGAAATTGCC
oJW38	4810		GGCAATTTCTGGTGAAATTTCGTTAGGAGTTCCACA
oJW39	4811	mutagenesis Y177F	TGTGGAACTCCTAACTTCATTTCACCAGAAATTGCC
oJW40	4812		GGCAATTTCTGGTGAAATGAAGTTAGGAGTTCCACA
oJW41	4813	mutagenesis T138A	CTACACCGGGACCTCGCACTTTCTAACCTCCTACTG
oJW42	4814		CAGTAGGAGGTTAGAAAGTGCGAGGTCCCGGTGTAG
oJW43	4815	mutagenesis T138D	CTACACCGGGACCTCGATCTTTCTAACCTCCTACTG
oJW44	4816		CAGTAGGAGGTTAGAAAGATCGAGGTCCCGGTGTAG
oJW45	4845	mutagenesis T170V	CATGAAAAGCACTATGTATTATGTGGAACTCC
oJW46	4846		GGAGTTCCACATAATACATAGTGCTTTTCATG
oJW64	6025	mutagenesis S285A / T289A	GAAGACTCAATTGATGCTGGGCATGCCGCAATTTCTACTGC
oJW65	6026		GCAGTAGAAATTGCGGCATGCCCAGCATCAATTGAGTCTTC
oJW66	6027	mutagenesis S285D / T289D	GAAGACTCAATTGATGACGGGCATGCCGACATTTCTACTGC
oJW67	6028		GCAGTAGAAATGTCGGCATGCCCGTCATCAATTGAGTCTTC
oJW79	6084	mutagenesis S282A	TTAGGAACTGTGGAAGACGCAATTGATAGTGGGCATGCC
oJW80	6085		GGCATGCCCACTATCAATTGCGTCTTCCACAGTTCCTAA
oJW81	6086	mutagenesis S282D	TTAGGAACTGTGGAAGACGACATTGATAGTGGGCATGCC
oJW82	6087		GGCATGCCCACTATCAATGTCGTCTTCCACAGTTCCTAA
oJW91	6133	mutagenesis G277R	ACAAAAAGTAAAGATTTACGAACTGTGGAAGACTCAATTG
oJW92	6134		CAATTGAGTCTTCCACAGTTCGTAAATCTTTACTTTTTGT
oJW93	6135	mutagenesis I294K	GCCACAATTTCTACTGCAAAGACAGCTTCTTCCAGTACC
oJW94	6136		GGTACTGGAAGAAGCTGTCTTTGCAGTAGAAATTGTGGC
oHR41	*1575*	*mutagenesis T170D*	*CATGAAAAGCACTATGACTTATGTGGAACTCC*
oHR44	*1583*		*GGAGTTCCACATAAGTCATAGTGCTTTTCATG*

Table 4: Plasmids relevant to this study.

Name	Insert	Vector
pJW 3	N-myc-Plk4 FL D154A	pcDNA3.1-3xmyc-TO
pJW 4	N-myc-Plk4 WT FL	pcDNA3.1-3xmyc-TO
pJW 14	N-myc-Plk4 WT aa1-608	pcDNA3.1-3xmyc-TO
pJW 18	N-FLAG-Plk4 WT aa1-608	pcDNA3.1-NFLAG-TO
pJW34b	N-GST-Plk4 aa1-265 S22A	pGEX-5X-2
pJW 35	N-GST-Plk4 aa1-265 S22D	pGEX-5X-2
pJW 38	N-myc-Plk4 FL S22A	pcDNA3.1-3xmyc-TO
pJW 39	N-myc-Plk4 FL S22D	pcDNA3.1-3xmyc-TO
pJW 40	N-myc-Plk4 FL S401A	pcDNA3.1-3xmyc-TO
pJW 41	N-myc-Plk4 FL S401D	pcDNA3.1-3xmyc-TO
pJW 42	N-myc-Plk4 FL S592A	pcDNA3.1-3xmyc-TO
pJW 43	N-myc-Plk4 FL S592D	pcDNA3.1-3xmyc-TO
pJW 44	N-myc-Plk4 FL S665A	pcDNA3.1-3xmyc-TO
pJW 45	N-myc-Plk4 FL S665D	pcDNA3.1-3xmyc-TO
pJW 46	N-myc-Plk4 FL S817A	pcDNA3.1-3xmyc-TO
pJW 47	N-myc-Plk4 FL S817D	pcDNA3.1-3xmyc-TO
pJW 48	N-FLAG-Plk4 FL S22A	pcDNA3.1-NFLAG-TO
pJW 49	N-FLAG-Plk4 FL S22D	pcDNA3.1-NFLAG-TO
pJW 50	N-FLAG-Plk4 FL S401A	pcDNA3.1-NFLAG-TO
pJW 51	N-FLAG-Plk4 FL S401D	pcDNA3.1-NFLAG-TO
pJW 52	N-FLAG-Plk4 FL S592A	pcDNA3.1-NFLAG-TO
pJW 53	N-FLAG-Plk4 FL S592D	pcDNA3.1-NFLAG-TO
pJW 54	N-FLAG-Plk4 FL S665A	pcDNA3.1-NFLAG-TO
pJW 55	N-FLAG-Plk4 FL S665D	pcDNA3.1-NFLAG-TO
pJW 56	N-FLAG-Plk4 FL S817A	pcDNA3.1-NFLAG-TO
pJW 57	N-FLAG-Plk4 FL S817D	pcDNA3.1-NFLAG-TO
pJW 58	N-FLAG Plk4 WT aa1-889	pcDNA3.1-NFLAG-TO
pJW66	N-myc-Plk4 WT aa1-750	pcDNA3.1-3xmyc-TO
pJW67	N-myc-Plk4 WT aa1-778	pcDNA3.1-3xmyc-TO
pJW70	N-myc-Plk4 WT aa609-970	pcDNA3.1-3xmyc-TO
pJW73	N-FLAG-Plk4 WT aa1-750	pcDNA3.1-NFLAG-TO
pJW74	N- FLAG-Plk4 WT aa1-778	pcDNA3.1-NFLAG-TO
pJW77	N- FLAG-Plk4 WT aa609-970	pcDNA3.1-NFLAG-TO
pJW83	N-myc-Plk4 FL S499A	pcDNA3.1-3xmyc-TO
pJW84	N-FLAG-Plk4 FL S499A	pcDNA3.1-NFLAG-TO
pJW85	N-myc-Plk4 FL S499D	pcDNA3.1-3xmyc-TO
pJW86	N-FLAG-Plk4 FL S499D	pcDNA3.1-NFLAG-TO
pJW87	N-myc-Plk4 FL S22E	pcDNA3.1-3xmyc-TO
pJW88	N-FLAG-Plk4 FL S22E	pcDNA3.1-NFLAG-TO
pJW94	N-GST-Plk4 aa1-430 WT	pGEX-5X-2
pJW95	N-GST-Plk4 aa1-430 D154A	pGEX-5X-2

pJW98	N-GST-Plk4 aa1-608 WT	pGEX-5X-2
pJW100	N-GST-Plk4 aa1-608 D154A	pGEX-5X-2
pJW101	N-GST-Plk4 aa609-970	pGEX-5X-2
pJW108	N-GST-Plk4 aa1-889 WT	pGEX-5X-2
pJW109b	N-GST-Plk4 aa1-889 D154A	pGEX-5X-2
pJW111	N-GST-Plk4 aa1-265 T170V	pGEX-5X-2
pJW112	N-GST-Plk4 aa1-265 T170D	pGEX-5X-2
pJW113	N-GST-Plk4 aa1-265 Y177F	pGEX-5X-2
pJW114	N-GST-Plk4 aa1-265 Y177E	pGEX-5X-2
pJW115	N-GST-Plk4 aa1-265 T138A	pGEX-5X-2
pJW116	N-GST-Plk4 aa1-265 T138D	pGEX-5X-2
pJW167	N-myc-Plk4 D154A aa1-750	pcDNA3.1-3xmyc-TO
pJW168	N-myc-Plk4 D154A aa1-778	pcDNA3.1-3xmyc-TO
pJW169	N-FLAG-Plk4 D154A aa1-750	pcDNA3.1-NFLAG-TO
pJW170	N-FLAG-Plk4 D154A aa1-778	pcDNA3.1-NFLAG-TO
pJW185	N-myc-Plk4 FL S285A/T289A	pcDNA3.1-3xmyc-TO
pJW186	N-myc-Plk4 FL S285D/T289D	pcDNA3.1-3xmyc-TO
pJW187	N-FLAG-Plk4 FL S285A/T289A	pcDNA3.1-NFLAG-TO
pJW188	N-FLAG-Plk4 FL S285D/T289D	pcDNA3.1-NFLAG-TO
pJW189	N-myc-Plk4 D154A aa1-608	pcDNA3.1-3xmyc-TO
pJW190	N-myc-Plk4 D154A aa1-889	pcDNA3.1-3xmyc-TO
pJW191	N-FLAG-Plk4 D154A aa1-608	pcDNA3.1-NFLAG-TO
pJW192	N-FLAG-Plk4 D154A aa1-889	pcDNA3.1-NFLAG-TO

7. Abbreviations

All units are abbreviated according to the International Unit System.

aa: amino acid(s)

ATP: adenosine 5´-triphosphate

βTrCP: β-transducin repeat containing protein

BSA: bovine serum albumin

Cep: centrosomal protein

CHX: Cycloheximide

DAPI: 4´,6-diamidino-2-phenylindole

DTT: dithiothreitol

ECL: enhanced chemiluminescence

EDTA: ethylenedinitrilotetraacetic acid

EGFP: enhanced green fluorescent protein

EM: electron microscopy

FCS: Fetal calf serum

GFP: green fluorescent protein

HCl: hydrochloric acid

HEPES: N-2-Hydroxyethylpiperazine-N`-2-ethane sulfonic acid

IgG: Immunoglobulin G

IF: Immunofluorescence

IP: Immunoprecipitation

IPTG: isopropyl-beta-D-thiogalactopyranoside

mAb: monoclonal antibody

MS: mass spectrometry

MT: microtubule

MTOC: microtubule organising centre

pAb: polyclonal antibody

PCM: pericentriolar material

PBS: Phosphate-buffered saline

PCR: Polymerase chain reaction

Plk4: Polo-like kinase 4

PMSF: phenylmethylsulfonyl fluoride

pY: phosphotyrosine

RNA: Ribonucleic Acid

RT: room temperature; reverse transcription

SAK: Snk/Fnk akin kinase

SDS-PAGE: Sodium dodecylsulfate polyacrylamid gelelectrophoresis

SILAC: Stable isotope labelling of amino acids in cell culture

siRNA: small interference Ribonucleic Acid

SPB: Spindle Pole Body

UTR: untranslated region (of mRNA)

WB: western blot

WT: wild-type

8. References

Acquaviva C & Pines J (2006) The anaphase-promoting complex/cyclosome: APC/C. *J Cell Sci* 119:2401-2404.

Alvey PL (1985) An investigation of the centriole cycle using 3T3 and CHO cells. *J Cell Sci* 78:147-162.

Alvey PL (1986) Do adult centrioles contain cartwheels and lie at right angles to each other? *Cell Biol Int Rep* 10:589-598.

Andersen JS, Wilkinson CJ, Mayor T, Mortensen P, Nigg EA & Mann M (2003) Proteomic characterization of the human centrosome by protein correlation profiling. *Nature* 426:570-574.

Anderson RG & Brenner RM (1971) The formation of basal bodies (centrioles) in the Rhesus monkey oviduct. *J Cell Biol* 50:10-34.

Askham JM, Vaughan KT, Goodson HV & Morrison EE (2002) Evidence that an interaction between EB1 and p150(Glued) is required for the formation and maintenance of a radial microtubule array anchored at the centrosome. *Mol Biol Cell* 13:3627-3645.

Azimzadeh J & Bornens M (2007) Structure and duplication of the centrosome. *J Cell Sci* 120:2139-2142.

Badano JL, Leitch CC, *et al.* (2006) Dissection of epistasis in oligogenic Bardet-Biedl syndrome. *Nature* 439:326-330.

Bahe S, Stierhof YD, Wilkinson CJ, Leiss F & Nigg EA (2005) Rootletin forms centriole-associated filaments and functions in centrosome cohesion. *J Cell Biol* 171:27-33.

Bai C, Sen P, Hofmann K, Ma L, Goebl M, Harper JW & Elledge SJ (1996) SKP1 connects cell cycle regulators to the ubiquitin proteolysis machinery through a novel motif, the F-box. *Cell* 86:263-274.

Balczon R, Bao L, Zimmer WE, Brown K, Zinkowski RP & Brinkley BR (1995) Dissociation of centrosome replication events from cycles of DNA synthesis and mitotic division in hydroxyurea-arrested Chinese hamster ovary cells. *J Cell Biol* 130:105-115.

Barr FA, Sillje HH & Nigg EA (2004) Polo-like kinases and the orchestration of cell division. *Nat Rev Mol Cell Biol* 5:429-440.

Barros TP, Kinoshita K, Hyman AA & Raff JW (2005) Aurora A activates D-TACC-Msps complexes exclusively at centrosomes to stabilize centrosomal microtubules. *J Cell Biol* 170:1039-1046.

Bartolini F & Gundersen GG (2006) Generation of noncentrosomal microtubule arrays. *J Cell Sci* 119:4155-4163.

Basto R, Brunk K, Vinadogrova T, Peel N, Franz A, Khodjakov A & Raff JW (2008) Centrosome amplification can initiate tumorigenesis in flies. *Cell* 133:1032-1042.

Beisson J & Wright M (2003) Basal body/centriole assembly and continuity. *Curr Opin Cell Biol* 15:96-104.

Berthet C, Aleem E, Coppola V, Tessarollo L & Kaldis P (2003) Cdk2 knockout mice are viable. *Curr Biol* 13:1775-1785.

Bettencourt-Dias M & Glover DM (2007) Centrosome biogenesis and function: centrosomics brings new understanding. *Nat Rev Mol Cell Biol* 8:451-463.

Bettencourt-Dias M & Glover DM (2009) SnapShot: centriole biogenesis. *Cell* 136:188-188 e181.

Bettencourt-Dias M, Rodrigues-Martins A, *et al.* (2005) SAK/PLK4 is required for centriole duplication and flagella development. *Curr Biol* 15:2199-2207.

Blagden SP & Glover DM (2003) Polar expeditions--provisioning the centrosome for mitosis. *Nat Cell Biol* 5:505-511.

Blangy A, Chaussepied P & Nigg EA (1998) Rigor-type mutation in the kinesin-related protein HsEg5 changes its subcellular localization and induces microtubule bundling. *Cell Motil Cytoskeleton* 40:174-182.

Blangy A, Lane HA, d'Herin P, Harper M, Kress M & Nigg EA (1995) Phosphorylation by p34cdc2 regulates spindle association of human Eg5, a kinesin-related motor essential for bipolar spindle formation in vivo. *Cell* 83:1159-1169.

Blow JJ & Dutta A (2005) Preventing re-replication of chromosomal DNA. *Nat Rev Mol Cell Biol* 6:476-486.

Bobinnec Y, Khodjakov A, Mir LM, Rieder CL, Edde B & Bornens M (1998) Centriole disassembly in vivo and its effect on centrosome structure and function in vertebrate cells. *J Cell Biol* 143:1575-1589.

Booher RN, Holman PS & Fattaey A (1997) Human Myt1 is a cell cycle-regulated kinase that inhibits Cdc2 but not Cdk2 activity. *J Biol Chem* 272:22300-22306.

Bornens M (2002) Centrosome composition and microtubule anchoring mechanisms. *Curr Opin Cell Biol* 14:25-34.

Bornens M (2008) Organelle positioning and cell polarity. *Nat Rev Mol Cell Biol* 9:874-886.

Boveri T (1887) Ueber die Befruchtung der Eier von Ascaris megalocephala. *SitzBer Ges Morph Phys München* 71-80.

Boveri T. 1914. Zur Frage der Entstehung maligner Tumoren. (English Translation: The Origin of Malignant Tumors, Williams and Wilkins, Baltimore, Maryland, 1929).

Brittle AL & Ohkura H (2005) Mini spindles, the XMAP215 homologue, suppresses pausing of interphase microtubules in Drosophila. *EMBO J* 24:1387-1396.

Brouhard GJ, Stear JH, Noetzel TL, Al-Bassam J, Kinoshita K, Harrison SC, Howard J & Hyman AA (2008) XMAP215 is a processive microtubule polymerase. *Cell* 132:79-88.

Busino L, Donzelli M, Chiesa M, Guardavaccaro D, Ganoth D, Dorrello NV, Hershko A, Pagano M & Draetta GF (2003) Degradation of Cdc25A by beta-TrCP during S phase and in response to DNA damage. *Nature* 426:87-91.

Callaini G, Whitfield WG & Riparbelli MG (1997) Centriole and centrosome dynamics during the embryonic cell cycles that follow the formation of the cellular blastoderm in Drosophila. *Exp Cell Res* 234:183-190.

Cardozo T & Pagano M (2004) The SCF ubiquitin ligase: insights into a molecular machine. *Nat Rev Mol Cell Biol* 5:739-751.

Carroll PE, Okuda M, Horn HF, Biddinger P, Stambrook PJ, Gleich LL, Li YQ, Tarapore P & Fukasawa K (1999) Centrosome hyperamplification in human cancer: chromosome instability induced by p53 mutation and/or Mdm2 overexpression. *Oncogene* 18:1935-1944.

Casenghi M, Barr FA & Nigg EA (2005) Phosphorylation of Nlp by Plk1 negatively regulates its dynein-dynactin-dependent targeting to the centrosome. *J Cell Sci* 118:5101-5108.

Casenghi M, Meraldi P, Weinhart U, Duncan PI, Korner R & Nigg EA (2003) Polo-like kinase 1 regulates Nlp, a centrosome protein involved in microtubule nucleation. *Dev Cell* 5:113-125.

Castellanos E, Dominguez P & Gonzalez C (2008) Centrosome dysfunction in Drosophila neural stem cells causes tumors that are not due to genome instability. *Curr Biol* 18:1209-1214.

Cavalier-Smith T (1974) Basal body and flagellar development during the vegetative cell cycle and the sexual cycle of Chlamydomonas reinhardii. *J Cell Sci* 16:529-556.

Cenciarelli C, Chiaur DS, Guardavaccaro D, Parks W, Vidal M & Pagano M (1999) Identification of a family of human F-box proteins. *Curr Biol* 9:1177-1179.

Chang P, Giddings TH, Jr., Winey M & Stearns T (2003) Epsilon-tubulin is required for centriole duplication and microtubule organization. *Nat Cell Biol* 5:71-76.

Cheng KY, Lowe ED, Sinclair J, Nigg EA & Johnson LN (2003) The crystal structure of the human polo-like kinase-1 polo box domain and its phospho-peptide complex. *EMBO J* 22:5757-5768.

Chretien D, Buendia B, Fuller SD & Karsenti E (1997) Reconstruction of the centrosome cycle from cryoelectron micrographs. *J Struct Biol* 120:117-133.

Chu IM, Hengst L & Slingerland JM (2008) The Cdk inhibitor p27 in human cancer: prognostic potential and relevance to anticancer therapy. *Nat Rev Cancer* 8:253-267.

Ciosk R, Zachariae W, Michaelis C, Shevchenko A, Mann M & Nasmyth K (1998) An ESP1/PDS1 complex regulates loss of sister chromatid cohesion at the metaphase to anaphase transition in yeast. *Cell* 93:1067-1076.

Coats S, Flanagan WM, Nourse J & Roberts JM (1996) Requirement of p27Kip1 for restriction point control of the fibroblast cell cycle. *Science* 272:877-880.

Cohen-Fix O, Peters JM, Kirschner MW & Koshland D (1996) Anaphase initiation in Saccharomyces cerevisiae is controlled by the APC-dependent degradation of the anaphase inhibitor Pds1p. *Genes Dev* 10:3081-3093.

Cowan CR & Hyman AA (2006) Cyclin E-Cdk2 temporally regulates centrosome assembly and establishment of polarity in Caenorhabditis elegans embryos. *Nat Cell Biol* 8:1441-1447.

Cox J & Mann M (2008) MaxQuant enables high peptide identification rates, individualized p.p.b.-range mass accuracies and proteome-wide protein quantification. *Nat Biotechnol* 26:1367-1372.

Cunha-Ferreira I, Bento I & Bettencourt-Dias M (2009a) From zero to many: control of centriole number in development and disease. *Traffic* 10:482-498.

Cunha-Ferreira I, Rodrigues-Martins A, Bento I, Riparbelli M, Zhang W, Laue E, Callaini G, Glover DM & Bettencourt-Dias M (2009b) The SCF/Slimb ubiquitin ligase limits centrosome amplification through degradation of SAK/PLK4. *Curr Biol* 19:43-49.

Dammermann A, Muller-Reichert T, Pelletier L, Habermann B, Desai A & Oegema K (2004) Centriole assembly requires both centriolar and pericentriolar material proteins. *Dev Cell* 7:815-829.

Daub H, Olsen JV*, et al.* (2008) Kinase-selective enrichment enables quantitative phosphoproteomics of the kinome across the cell cycle. *Mol Cell* 31:438-448.

Delattre M, Canard C & Gonczy P (2006) Sequential protein recruitment in C. elegans centriole formation. *Curr Biol* 16:1844-1849.

Delattre M & Gonczy P (2004) The arithmetic of centrosome biogenesis. *J Cell Sci* 117:1619-1630.

Delattre M, Leidel S, Wani K, Baumer K, Bamat J, Schnabel H, Feichtinger R, Schnabel R & Gonczy P (2004) Centriolar SAS-5 is required for centrosome duplication in C. elegans. *Nat Cell Biol* 6:656-664.

Dhanasekaran N & Premkumar Reddy E (1998) Signaling by dual specificity kinases. *Oncogene* 17:1447-1455.

Diffley JF (2001) DNA replication: building the perfect switch. *Curr Biol* 11:R367-370.

Dirksen ER (1991) Centriole and basal body formation during ciliogenesis revisited. *Biol Cell* 72:31-38.

Dix CI & Raff JW (2007) Drosophila Spd-2 recruits PCM to the sperm centriole, but is dispensable for centriole duplication. *Curr Biol* 17:1759-1764.

do Carmo Avides M, Tavares A & Glover DM (2001) Polo kinase and Asp are needed to promote the mitotic organizing activity of centrosomes. *Nat Cell Biol* 3:421-424.

Doxsey S (2001) Re-evaluating centrosome function. *Nat Rev Mol Cell Biol* 2:688-698.

Doxsey SJ, Stein P, Evans L, Calarco PD & Kirschner M (1994) Pericentrin, a highly conserved centrosome protein involved in microtubule organization. *Cell* 76:639-650.

Duensing A, Liu Y, Perdreau SA, Kleylein-Sohn J, Nigg EA & Duensing S (2007) Centriole overduplication through the concurrent formation of multiple daughter centrioles at single maternal templates. *Oncogene* 26:6280-6288.

Dutcher SK (2003) Elucidation of basal body and centriole functions in Chlamydomonas reinhardtii. *Traffic* 4:443-451.

Elbashir SM, Harborth J, Lendeckel W, Yalcin A, Weber K & Tuschl T (2001) Duplexes of 21-nucleotide RNAs mediate RNA interference in cultured mammalian cells. *Nature* 411:494-498.

Elia AE, Rellos P, *et al.* (2003) The molecular basis for phosphodependent substrate targeting and regulation of Plks by the Polo-box domain. *Cell* 115:83-95.

Evan GI, Lewis GK, Ramsay G & Bishop JM (1985) Isolation of monoclonal antibodies specific for human c-myc proto-oncogene product. *Mol Cell Biol* 5:3610-3616.

Finley D (2009) Recognition and processing of ubiquitin-protein conjugates by the proteasome. *Annu Rev Biochem* 78:477-513.

Fliegauf M, Benzing T & Omran H (2007) When cilia go bad: cilia defects and ciliopathies. *Nat Rev Mol Cell Biol* 8:880-893.

Fode C, Binkert C & Dennis JW (1996) Constitutive expression of murine Sak-a suppresses cell growth and induces multinucleation. *Mol Cell Biol* 16:4665-4672.

Fode C, Motro B, Yousefi S, Heffernan M & Dennis JW (1994) Sak, a murine protein-serine/threonine kinase that is related to the Drosophila polo kinase and involved in cell proliferation. *Proc Natl Acad Sci U S A* 91:6388-6392.

Freed E, Lacey KR, Huie P, Lyapina SA, Deshaies RJ, Stearns T & Jackson PK (1999) Components of an SCF ubiquitin ligase localize to the centrosome and regulate the centrosome duplication cycle. *Genes Dev* 13:2242-2257.

Frescas D & Pagano M (2008) Deregulated proteolysis by the F-box proteins SKP2 and beta-TrCP: tipping the scales of cancer. *Nat Rev Cancer* 8:438-449.

Ganem NJ, Godinho SA & Pellman D (2009) A mechanism linking extra centrosomes to chromosomal instability. *Nature*

Gavin RH (1984) In vitro reassembly of basal body components. *J Cell Sci* 66:147-154.

Geng Y, Yu Q, *et al.* (2003) Cyclin E ablation in the mouse. *Cell* 114:431-443.

Gibbs CS & Zoller MJ (1991) Rational scanning mutagenesis of a protein kinase identifies functional regions involved in catalysis and substrate interactions. *J Biol Chem* 266:8923-8931.

Giehl M, Fabarius A, Frank O, Hochhaus A, Hafner M, Hehlmann R & Seifarth W (2005) Centrosome aberrations in chronic myeloid leukemia correlate with stage of disease and chromosomal instability. *Leukemia* 19:1192-1197.

Giet R, McLean D, Descamps S, Lee MJ, Raff JW, Prigent C & Glover DM (2002) Drosophila Aurora A kinase is required to localize D-TACC to centrosomes and to regulate astral microtubules. *J Cell Biol* 156:437-451.

Glotzer M, Murray AW & Kirschner MW (1991) Cyclin is degraded by the ubiquitin pathway. *Nature* 349:132-138.

Godinho SA, Kwon M & Pellman D (2009) Centrosomes and cancer: how cancer cells divide with too many centrosomes. *Cancer Metastasis Rev* 28:85-98.

Golan A, Yudkovsky Y & Hershko A (2002) The cyclin-ubiquitin ligase activity of cyclosome/APC is jointly activated by protein kinases Cdk1-cyclin B and Plk. *J Biol Chem* 277:15552-15557.

Gomez-Ferreria MA, Rath U, Buster DW, Chanda SK, Caldwell JS, Rines DR & Sharp DJ (2007) Human Cep192 is required for mitotic centrosome and spindle assembly. *Curr Biol* 17:1960-1966.

Gonzalez C, Sunkel CE & Glover DM (1998) Interactions between mgr, asp, and polo: asp function modulated by polo and needed to maintain the poles of monopolar and bipolar spindles. *Chromosoma* 107:452-460.

Graser S, Stierhof YD, Lavoie SB, Gassner OS, Lamla S, Le Clech M & Nigg EA (2007) Cep164, a novel centriole appendage protein required for primary cilium formation. *J Cell Biol* 179:321-330.

Griffith LC (2004) Regulation of calcium/calmodulin-dependent protein kinase II activation by intramolecular and intermolecular interactions. *J Neurosci* 24:8394-8398.

Gstaiger M, Marti A & Krek W (1999) Association of human SCF(SKP2) subunit p19(SKP1) with interphase centrosomes and mitotic spindle poles. *Exp Cell Res* 247:554-562.

Guardavaccaro D, Frescas D, *et al.* (2008) Control of chromosome stability by the beta-TrCP-REST-Mad2 axis. *Nature* 452:365-369.

Guardavaccaro D, Kudo Y, *et al.* (2003) Control of meiotic and mitotic progression by the F box protein beta-Trcp1 in vivo. *Dev Cell* 4:799-812.

Guarguaglini G, Duncan PI, Stierhof YD, Holmstrom T, Duensing S & Nigg EA (2005) The forkhead-associated domain protein Cep170 interacts with Polo-like kinase 1 and serves as a marker for mature centrioles. *Mol Biol Cell* 16:1095-1107.

Habedanck R (2006) The human Polo-like kinase 4 is a regulator of centrosome duplication. *Dissertation zur Erlangung des Doktorgrades der Naturwissenschaften*, Ludwig-Maximilians-Universität München.

Habedanck R, Stierhof YD, Wilkinson CJ & Nigg EA (2005) The Polo kinase Plk4 functions in centriole duplication. *Nat Cell Biol* 7:1140-1146.

Hagiwara H, Ohwada N & Takata K (2004) Cell biology of normal and abnormal ciliogenesis in the ciliated epithelium. *Int Rev Cytol* 234:101-141.

Hammond C, Jeffers L, Carr BI & Simon D (1999) Multiple genetic alterations, 4q28, a new suppressor region, and potential gender differences in human hepatocellular carcinoma. *Hepatology* 29:1479-1485.

Hanks SK & Hunter T (1995) Protein kinases 6. The eukaryotic protein kinase superfamily: kinase (catalytic) domain structure and classification. *FASEB J* 9:576-596.

Hanks SK & Quinn AM (1991) Protein kinase catalytic domain sequence database: identification of conserved features of primary structure and classification of family members. *Methods Enzymol* 200:38-62.

Hanks SK, Quinn AM & Hunter T (1988) The protein kinase family: conserved features and deduced phylogeny of the catalytic domains. *Science* 241:42-52.

Hershko A & Ciechanover A (1998) The ubiquitin system. *Annu Rev Biochem* 67:425-479.

Hildebrandt F & Zhou W (2007) Nephronophthisis-associated ciliopathies. *J Am Soc Nephrol* 18:1855-1871.

Hinchcliffe EH & Linck RW (1998) Two proteins isolated from sea urchin sperm flagella: structural components common to the stable microtubules of axonemes and centrioles. *J Cell Sci* 111 (Pt 5):585-595.

Hinchcliffe EH, Miller FJ, Cham M, Khodjakov A & Sluder G (2001) Requirement of a centrosomal activity for cell cycle progression through G1 into S phase. *Science* 291:1547-1550.

Hiraki M, Nakazawa Y, Kamiya R & Hirono M (2007) Bld10p constitutes the cartwheel-spoke tip and stabilizes the 9-fold symmetry of the centriole. *Curr Biol* 17:1778-1783.

Hochstrasser M (1996) Ubiquitin-dependent protein degradation. *Annu Rev Genet* 30:405-439.

Hook SS, Lin JJ & Dutta A (2007) Mechanisms to control rereplication and implications for cancer. *Curr Opin Cell Biol* 19:663-671.

Hudson JW, Kozarova A, Cheung P, Macmillan JC, Swallow CJ, Cross JC & Dennis JW (2001) Late mitotic failure in mice lacking Sak, a polo-like kinase. *Curr Biol* 11:441-446.

Hunter T (2000) Signaling--2000 and beyond. *Cell* 100:113-127.

Hunter T (2007) The age of crosstalk: phosphorylation, ubiquitination, and beyond. *Mol Cell* 28:730-738.

Ishikawa H, Kubo A & Tsukita S (2005) Odf2-deficient mother centrioles lack distal/subdistal appendages and the ability to generate primary cilia. *Nat Cell Biol* 7:517-524.

Janke C, Rogowski K*, et al.* (2005) Tubulin polyglutamylase enzymes are members of the TTL domain protein family. *Science* 308:1758-1762.

Jiang J & Struhl G (1998) Regulation of the Hedgehog and Wingless signalling pathways by the F-box/WD40-repeat protein Slimb. *Nature* 391:493-496.

Jin J, Shirogane T, Xu L, Nalepa G, Qin J, Elledge SJ & Harper JW (2003) SCFbeta-TRCP links Chk1 signaling to degradation of the Cdc25A protein phosphatase. *Genes Dev* 17:3062-3074.

Jones MH & Winey M (2006) Centrosome duplication: is asymmetry the clue? *Curr Biol* 16:R808-810.

Kang BS, French OG, Sando JJ & Hahn CS (2000) Activation-dependent degradation of protein kinase C eta. *Oncogene* 19:4263-4272.

Karn T, Holtrich U, Wolf G, Hock B, Strebhardt K & RubsamenWaigmann H (1997) Human SAK related to the PLK/polo family of cell cycle kinases shows high mRNA expression in testis. *Oncology Reports* 4:505-510.

Kemp CA, Kopish KR, Zipperlen P, Ahringer J & O'Connell KF (2004) Centrosome maturation and duplication in C. elegans require the coiled-coil protein SPD-2. *Dev Cell* 6:511-523.

Khodjakov A, Rieder CL, Sluder G, Cassels G, Sibon O & Wang CL (2002) De novo formation of centrosomes in vertebrate cells arrested during S phase. *J Cell Biol* 158:1171-1181.

Kipreos ET & Pagano M (2000) The F-box protein family. *Genome Biol* 1:REVIEWS3002.

Kleylein-Sohn J, Westendorf J, Le Clech M, Habedanck R, Stierhof YD & Nigg EA (2007) Plk4-induced centriole biogenesis in human cells. *Dev Cell* 13:190-202.

Ko MA, Rosario CO, Hudson JW, Kulkarni S, Pollett A, Dennis JW & Swallow CJ (2005) Plk4 haploinsufficiency causes mitotic infidelity and carcinogenesis. *Nat Genet* 37:883-888.

Kochanski RS & Borisy GG (1990) Mode of centriole duplication and distribution. *J Cell Biol* 110:1599-1605.

Koepp DM, Schaefer LK, Ye X, Keyomarsi K, Chu C, Harper JW & Elledge SJ (2001) Phosphorylation-dependent ubiquitination of cyclin E by the SCFFbw7 ubiquitin ligase. *Science* 294:173-177.

Kohlmaier G, Loncarek J, Meng X, McEwen BF, Mogensen MM, Spektor A, Dynlacht BD, Khodjakov A & Gonczy P (2009) Overly long centrioles and defective cell division upon excess of the SAS-4-related protein CPAP. *Curr Biol* 19:1012-1018.

Kollberg H, Mossberg B, Afzelius BA, Philipson K & Camner P (1978) Cystic fibrosis compared with the immotile-cilia syndrome. A study of mucociliary clearance, ciliary ultrastructure, clinical picture and ventilatory function. *Scand J Respir Dis* 59:297-306.

Kraft C, Vodermaier HC, Maurer-Stroh S, Eisenhaber F & Peters JM (2005) The WD40 propeller domain of Cdh1 functions as a destruction box receptor for APC/C substrates. *Mol Cell* 18:543-553.

Kramer A, Neben K & Ho AD (2005) Centrosome aberrations in hematological malignancies. *Cell Biol Int* 29:375-383.

Kramer ER, Scheuringer N, Podtelejnikov AV, Mann M & Peters JM (2000) Mitotic regulation of the APC activator proteins CDC20 and CDH1. *Mol Biol Cell* 11:1555-1569.

Kuriyama R & Borisy GG (1981) Centriole cycle in Chinese hamster ovary cells as determined by whole-mount electron microscopy. *J Cell Biol* 91:814-821.

La Terra S, English CN, Hergert P, McEwen BF, Sluder G & Khodjakov A (2005) The de novo centriole assembly pathway in HeLa cells: cell cycle progression and centriole assembly/maturation. *J Cell Biol* 168:713-722.

Lacey KR, Jackson PK & Stearns T (1999) Cyclin-dependent kinase control of centrosome duplication. *Proc Natl Acad Sci U S A* 96:2817-2822.

Leidel S, Delattre M, Cerutti L, Baumer K & Gonczy P (2005) SAS-6 defines a protein family required for centrosome duplication in C. elegans and in human cells. *Nat Cell Biol* 7:115-125.

Leidel S & Gonczy P (2003) SAS-4 is essential for centrosome duplication in C elegans and is recruited to daughter centrioles once per cell cycle. *Dev Cell* 4:431-439.

Leung GC, Ho CS, Blasutig IM, Murphy JM & Sicheri F (2007) Determination of the Plk4/Sak consensus phosphorylation motif using peptide spots arrays. *FEBS Lett* 581:77-83.

Leung GC, Hudson JW, Kozarova A, Davidson A, Dennis JW & Sicheri F (2002) The Sak polo-box comprises a structural domain sufficient for mitotic subcellular localization. *Nat Struct Biol* 9:719-724.

Lindberg RA, Quinn AM & Hunter T (1992) Dual-specificity protein kinases: will any hydroxyl do? *Trends Biochem Sci* 17:114-119.

Lindon C & Pines J (2004) Ordered proteolysis in anaphase inactivates Plk1 to contribute to proper mitotic exit in human cells. *J Cell Biol* 164:233-241.

Lingle WL, Lutz WH, Ingle JN, Maihle NJ & Salisbury JL (1998) Centrosome hypertrophy in human breast tumors: implications for genomic stability and cell polarity. *Proc Natl Acad Sci U S A* 95:2950-2955.

Liu F, Stanton JJ, Wu Z & Piwnica-Worms H (1997) The human Myt1 kinase preferentially phosphorylates Cdc2 on threonine 14 and localizes to the endoplasmic reticulum and Golgi complex. *Mol Cell Biol* 17:571-583.

Loncarek J, Hergert P, Magidson V & Khodjakov A (2008) Control of daughter centriole formation by the pericentriolar material. *Nat Cell Biol* 10:322-328.

Loncarek J & Khodjakov A (2009) Ab ovo or de novo? Mechanisms of centriole duplication. *Mol Cells* 27:135-142.

Lu Z & Hunter T (2009) Degradation of activated protein kinases by ubiquitination. *Annu Rev Biochem* 78:435-475.

Lu Z, Liu D, Hornia A, Devonish W, Pagano M & Foster DA (1998) Activation of protein kinase C triggers its ubiquitination and degradation. *Mol Cell Biol* 18:839-845.

Ma S, Charron J & Erikson RL (2003) Role of Plk2 (Snk) in mouse development and cell proliferation. *Mol Cell Biol* 23:6936-6943.

Macmillan JC, Hudson JW, Bull S, Dennis JW & Swallow CJ (2001) Comparative expression of the mitotic regulators SAK and PLK in colorectal cancer. *Ann Surg Oncol* 8:729-740.

Marshall WF, Vucica Y & Rosenbaum JL (2001) Kinetics and regulation of de novo centriole assembly. Implications for the mechanism of centriole duplication. *Curr Biol* 11:308-317.

Martindill DM, Risebro CA, Smart N, Franco-Viseras Mdel M, Rosario CO, Swallow CJ, Dennis JW & Riley PR (2007) Nucleolar release of Hand1 acts as a molecular switch to determine cell fate. *Nat Cell Biol* 9:1131-1141.

Matsumoto Y, Hayashi K & Nishida E (1999) Cyclin-dependent kinase 2 (Cdk2) is required for centrosome duplication in mammalian cells. *Curr Biol* 9:429-432.

Matsuura K, Lefebvre PA, Kamiya R & Hirono M (2004) Bld10p, a novel protein essential for basal body assembly in Chlamydomonas: localization to the cartwheel, the first ninefold symmetrical structure appearing during assembly. *J Cell Biol* 165:663-671.

Mayor T, Hacker U, Stierhof YD & Nigg EA (2002) The mechanism regulating the dissociation of the centrosomal protein C-Nap1 from mitotic spindle poles. *J Cell Sci* 115:3275-3284.

Mayor T, Stierhof YD, Tanaka K, Fry AM & Nigg EA (2000) The centrosomal protein C-Nap1 is required for cell cycle-regulated centrosome cohesion. *J Cell Biol* 151:837-846.

McGuffin LJ, Bryson K & Jones DT (2001) What are the baselines for protein fold recognition? *Bioinformatics* 17:63-72.

Meraldi P, Honda R & Nigg EA (2002) Aurora-A overexpression reveals tetraploidization as a major route to centrosome amplification in p53-/- cells. *EMBO J* 21:483-492.

Meraldi P, Lukas J, Fry AM, Bartek J & Nigg EA (1999) Centrosome duplication in mammalian somatic cells requires E2F and Cdk2-cyclin A. *Nat Cell Biol* 1:88-93.

Mills GB, Schmandt R, *et al.* (1992) Expression of TTK, a novel human protein kinase, is associated with cell proliferation. *J Biol Chem* 267:16000-16006.

Mitchison T & Kirschner M (1984) Dynamic instability of microtubule growth. *Nature* 312:237-242.

Moberg KH, Bell DW, Wahrer DC, Haber DA & Hariharan IK (2001) Archipelago regulates Cyclin E levels in Drosophila and is mutated in human cancer cell lines. *Nature* 413:311-316.

Mogensen MM, Malik A, Piel M, Bouckson-Castaing V & Bornens M (2000) Microtubule minus-end anchorage at centrosomal and non-centrosomal sites: the role of ninein. *J Cell Sci* 113 (Pt 17):3013-3023.

Moller W, Haussinger K, Ziegler-Heitbrock L & Heyder J (2006) Mucociliary and long-term particle clearance in airways of patients with immotile cilia. *Respir Res* 7:10.

Moritz MRLMADA (2004) Microtubule Nucleation. In: Nigg EA, ed. *Centrosomes in Development and Disease*. Weinheim: Wiley-VCH. 27-41.

Murphy TD (2003) Drosophila skpA, a component of SCF ubiquitin ligases, regulates centrosome duplication independently of cyclin E accumulation. *J Cell Sci* 116:2321-2332.

Murray AW & Kirschner MW (1989) Cyclin synthesis drives the early embryonic cell cycle. *Nature* 339:275-280.

Nakayama K, Nagahama H, *et al.* (2000) Targeted disruption of Skp2 results in accumulation of cyclin E and p27(Kip1), polyploidy and centrosome overduplication. *EMBO J* 19:2069-2081.

Nakayama KI & Nakayama K (2005) Regulation of the cell cycle by SCF-type ubiquitin ligases. *Semin Cell Dev Biol* 16:323-333.

Nakayama KI & Nakayama K (2006) Ubiquitin ligases: cell-cycle control and cancer. *Nat Rev Cancer* 6:369-381.

Nakazawa Y, Hiraki M, Kamiya R & Hirono M (2007) SAS-6 is a cartwheel protein that establishes the 9-fold symmetry of the centriole. *Curr Biol* 17:2169-2174.

Nasmyth K (2001) Disseminating the genome: joining, resolving, and separating sister chromatids during mitosis and meiosis. *Annu Rev Genet* 35:673-745.

Newton AC (2003) Regulation of the ABC kinases by phosphorylation: protein kinase C as a paradigm. *Biochem J* 370:361-371.

Nigg EA (2002) Centrosome aberrations: cause or consequence of cancer progression? *Nat Rev Cancer* 2:815-825.

Nigg EA (2006) Cell biology: a licence for duplication. *Nature* 442:874-875.

Nigg EA (2007) Centrosome duplication: of rules and licenses. *Trends Cell Biol* 17:215-221.

Nolen B, Taylor S & Ghosh G (2004) Regulation of protein kinases; controlling activity through activation segment conformation. *Mol Cell* 15:661-675.

Nonaka S, Tanaka Y, Okada Y, Takeda S, Harada A, Kanai Y, Kido M & Hirokawa N (1998) Randomization of left-right asymmetry due to loss of nodal cilia generating leftward flow of extraembryonic fluid in mice lacking KIF3B motor protein. *Cell* 95:829-837.

O'Connell KF, Caron C, Kopish KR, Hurd DD, Kemphues KJ, Li Y & White JG (2001) The C. elegans zyg-1 gene encodes a regulator of centrosome duplication with distinct maternal and paternal roles in the embryo. *Cell* 105:547-558.

Ortega S, Prieto I, Odajima J, Martin A, Dubus P, Sotillo R, Barbero JL, Malumbres M & Barbacid M (2003) Cyclin-dependent kinase 2 is essential for meiosis but not for mitotic cell division in mice. *Nat Genet* 35:25-31.

Paintrand M, Moudjou M, Delacroix H & Bornens M (1992) Centrosome organization and centriole architecture: their sensitivity to divalent cations. *J Struct Biol* 108:107-128.

Palazzo RE, Vogel JM, Schnackenberg BJ, Hull DR & Wu X (2000) Centrosome maturation. *Curr Top Dev Biol* 49:449-470.

Peel N, Stevens NR, Basto R & Raff JW (2007) Overexpressing centriole-replication proteins in vivo induces centriole overduplication and de novo formation. *Curr Biol* 17:834-843.

Pelletier L, Muller-Reichert, T., Srayko, M., Ozlu, N., Schlaitz, A., Hyman, AA (2004). In: Nigg EA, ed. *Centrosomes in Development and Disease*. Weinheim: Wiley-VCH. 227-250.

Pelletier L, O'Toole E, Schwager A, Hyman AA & Muller-Reichert T (2006) Centriole assembly in Caenorhabditis elegans. *Nature* 444:619-623.

Peset I, Seiler J, Sardon T, Bejarano LA, Rybina S & Vernos I (2005) Function and regulation of Maskin, a TACC family protein, in microtubule growth during mitosis. *J Cell Biol* 170:1057-1066.

Peters JM (2006) The anaphase promoting complex/cyclosome: a machine designed to destroy. *Nat Rev Mol Cell Biol* 7:644-656.

Pfleger CM & Kirschner MW (2000) The KEN box: an APC recognition signal distinct from the D box targeted by Cdh1. *Genes Dev* 14:655-665.

Pickart CM & Cohen RE (2004) Proteasomes and their kin: proteases in the machine age. *Nat Rev Mol Cell Biol* 5:177-187.

Pihan GA, Purohit A, Wallace J, Knecht H, Woda B, Quesenberry P & Doxsey SJ (1998) Centrosome defects and genetic instability in malignant tumors. *Cancer Res* 58:3974-3985.

Piva R, Liu J, Chiarle R, Podda A, Pagano M & Inghirami G (2002) In vivo interference with Skp1 function leads to genetic instability and neoplastic transformation. *Mol Cell Biol* 22:8375-8387.

Pomerening JR, Kim SY & Ferrell JE, Jr. (2005) Systems-level dissection of the cell-cycle oscillator: bypassing positive feedback produces damped oscillations. *Cell* 122:565-578.

Praetorius HA & Spring KR (2005) A physiological view of the primary cilium. *Annu Rev Physiol* 67:515-529.

Quarmby LM & Parker JD (2005) Cilia and the cell cycle? *J Cell Biol* 169:707-710.

Reed SI (2003) Ratchets and clocks: the cell cycle, ubiquitylation and protein turnover. *Nat Rev Mol Cell Biol* 4:855-864.

Rodrigues-Martins A, Riparbelli M, Callaini G, Glover DM & Bettencourt-Dias M (2007) Revisiting the role of the mother centriole in centriole biogenesis. *Science* 316:1046-1050.

Rogers GC, Rusan NM, Roberts DM, Peifer M & Rogers SL (2009) The SCF Slimb ubiquitin ligase regulates Plk4/Sak levels to block centriole reduplication. *J Cell Biol* 184:225-239.

Rogers S, Wells R & Rechsteiner M (1986) Amino acid sequences common to rapidly degraded proteins: the PEST hypothesis. *Science* 234:364-368.

Rudner AD & Murray AW (2000) Phosphorylation by Cdc28 activates the Cdc20-dependent activity of the anaphase-promoting complex. *J Cell Biol* 149:1377-1390.

Satir P & Christensen ST (2007) Overview of structure and function of mammalian cilia. *Annu Rev Physiol* 69:377-400.

Schmidt TI, Kleylein-Sohn J, Westendorf J, Le Clech M, Lavoie SB, Stierhof YD & Nigg EA (2009) Control of centriole length by CPAP and CP110. *Curr Biol* 19:1005-1011.

Seo E, Kim H, Kim R, Yun S, Kim M, Han JK, Costantini F & Jho EH (2009) Multiple isoforms of beta-TrCP display differential activities in the regulation of Wnt signaling. *Cell Signal* 21:43-51.

Shi Z, Resing KA & Ahn NG (2006) Networks for the allosteric control of protein kinases. *Curr Opin Struct Biol* 16:686-692.

Skowyra D, Craig KL, Tyers M, Elledge SJ & Harper JW (1997) F-box proteins are receptors that recruit phosphorylated substrates to the SCF ubiquitin-ligase complex. *Cell* 91:209-219.

Sluder G (2004) Centrosome Duplication and its Regulation in the Higher Animal Cell. In: Nigg EA, ed. *Centrosomes in Development and Disease*. Weinheim: Wiley-VCH. 167-183.

Song MH, Aravind L, Muller-Reichert T & O'Connell KF (2008a) The conserved protein SZY-20 opposes the Plk4-related kinase ZYG-1 to limit centrosome size. *Dev Cell* 15:901-912.

Song MH, Miliaras NB, Peel N & O'Connell KF (2008b) Centrioles: some self-assembly required. *Curr Opin Cell Biol* 20:688-693.

Sorokin SP (1968) Reconstructions of centriole formation and ciliogenesis in mammalian lungs. *J Cell Sci* 3:207-230.

Spevak W, Keiper BD, Stratowa C & Castanon MJ (1993) Saccharomyces cerevisiae cdc15 mutants arrested at a late stage in anaphase are rescued by Xenopus cDNAs encoding N-ras or a protein with beta-transducin repeats. *Mol Cell Biol* 13:4953-4966.

Spruck CH, Won KA & Reed SI (1999) Deregulated cyclin E induces chromosome instability. *Nature* 401:297-300.

Steffen W & Linck RW (1988) Evidence for tektins in centrioles and axonemal microtubules. *Proc Natl Acad Sci U S A* 85:2643-2647.

Strnad P & Gonczy P (2008) Mechanisms of procentriole formation. *Trends Cell Biol* 18:389-396.

Strnad P, Leidel S, Vinogradova T, Euteneuer U, Khodjakov A & Gonczy P (2007) Regulated HsSAS-6 levels ensure formation of a single procentriole per centriole during the centrosome duplication cycle. *Dev Cell* 13:203-213.

Strohmaier H, Spruck CH, Kaiser P, Won KA, Sangfelt O & Reed SI (2001) Human F-box protein hCdc4 targets cyclin E for proteolysis and is mutated in a breast cancer cell line. *Nature* 413:316-322.

Sutterluty H, Chatelain E, Marti A, Wirbelauer C, Senften M, Muller U & Krek W (1999) p45SKP2 promotes p27Kip1 degradation and induces S phase in quiescent cells. *Nat Cell Biol* 1:207-214.

Swallow CJ, Ko MA, Siddiqui NU, Hudson JW & Dennis JW (2005) Sak/Plk4 and mitotic fidelity. *Oncogene* 24:306-312.

Szollosi D, Calarco P & Donahue RP (1972) Absence of centrioles in the first and second meiotic spindles of mouse oocytes. *J Cell Sci* 11:521-541.

Tang CJ, Fu RH, Wu KS, Hsu WB & Tang TK (2009) CPAP is a cell-cycle regulated protein that controls centriole length. *Nat Cell Biol*

Taylor SS, Knighton DR, Zheng J, Sowadski JM, Gibbs CS & Zoller MJ (1993) A template for the protein kinase family. *Trends Biochem Sci* 18:84-89.

Theodosiou NA, Zhang S, Wang WY & Xu T (1998) slimb coordinates wg and dpp expression in the dorsal-ventral and anterior-posterior axes during limb development. *Development* 125:3411-3416.

Trinkle-Mulcahy L & Lamond AI (2006) Mitotic phosphatases: no longer silent partners. *Curr Opin Cell Biol* 18:623-631.

Tsang WY, Spektor A, Vijayakumar S, Bista BR, Li J, Sanchez I, Duensing S & Dynlacht BD (2009) Cep76, a centrosomal protein that specifically restrains centriole reduplication. *Dev Cell* 16:649-660.

Tsou MF & Stearns T (2006a) Controlling centrosome number: licenses and blocks. *Curr Opin Cell Biol* 18:74-78.

Tsou MF & Stearns T (2006b) Mechanism limiting centrosome duplication to once per cell cycle. *Nature* 442:947-951.

Tsvetkov LM, Yeh KH, Lee SJ, Sun H & Zhang H (1999) p27(Kip1) ubiquitination and degradation is regulated by the SCF(Skp2) complex through phosphorylated Thr187 in p27. *Curr Biol* 9:661-664.

Uetake Y, Loncarek J, Nordberg JJ, English CN, La Terra S, Khodjakov A & Sluder G (2007) Cell cycle progression and de novo centriole assembly after centrosomal removal in untransformed human cells. *J Cell Biol* 176:173-182.

Van Beneden A. 1883. Recherches sur la maturation de l'oeuf, la Fé-condation et la division cellulaire. Bruxelles.

Vorobjev IA & Chentsov Yu S (1982) Centrioles in the cell cycle. I. Epithelial cells. *J Cell Biol* 93:938-949.

Watanabe N, Arai H, Nishihara Y, Taniguchi M, Hunter T & Osada H (2004) M-phase kinases induce phospho-dependent ubiquitination of somatic Wee1 by SCFbeta-TrCP. *Proc Natl Acad Sci U S A* 101:4419-4424.

Watanabe N, Broome M & Hunter T (1995) Regulation of the human WEE1Hu CDK tyrosine 15-kinase during the cell cycle. *EMBO J* 14:1878-1891.

Westbrook TF, Hu G, *et al.* (2008) SCFbeta-TRCP controls oncogenic transformation and neural differentiation through REST degradation. *Nature* 452:370-374.

Winston JT, Koepp DM, Zhu C, Elledge SJ & Harper JW (1999) A family of mammalian F-box proteins. *Curr Biol* 9:1180-1182.

Wojcik EJ, Glover DM & Hays TS (2000) The SCF ubiquitin ligase protein slimb regulates centrosome duplication in Drosophila. *Curr Biol* 10:1131-1134.

Wong C & Stearns T (2003) Centrosome number is controlled by a centrosome-intrinsic block to reduplication. *Nat Cell Biol* 5:539-544.

Yamaguchi T, Goto H, *et al.* (2005) Phosphorylation by Cdk1 induces Plk1-mediated vimentin phosphorylation during mitosis. *J Cell Biol* 171:431-436.

Yamashita Y, Kajigaya S, *et al.* (2001) Sak serine-threonine kinase acts as an effector of Tec tyrosine kinase. *J Biol Chem* 276:39012-39020.

Yang J, Adamian M & Li T (2006) Rootletin interacts with C-Nap1 and may function as a physical linker between the pair of centrioles/basal bodies in cells. *Mol Biol Cell* 17:1033-1040.

Zariwala MA, Knowles MR & Omran H (2007) Genetic defects in ciliary structure and function. *Annu Rev Physiol* 69:423-450.

Zheng Y, Wong ML, Alberts B & Mitchison T (1995) Nucleation of microtubule assembly by a gamma-tubulin-containing ring complex. *Nature* 378:578-583.

Zhu F, Lawo S, *et al.* (2008) The mammalian SPD-2 ortholog Cep192 regulates centrosome biogenesis. *Curr Biol* 18:136-141.

9. Appendix

Parts of this work have been published in:

Kleylein-Sohn J, Westendorf J, Le Clech M, Habedanck R, Stierhof YD & Nigg EA (2007) Plk4-induced centriole biogenesis in human cells. *Dev Cell 13:190-202.*

10. Curriculum Vitae

Jens Westendorf

Date of birth: January 14th, 1978

Place of birth: Sögel

Nationality: German

July 2005 – June 2009

PhD Student at the Max-Planck Institute of Biochemistry, Martinsried, Germany

Department of Cell Biology

Prof. Dr. Erich A. Nigg

July 2004 – June 2005

Research assistant at the University of British Columbia, Vancouver, Canada

Department of Microbiology & Immunology

Prof. Dr. Michael R. Gold

October 1998 – February 2004

Diploma in Biology at the Westfälische Wilhelms-Universität Münster, Germany

Department of Microbiology & Botany

Supervisor: Prof. Dr. Paul Tudzynski

August 1997 – October 1998

Public service as Paramedic

Rettungsdienst des Landkreises Emsland

August 1990 – June 1997

High School Diploma (Abitur)

Hümmling Gymnasium, Sögel, Germany

Publications:

Durand CA, **Westendorf J**, Tse KW, Gold MR (2006) The Rap GTPases mediate CXCL13- and sphingosine1-phosphate-induced chemotaxis, adhesion, and Pyk2 tyrosine phosphorylation in B lymphocytes. *Eur J Immunol 36(8): 2235-49.*

Lee RL, **Westendorf J**, Gold MR (2007) Differential role of reactive oxygen species in the activation of mitogen-activated protein kinases and Akt by key receptors on B-lymphocytes: CD40, the B cell antigen receptor, and CXCR4. *J Cell Commun Signal 1(1): 33-43.*

Kleylein-Sohn J, Stierhof Y-D, **Westendorf J**, Le Clech M, Habedanck R and Nigg EA (2007) Plk4-induced centriole biogenesis in human cells. *Dev Cell 13(2): 190-202.*

Schmidt TI, Kleylein-Sohn J, **Westendorf J**, Le Clech M, Lavoie SB, Stierhof YD, Nigg EA (2009) Control of Centriole Length by CPAP and CP110. *Curr Biol 19: 1005-1011.*

11. Acknowledgements

First, I would like to express my thanks to Erich Nigg for the opportunity to graduate in his group, and for his patience and guidance towards the end of this work. Furthermore, I am grateful to Heinrich Leonhardt for his committment to reviewing this study and for participating in my Thesis Advisory Committee. Similarly, I would like to thank Thomas Cremer for his participation in my Thesis Advisory Committee.
At this point, also a big thanks to my former supervisor Mike Gold and my labmates in Vancouver – particularly Caylib and Kevin – for all their support and the best time of my life.
Thanks a lot to Maxi Reif and Hans-Jörg Schäffer for their extraordinary energy to make the IMPRS live, and for their support during the last 4 years.

In every moment of lab frustration, my great colleagues and friends in the lab kept me going, and thus I would like to express my deepest 'thank you all' to the people in the department. Particular thanks go to Klaus Weber and Alison Dalfovo, as they have always been helpful in every situation.
Furthermore, I am grateful to the MassSpec group and to Roman Körner ("Da ist doch eh wieder kein Plk4 drin...!") for help with the endless Plk4 analyses. Roman and Rainer, I count on you for our Ex-Nigg-Stammtisch!

"Centrosomics brings new understanding" of friendship among colleagues... Julia, Thorsten, Gernot and Ina, I enjoyed my time with you 'downstairs' to the full, all the endless discussions, mutual support, jokes, laughs and our supernumerary Schlagerparties. Thanks, the time was just great fun. Thanks also to Kiwi-Tom for all the distractions and fun stuff... Glad to know that you and Louise are staying in Munich.
Robert and Xiumin – thanks a lot for all your support to get things going and finally for your friendship over the time.

Schließlich und endlich möchte ich denjenigen danken, die mich privat in allen Höhen und Tiefen immer unterstützt haben.
Heike & Helmut Schreck: Vielen Dank für Euer stetiges Interesse, Eure Erfahrung und all Eure Hilfe, ich freue mich auf die vielen weiteren Jahre!
Meinen Eltern Anneliese & Hans Westendorf: Es ist schwer, die richtigen Worte für Eure Aufopferung in all den zurückliegenden Jahren zu finden. Deshalb an dieser Stelle einfach nur ein schlichtes 'Danke'.
Und schließlich meiner Heidrun: Danke für Deine unerschöpfliche Geduld, bedingungslose Unterstützung, und schließlich für die wundervolle Zeit, die wir zusammen verbracht haben und weiterhin verbringen werden. *....* :)